

Statement

Position Statement on the Use of Myocardial Strain in Cardiology Routines by the Brazilian Society of Cardiology's Department Of Cardiovascular Imaging – 2023

Development: Department of Cardiovascular Imaging of Brazilian Society of Cardiology (Departamento de Imagem Cardiovascular da Sociedade Brasileira de Cardiologia – DIC/SBC)

Statement Authors: André Luiz Cerqueira Almeida,¹ Marcelo Dantas Tavares de Melo,² David Costa de Souza Le Bihan,³ Marcelo Luiz Campos Vieira,³ José Luiz Barros Pena,^{4,5} José Maria Del Castillo,⁶ Henry Abensur,⁷ Renato de Aguiar Hortegal,⁸ Maria Estefania Bosco Otto,⁹ Rafael Bonafim Piveta,¹⁰ Maria Rosa Dantas,¹¹ Jorge Eduardo Assef,⁸ Adenvalva Lima de Souza Beck,¹² Thais Harada Campos Espirito Santo,^{13,14} Tonnison de Oliveira Silva,¹⁵ Vera Maria Cury Salemi,³ Camila Rocon,¹⁶ Márcio Silva Miguel Lima,³ Silvio Henrique Barberato,¹⁷ Ana Clara Rodrigues,¹⁰ Arnaldo Rabschkowsky,¹⁸ Daniela do Carmo Rassi Frotta,¹⁹ Eliza de Almeida Gripp,^{20,21} Rodrigo Bellio de Mattos Barretto,³ Sandra Marques e Silva,²² Sanderson Antonio Cauduro,²³ Aurélio Carvalho Pinheiro,²⁴ Salustiano Pereira de Araujo,²⁵ Cintia Galhardo Tressino,⁸ Carlos Eduardo Suaide Silva,²⁶ Claudia Gianini Monaco,¹⁰ Marcelo Goulart Paiva,²⁷ Cláudio Henrique Fisher,¹⁰ Marco Stephan Lofrano Alves,²⁸ Cláudia R. Pinheiro de Castro Grau,³ Maria Veronica Camara dos Santos,^{29,30} Isabel Cristina Britto Guimarães,³¹ Samira Saady Morhy,¹⁰ Gabriela Nunes Leal,³² Andressa Mussi Soares,³³ Cecília Beatriz Bittencourt Viana Cruz,³ Fabio Villaça Guimarães Filho,³⁴ Bruna Morhy Borges Leal Assunção,³⁵ Rafael Modesto Fernandes,³⁶ Roberto Magalhães Saraiva,³⁷ Jeane Mike Tsutsui,³⁸ Fábio Luis de Jesus Soares,³⁹ Sandra Nívea dos Reis Saraiva Falcão,⁴⁰ Viviane Tiemi Hotta,^{3,38} Anderson da Costa Armstrong,⁴¹ Daniel de Andrade Hygídio,^{42,43} Marcelo Haertel Miglioranza,^{44,45} Ana Cristina Camarozano,²⁸ Marly Maria Uellendahl Lopes,⁴⁶ Rodrigo Julio Cerci,⁴⁷ Maria Eduarda Menezes de Siqueira,⁴⁶ Jorge Andion Torreão,^{48,49} Carlos Eduardo Rochitte,^{3,16} Alex Felix^{26,50}

Santa Casa de Misericórdia de Feira de Santana,¹ Feira de Santana, BA – Brazil

Universidade Federal da Paraíba,² João Pessoa, PB – Brazil

Instituto do Coração da Faculdade de Medicina da Universidade de São Paulo (Incor/FMUSP),³ São Paulo, SP – Brazil

Faculdade Ciências Médicas de Minas Gerais, Belo Horizonte,⁴ MG – Brazil

Hospital Felício Rocho,⁵ Belo Horizonte, MG – Brazil

Escola de Ecografia de Pernambuco (ECOPE),⁶ Recife, PE – Brazil

Beneicência Portuguesa de São Paulo,⁷ São Paulo, SP – Brazil

Instituto Dante Pazzanese de Cardiologia,⁸ São Paulo, SP – Brazil

DF Star, Rede D'Or São Luiz,⁹ Brasília, DF – Brazil

Hospital Israelita Albert Einstein,¹⁰ São Paulo, SP – Brazil

Santa Casa de Feira de Santana,¹¹ Feira de Santana, BA – Brazil

Instituto de Cardiologia e Transplantes do DF,¹² Brasília, DF – Brazil

Diagnoson, Grupo Fleury,¹³ Salvador, BA – Brazil

Hospital da Bahia,¹⁴ Salvador, BA – Brazil

Escola Bahiana de Medicina e Saúde Pública,¹⁵ Salvador, BA – Brazil

Hospital do Coração (HCor),¹⁶ São Paulo, SP – Brazil

CardioEco Centro de Diagnóstico Cardiovascular e Ecocardiografia,¹⁷ Curitiba, PR – Brazil

UnitedHealth Group,¹⁸ Rio de Janeiro, RJ – Brazil

Faculdade de Medicina da Universidade Federal de Goiás,¹⁹ Goiânia, GO – Brazil

Hospital Pró-Cardiaco,²⁰ Rio de Janeiro, RJ – Brazil

Hospital Universitário Antônio Pedro da Universidade Federal Fluminense (UFF),²¹ Rio de Janeiro, RJ – Brazil

Secretaria de Estado de Saúde do Distrito Federal,²² Brasília, DF – Brazil

Clínica Cardio & Saúde,²³ Curitiba, PR – Brazil

Heart & Mind Care Serviços Médicos (HMC),²⁴ Manaus, AM – Brazil

Cardiologia Não Invasiva, Clínica CNI,²⁵ Uberlândia, MG – Brazil

Diagnósticos da América SA (DASA),²⁶ São Paulo, SP – Brazil

Hospital 9 de Julho,²⁷ São Paulo, SP – Brazil

Universidade Federal do Paraná (UFPR),²⁸ Curitiba, PR – Brazil

Departamento de Cardiologia Pediátrica (DCC/CP) da Sociedade Brasileira de Cardiologia (SBC),²⁹ São Paulo, SP – Brazil

DOI: <https://doi.org/10.36660/abc.20230646>

Sociedade Brasileira de Oncologia Pediátrica,³⁰ São Paulo, SP – Brazil
Universidade Federal da Bahia (UFBA),³¹ Salvador, BA – Brazil
Instituto da Criança e do Adolescente do Hospital das Clínicas Faculdade de Medicina da Universidade de São Paulo (FMUSP),³² São Paulo, SP – Brazil
Hospital Evangélico,³³ Cachoeiro de Itapemirim, ES – Brazil
Instituto do Coração de Marília (ICM),³⁴ Marília, SP – Brazil
Instituto do Câncer do Estado de São Paulo (ICESP),³⁵ São Paulo, SP – Brazil
Hospital Aliança Rede D'Or São Luiz,³⁶ Salvador, BA – Brazil
Fundação Oswaldo Cruz (FIOCRUZ),³⁷ Rio de Janeiro, RJ – Brazil
Grupo Fleury,³⁸ São Paulo, SP – Brazil
Hospital Cardio Pulmonar Rede D'Or São Luiz,³⁹ Salvador, BA – Brazil
Universidade Federal do Ceará,⁴⁰ Fortaleza, CE – Brazil
Universidade Federal do Vale do São Francisco (UNIVASF),⁴¹ Petrolina, PE – Brazil
Hospital Nossa Senhora da Conceição,⁴² Tubarão, SC – Brazil
Universidade do Sul de Santa Catarina (UNISUL),⁴³ Tubarão, SC – Brazil
EcoHaertel - Hospital Mae de Deus,⁴⁴ Porto Alegre, RS – Brazil
Universidade Federal de Ciências da Saúde de Porto Alegre,⁴⁵ Porto Alegre, RS – Brazil
Universidade Federal de São Paulo (UNIFESP),⁴⁶ São Paulo, SP – Brazil
Quanta Diagnóstico por Imagem,⁴⁷ Curitiba, PR – Brazil
Hospital Santa Izabel,⁴⁸ Salvador, BA – Brazil
Santa Casa da Bahia,⁴⁹ Salvador, BA – Brazil
Instituto Nacional de Cardiologia (INC),⁵⁰ Rio de Janeiro, RJ – Brazil

Presidents of the Department of Cardiovascular Imaging: Carlos Eduardo Rochitte (2020/2021) and André Luiz Cerqueira de Almeida (2022/2023)

Coordinating Editors: André Luiz Cerqueira de Almeida, Marcelo Dantas Tavares de Melo, Alex dos Santos Felix and David Costa de Souza Le Bihan

Co-Editors: Marcelo Luiz Campos Vieira and José Luiz Barros Pena

SBC Clinical Practice Guidelines Committee: Carisi Anne Polanczyk (Coordinator), Humberto Graner Moreira, Mário de Seixas Rocha, Jose Airton de Arruda, Pedro Gabriel Melo de Barros e Silva – Period 2022-2024

How to cite this Guideline: Almeida ALC, Melo MDT, Bihan DCSL, Vieira MLC, Pena JLB, Castillo JMD, et al. Position Statement on the Use of Myocardial Strain in Cardiology Routines by the Brazilian Society of Cardiology's Department Of Cardiovascular Imaging – 2023. *Arq Bras Cardiol.* 2023; 120(12):e20230646

Note: These statements are for information purposes and should not replace the clinical judgment of a physician, who must ultimately determine the appropriate treatment for each patient.

Correspondence: Sociedade Brasileira de Cardiologia – Av. Marechal Câmara, 360/330 – Centro – Rio de Janeiro, Brazil – Posta Code 20020-907. E-mail: diretrizes@cardiol.br

Statement

Position Statement on the Use of Myocardial Strain in Cardiology Routines by the Brazilian Society of Cardiology's Department Of Cardiovascular Imaging – 2023

The report below lists declarations of interest as reported to the SBC by the experts during the period of the development of these statement, 2022/2023.

Expert	Type of relationship with industry
Adenálva Lima de Souza Beck	Nothing to be declared
Alex Felix	Nothing to be declared
Ana Clara Rodrigues	Nothing to be declared
Ana Cristina Camarozano	Nothing to be declared
Anderson da Costa Armstrong	<p>Financial declaration</p> <p>A - Economically relevant payments of any kind made to (i) you, (ii) your spouse/partner or any other person living with you, (iii) any legal person in which any of these is either a direct or indirect controlling owner, business partner, shareholder or participant; any payments received for lectures, lessons, training instruction, compensation, fees paid for participation in advisory boards, investigative boards or other committees, etc. From the brazilian or international pharmaceutical, orthosis, prosthesis, equipment and implants industry:</p> <p>- Amyloidosis: Anylam.</p> <p>Other relationships</p> <p>Funding of continuing medical education activities, including travel, accommodation and registration in conferences and courses, from the brazilian or international pharmaceutical, orthosis, prosthesis, equipment and implants industry:</p> <p>- Health area; CARDIOVASF.</p>
André Luiz Cerqueira de Almeida	<p>Financial declaration</p> <p>A - Economically relevant payments of any kind made to (i) you, (ii) your spouse/partner or any other person living with you, (iii) any legal person in which any of these is either a direct or indirect controlling owner, business partner, shareholder or participant; any payments received for lectures, lessons, training instruction, compensation, fees paid for participation in advisory boards, investigative boards or other committees, etc. From the brazilian or international pharmaceutical, orthosis, prosthesis, equipment and implants industry:</p> <p>- Boston Scientific: Speaker.</p>
Andressa Mussi Soares	<p>Financial declaration</p> <p>A - Economically relevant payments of any kind made to (i) you, (ii) your spouse/partner or any other person living with you, (iii) any legal person in which any of these is either a direct or indirect controlling owner, business partner, shareholder or participant; any payments received for lectures, lessons, training instruction, compensation, fees paid for participation in advisory boards, investigative boards or other committees, etc. From the brazilian or international pharmaceutical, orthosis, prosthesis, equipment and implants industry:</p> <p>- Bayer: Anticoagulation and heart failure; Pfizer: Anticoagulation and amyloidosis; Janssen: Leukemia.</p> <p>Other relationships</p> <p>Funding of continuing medical education activities, including travel, accommodation and registration in conferences and courses, from the brazilian or international pharmaceutical, orthosis, prosthesis, equipment and implants industry:</p> <p>- Bayer: Heart failure.</p>
Arnaldo Rabischoffsky	Nothing to be declared
Aurélio Carvalho Pinheiro	Nothing to be declared
Bruna Morhy Borges Leal Assunção	Nothing to be declared
Camila Rocon	Nothing to be declared
Carlos Eduardo Suaide Silva	Nothing to be declared
Carlos Eduardo Rochitte	Nothing to be declared
Cecilia Beatriz Bittencourt Viana Cruz	Nothing to be declared
Cintia Galhardo Tressino	Nothing to be declared
Claudia Gianini Monaco	Nothing to be declared
Claudia R. Pinheiro de Castro Grau	Nothing to be declared
Cláudio Henrique Fischer	Nothing to be declared
Daniel de Andrade Hygídio	Nothing to be declared
Daniela do Carmo Rassi Frota	Nothing to be declared

David Costa de Souza Le Bihan	Financial declaration A - Economically relevant payments of any kind made to (i) you, (ii) your spouse/partner or any other person living with you, (iii) any legal person in which any of these is either a direct or indirect controlling owner, business partner, shareholder or participant; any payments received for lectures, lessons, training instruction, compensation, fees paid for participation in advisory boards, investigative boards or other committees, etc. From the brazilian or international pharmaceutical, orthosis, prosthesis, equipment and implants industry: - Edwards Lifescience; Abbott; GE Healthcare; Philips.
Eliza de Almeida Gripp	Nothing to be declared
Fábio Luis de Jesus Soares	Nothing to be declared
Fabio Villaça Guimarães Filho	Nothing to be declared
Gabriela Nunes Leal	Nothing to be declared
Henry Abensur	Nothing to be declared
Isabel Cristina Britto Guimarães	Nothing to be declared
Jeane Mike Tsutsui	Other relationships Any economically relevant equity interest in companies in the healthcare or education industry or in any companies competing with or supplying to SBC: - Health area: Grupo Fleury.
Jorge Andion Torreão	Other relationships Any economically relevant equity interest in companies in the healthcare or education industry or in any companies competing with or supplying to SBC: - Partner of an education company in the health sector.
Jorge Eduardo Assef	Nothing to be declared
José Luiz Barros Pena	Nothing to be declared
Jose Maria Del Castillo	Nothing to be declared
Marcelo Dantas Tavares de Melo	Nothing to be declared
Marcelo Goulart Paiva	Nothing to be declared
Marcelo Haertel Miglioranza	Nothing to be declared
Marcelo Luiz Campos Vieira	Nothing to be declared
Márcio Silva Miguel Lima	Nothing to be declared
Marco Stephan Lofrano Alves	Nothing to be declared
Maria Eduarda Menezes de Siqueira	Nothing to be declared
Maria Estefânia Bosco Otto	Nothing to be declared
Maria Rosa Dantas	Nothing to be declared
Maria Veronica Camara dos Santos	Nothing to be declared
Marly Maria Uellendahl Lopes	Nothing to be declared
Rafael Bonafim Piveta	Other relationships Any economically relevant equity interest in companies in the healthcare or education industry or in any companies competing with or supplying to SBC: - Partner at WavesMed (digital platform for continuing education/updates).
Rafael Modesto Fernandes	Nothing to be declared
Renato de Aguiar Hortegal	Nothing to be declared
Roberto Magalhães Saraiva	Nothing to be declared

Statement

Rodrigo Bellio de Mattos Barretto	<p>Financial declaration</p> <p>A - Economically relevant payments of any kind made to (i) you, (ii) your spouse/partner or any other person living with you, (iii) any legal person in which any of these is either a direct or indirect controlling owner, business partner, shareholder or participant; any payments received for lectures, lessons, training instruction, compensation, fees paid for participation in advisory boards, investigative boards or other committees, etc. From the brazilian or international pharmaceutical, orthosis, prosthesis, equipment and implants industry: - GE; Abbot; Edwards.</p>
Rodrigo Julio Cerci	Nothing to be declared
Salustiano Pereira de Araujo	Nothing to be declared
Samira Saady Morhy	Nothing to be declared
Sanderson Antonio Cauduro	Nothing to be declared
Sandra Marques e Silva	<p>Other relationships</p> <p>Funding of continuing medical education activities, including travel, accommodation and registration in conferences and courses, from the brazilian or international pharmaceutical, orthosis, prosthesis, equipment and implants industry: - Pfizer: Amyloidosis; Sanofi, Pint Pharma, Takeda and Chiesi: Fabry.</p>
Sandra Nívea dos Reis Saraiva Falcão	Nothing to be declared
Silvio Henrique Barberato	Nothing to be declared
Thais Harada Campos Espirito Santo	Nothing to be declared
Tonnison de Oliveira Silva	Nothing to be declared
Vera Maria Cury Salemi	Nothing to be declared
Viviane Tiemi Hotta	<p>Financial declaration</p> <p>B - Research funding under your direct/personal responsibility (directed to the department or institution) from the Brazilian or international pharmaceutical, orthosis, prosthesis, equipment and implants industry: - Pfizer: Amyloidosis.</p>

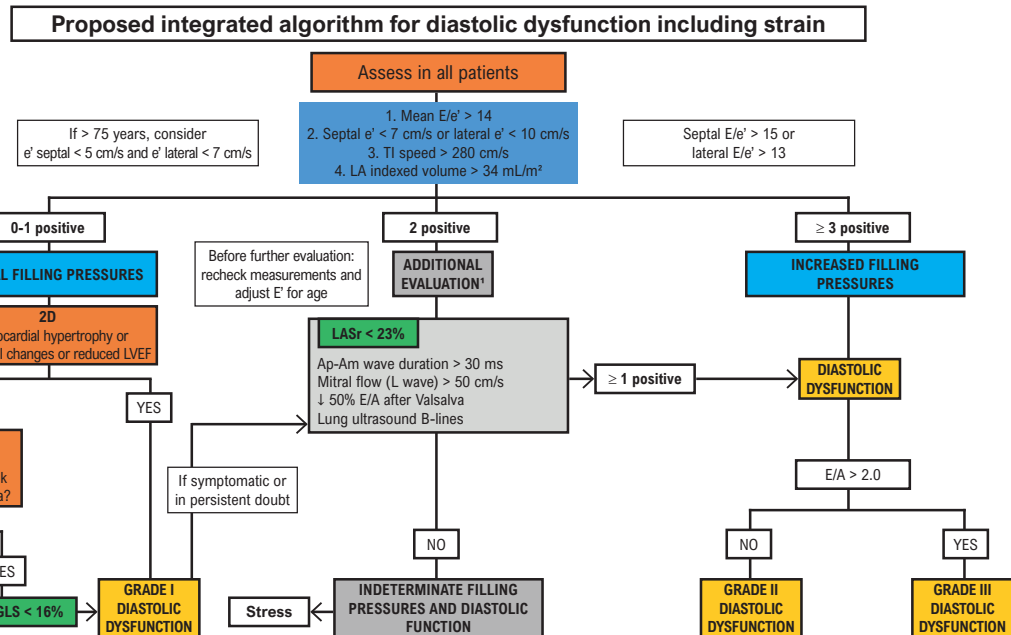
Table of contents

1. Basic Concepts in Left Ventricular Strain	7
1.1. Brief Introduction to the Physical Principles of Speckle Formation in Cardiovascular Imaging	7
1.2. Definitions	7
1.2.1. Strain and Strain Rate	7
1.2.2. Longitudinal, Circumferential, and Radial Deformation	7
1.2.3. Timing Mechanical Events	8
1.2.4. Peak Measurements Extracted from Strain Curves	8
1.3. Factors Affecting Strain Estimation	8
1.3.1. Image Quality	8
1.3.2. Cardiovascular Imaging Modality	8
1.3.3. Software Manufacturer and Version	8
1.3.4. Hemodynamic Conditions	8
1.4. Global Longitudinal Strain	9
2. General Recommendations for Using Strain: Clinical Applicability, Comparison with Ejection Fraction, and Adequate Description for Echocardiography Reports	10
2.1. Prognostic Value, Parametric Patterns, and Subclinical Detection of Heart Disease Through Myocardial Strain	10
2.2. Which is Better, Strain or Ejection Fraction?	11
2.3. General Recommendations for Reporting Strain Results and Normality Values	12
2.4. Conclusion	12
3. Strain in Cardio-oncology	13
4. Strain in Diastolic Dysfunction	15
4.1. Introduction	15
4.2. Left Ventricle Strain	15
4.3. Left Atrial Strain	15
4.4. Conclusion	16
5. Strain in Cardiomyopathies	16
5.1. Introduction	16
5.2. Dilated Cardiomyopathy	16
5.3. Arrhythmogenic Cardiomyopathy	16
5.4. Hypertrophic Cardiomyopathy	17
5.5. Endomyocardial Fibrosis	17
5.6. Noncompacted Myocardium	17
6. Strain in Valvular Heart Disease	18
7. Strain in Ischemic Heart Disease	19
7.1. Introduction	19
7.2. Strain in Acute Coronary Syndrome	19
7.3. Strain in Chronic Coronary Syndromes	20
7.4. Right Ventricular Strain in Ischemic Heart Disease	20
8. Strain Assessment in Systemic Diseases (Amyloidosis and Fabry Disease)	20
8.1. Strain Assessment in Cardiac Amyloidosis	20
8.1.1. Myocardial Strain Assessment in the Diagnosis of Cardiac Amyloidosis	21
8.2. Fabry Disease	23
9. Strain in Hypertension	24
9.1. Introduction	24
9.2. Hypertension without Left Ventricular Hypertrophy Criteria	24
9.3. Hypertension with Left Ventricular Hypertrophy Criteria	25
9.4. Clinical Treatment	25
9.5. Conclusion	25
10. Strain in Athletes	25
11. Strain in Stress Echocardiography	26
12. Strain in Congenital Heart Disease	26
13. Right Ventricle Strain	26
13.1. Introduction	26
13.2. Anatomical and Functional Characteristics of the Right Ventricle	28
13.3. Right Ventricle and Echocardiographic Parameters in Systolic Function Assessment	28
13.4. Acquisition and Limitations	28
13.5. Indications/Normal Values	30
14. Left and Right Atrial Strain	31
14.1. Left Atrial Strain Assessment Techniques	31
14.2. Normality Values	31
14.3. Clinical Applicability of Left Atrial Strain	32
14.3.1. Left Atrial Strain and Diastolic Function in Heart Failure	32
14.3.2. Atrial Fibrillation	32
14.3.3. Valvular Heart Disease	32
14.3.4. Coronary Artery Disease	32
14.4. Right Atrial Strain	32
15. Assessing Left Ventricular Torsion	32
15.1. Introduction	32
15.2. Definitions and Nomenclature	33
15.3. Step-by-step Assessment of Ventricular Torsion by Speckle Tracking Echocardiography	33
16. Strain in Ventricular Dyssynchrony Analysis	34
16.1. Introduction	34
16.2. Dyssynchrony Assessment when Selecting Patients for Cardiac Resynchronization Therapy	35
16.3. Myocardial Viability Assessment	35
16.4. Electrode Implantation Site	35
16.5. Prognostic Assessment after CRT	35
16.6. Adjustment of Resynchronization Parameters	36
17. Myocardial Work	36
17.1. Introduction	36
17.2. Calculating Myocardial Work	36
17.3. Normality Values	37
17.4. Potential Clinical Use	37
18. Three-dimensional Strain Assessment: What can be Added	40
18.1. Introduction	40
18.2. Left Ventricular Strain	41
18.3. Right Ventricular Strain	41
18.3.1. Full-volume 3D Acquisition and Analysis	41
18.4. Left Atrial Strain	41
19. The Role of Cardiac Resonance and Tomography in Strain Assessment	41
19.1. Introduction	41
19.2. Strain Acquisition Methods by Cardiac Magnetic Resonance Imaging	41
19.3. Determining Right Ventricle Strain Through Cardiac Magnetic Resonance Imaging	42
19.4. Determining Left Ventricular Strain Through Cardiac Magnetic Resonance Imaging	42
19.5. Determining Left Atrial Strain Through Cardiac Magnetic Resonance Imaging	42
19.6. Determining Strain Through Cardiac Tomography	43
References	43

Statement



Central Illustration: Position Statement on the Use of Myocardial Strain in Cardiology Routines by the Brazilian Society of Cardiology's Department Of Cardiovascular Imaging – 2023



Arq Bras Cardiol. 2023; 120(12):e20230646

Proposal for including strain in the integrated diastolic function assessment algorithm, adapted from Nagueh et al.⁶⁷ Am: mitral A-wave duration; Ap: reverse pulmonary A-wave duration; DD: diastolic dysfunction; LA: left atrium; LASr: LA strain reserve; LVGLS: left ventricular global longitudinal strain; TI: tricuspid insufficiency. Confirm concentric remodeling with LVGLS. In LVEF, mitral E wave deceleration time < 160 ms and pulmonary S-wave < D-wave are also parameters of increased filling pressure. This algorithm does not apply to patients with atrial fibrillation (AF), mitral annulus calcification, > mild mitral valve disease, left bundle branch block, paced rhythm, prosthetic valves, or severe primary pulmonary hypertension

1. Basic Concepts in Left Ventricular Strain

1.1. Brief Introduction to the Physical Principles of Speckle Formation in Cardiovascular Imaging

Optical coherence imaging systems such as laser, optical coherence tomography, or ultrasound produce grainy reflections known as speckle.^{1,2} In echocardiography, an emitted ultrasound pulse moves in a straight line, interacting with the acoustic interfaces of the thoracic cavity until it reaches the heart. Some of the beam is reflected by different cardiac structures, producing an echo that is partially captured by the transducer, and the software uses it as an input to produce images. In this case, the beam's wavelength is usually shorter than the structures that reflect it.

However, when the wavelength is longer than the microstructures it interacts with, the beam is a scattered, radiating in all directions (diffuse scattering). This phenomenon is the result of an interference pattern in all wavefronts scattered by the different phenomena (eg, local differences in tissue density and compressibility). Some this diffuse scattering, or speckle, is captured by the transducer. Although speckle makes the B-mode image less clear for human operators, it

should not be seen as noise, since it carries unique information, acting as a myocardial “fingerprint”.¹

1.2. Definitions

1.2.1. Strain and Strain Rate

Strain is the amount that an object deforms compared to its original shape.³ In cardiology, this concept is represented as the magnitude (%) of myocardial fiber contraction/relaxation in relation to its initial measurement. This concept can be applied to a single segment (regional strain) or to entire heart chambers (global strain), such as the left ventricle (LV). Strain rate indicates the rate of myocardial deformation (%) every second (s^{-1}), ie, the speed at which deformation occurs.³⁻⁴

1.2.2. Longitudinal, Circumferential, and Radial Deformation

Through the concept of strain, the contraction/relaxation of the LV myocardium from its orientation in different axes can be studied. In fact, due to the helical arrangement of

cardiac muscle fibers, LV systolic shortening is determined by the longitudinal and circumferential action of fibers,⁵ the two active force vectors of strain (Figure 1.1 A).

When longitudinal and circumferential forces are applied to a material with low compressibility, such as myocardial tissue, the myocardium is thickened radially (passive deformation component).⁶ Ultimately, this accounts for radial shrinkage of the ventricular cavity.⁴ The deformation process is much more complex than we can measure, since for each interaction between the force vectors, a new vector arises from the shear between the different deformations, called shear strain (Figure 1.1 B, C and D).

Systolic fiber shortening/thinning in the longitudinal and circumferential direction produces negative strain values, whereas systolic thickening results in positive strain values. Many authors express only the absolute value (modulus value), and we will do the same herein.

1.2.3. Timing Mechanical Events

Some fundamental definitions for clinical practice are provided below:^{1,7}

- **End-systole:** The point of aortic valve closure. Potential substitutes: peak global strain or the volume curve. The software should show which criterion is used to determine end-systole.
- **End-diastole:** The point at which the QRS complex peaks. Event timing should be performed using Doppler imaging in reference to the electrocardiogram.

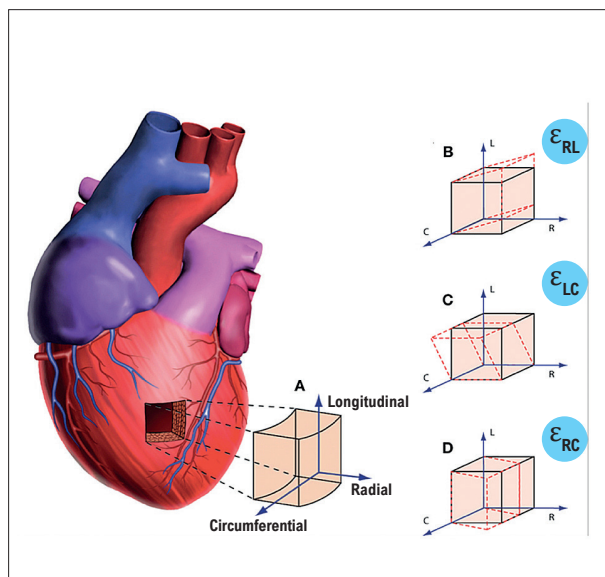


Figure 1.1 – Myocardial strain in different axes. A) Strain can be measured in the longitudinal, circumferential, and radial directions.⁴ A third vector results from the interaction of 2 of these force-vectors. B) Radial-circumferential shear strain. C) Longitudinal-circumferential shear strain (ie, ventricular twist/torsion). D) Radial-circumferential shear strain.

1.2.4. Peak Measurements Extracted from Strain Curves (Figure 1.2)

- **End-systolic strain:** The point of the strain curve at end-systole, as defined above (aortic valve closure). This is the standard parameter for describing myocardial deformation.
- **Peak systolic strain:** The point at which the peak of the strain curve occurs during systole.
- **Positive peak systolic strain:** the highest positive value of local myocardial stretching at some point during systole.
- **Peak strain:** the highest point of the strain curve during the entire heart cycle. Although this point is usually reached before aortic valve closure, when it occurs afterwards, it is described as post-systolic strain⁸ or post-systolic shortening. Post-systolic strain is the deformation of segments after aortic valve closure that does not contribute to ventricular ejection.

1.3. Factors Affecting Strain Estimation

1.3.1 Image Quality

Image quality is a critical factor in any software that estimates myocardial strain. Several authors have reported the sensitivity of strain and strain rate estimation proportional to the quality of the image and the tracking algorithm.⁹⁻¹¹

1.3.2. Cardiovascular Imaging Modality

Different cardiovascular imaging modalities provide different strain values. Tee et al.¹² reported differences between transthoracic echocardiography, computed tomography, and cardiac magnetic resonance imaging (MRI).

1.3.3. Software Manufacturer and Version

Two studies by the European Association of Cardiovascular Imaging and the American Society of Echocardiography tested the variability of global longitudinal strain (GLS) measurements among different equipment types and software, finding significant divergences.¹³⁻¹⁴ However, such differences are smaller than the ejection fraction (EF) variability reported in the literature.^{9-10,15} In addition to variability among manufacturers, measures can vary in different programs by the same manufacturer, with significant changes in GLS having been reported.^{11,15}

Thus, serial echocardiographic studies should ideally be performed using the same device and software and under similar hemodynamic conditions, especially when GLS variation in can restrict therapy options, such as when assessing chemotherapy-induced cardiotoxicity.⁴

1.3.4. Hemodynamic Conditions

LV deformation varies considerably according to the ventricle's preload and afterload conditions.

Statement

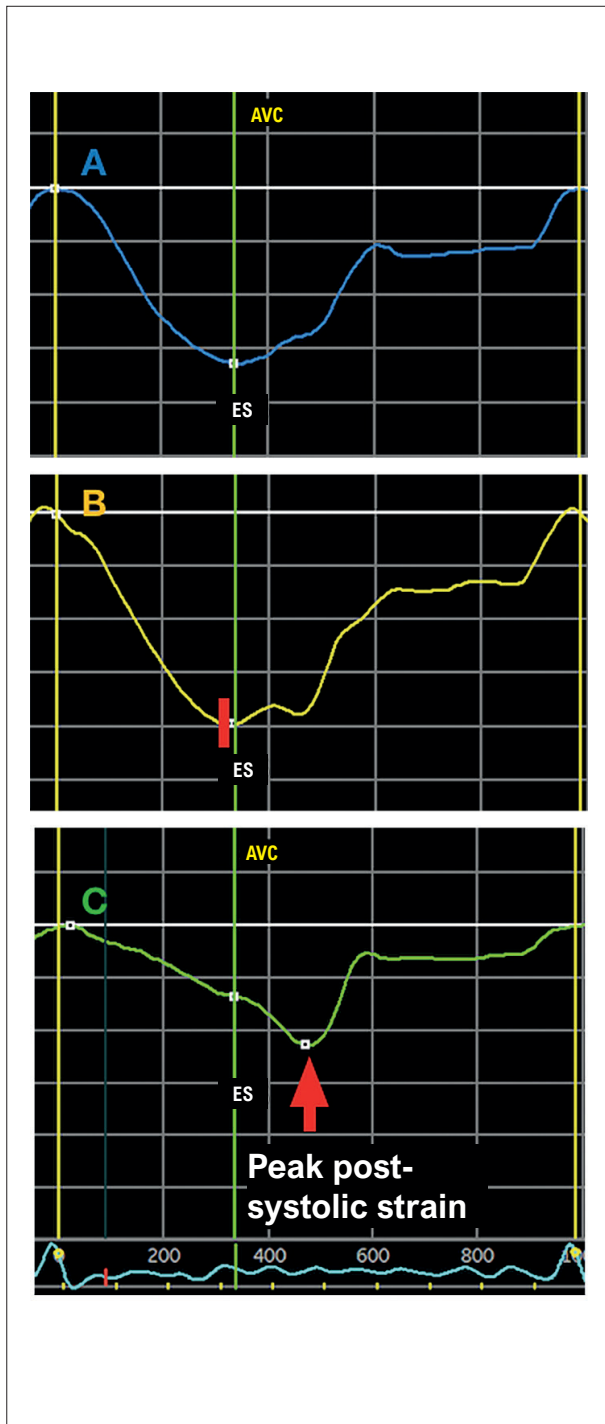


Figure 1.2 – Peak measurements derived from strain curves A) Peak systolic strain, peak strain, and end-systolic (ES) strain coincide upon aortic valve closure (AVC). B) Peak systolic strain and peak strain coincide, although both occur immediately before AVC (red bar), resulting in slight dissociation between these and ES strain. C) Peak and end-systolic strain coincide (both with lower absolute values), although peak strain occurs after AVC (post-systolic shortening phenomenon).

1.4. Global Longitudinal Strain

The evidence is more robust for GLS than for any other cardiac strain parameter, and it is the most relevant type for clinical practice.⁹ It reflects relative LS (%) in the LV myocardium, which occurs from the isovolumetric contraction until the end of the ejection period.^{1,5,15}

Mathematically, the contraction at any instant is computed using the algorithm: $GLS(t) = 100 [L(t) - L(ED)/L(ED)]$, in which $L(t)$ is the longitudinal length at time t , with $L(ED)$ being the end-diastolic length.¹

Programs vary significantly regarding $L(ED)$ length: the entire line of the region of interest \times the mean of a given number of points in a region of interest \times the mean value in each segment of the same frame. The normal GLS value is approximately 20%,⁹ although there is evidence that normality varies according to sex and age.⁷

To analyze LVGLS by speckle tracking, a series of image acquisition precautions are necessary:

- 1) The patient must be monitored electrocardiographically.
- 2) If possible, an attempt should be made to achieve expiratory apnea, avoiding translational movements of the heart with respiratory incursions.
- 3) Balance should be sought between the echocardiographic method's spatial and temporal resolution (focus, depth, and width adjustments) to optimize the cardiac chamber of interest vs frame rate. The latter should be kept between 40-80 frames per second in patients with a normal heart rate. The higher the heart rate, the higher the required RR values.
- 4) Avoid foreshortening in LV images.
- 5) Four-, 3-, and 2-chamber apical acoustic windows must be acquired, preferably with a minimum of 3 beats, excluding extrasystoles.

Table 1.1 and Figure 1.3 summarize the GLS measurement procedure.

Table 1.1 – Step-by-step measurement of global longitudinal strain for most manufacturers⁴

• Good quality cardiac electrocardiographic monitoring
• Obtain 3-, 4-, and 2-chamber acoustic windows with a frame rate between 40-80 frames per second.
• Mark aortic valve closure.
• Mark topographic definitions to determine the region of interest in the 3-, 4- and 2-chamber windows.
• Accept or discard the myocardial segments tracked in each window and make adjustments if necessary.
• Evaluate the curves and interpret the results of the polar map.
• Properly record the hemodynamic conditions under which GLS was measured.

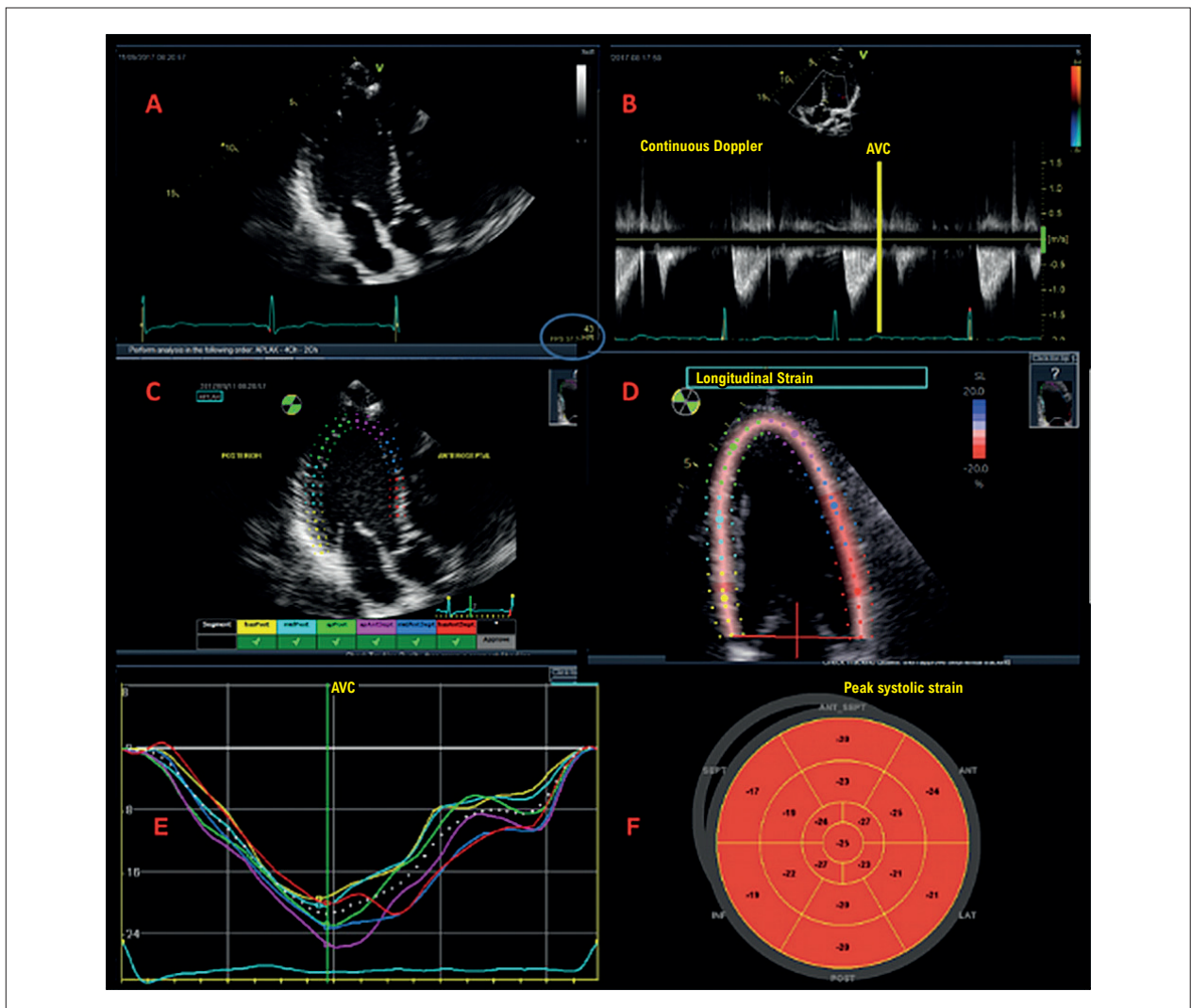


Figure 1.3 – Step by step to obtain the global longitudinal strain. Initially, images are acquired in 3, 4 and 2 chambers, with good quality EKG. Images must be acquired at an adequate frame rate (40-80 frames per second) (A: blue ovoid). Aortic valve closure (AVC) is marked using pulsed or continuous Doppler tracking (B). Three points (2 at the base and 1 at the apex) are then marked on the 3 acquired images, determining whether the software adequately tracked the 2D images (C and D). Finally, the curves (E), bull's eye map (F), and global longitudinal strain values are obtained. Adapted from Tressino et al.⁴

2. General Recommendations for Using Strain: Clinical Applicability, Comparison with Ejection Fraction, and Adequate Description for Echocardiography Reports

2.1. Prognostic Value, Parametric Patterns, and Subclinical Detection of Heart Disease Through Myocardial Strain

Myocardial strain analysis is a robust and versatile tool that offers additional information with less variability than normal prognosis parameters, in addition to parametric cardiomyopathy patterns, and subclinical lesion detection.

Recent studies have shown the increasing value of LVGLS in relation to left ventricular ejection fraction (LVEF).¹⁰ The inter- and intraobserver variability of strain analysis is 4.9-8.6%, which is much lower than LVEF, probably because it is less

influenced by ventricular preload and afterload.^{13,16} LVGLS is superior to LVEF in patients with heart failure (HF) and in those with reduced and preserved EF (HFrEF and HFpEF, respectively).^{17,18} In addition to LV analysis, worsening right ventricular (RV) strain provides additive prognostic value in patients with HFpEF.¹⁹

The morphological findings of cardiomyopathies usually overlap, which is a major diagnostic challenge in daily clinical practice. Increased ventricular mass and thickness is common, being associated with diastolic dysfunction (DD) and preserved LVEF in earlier stages. Parametric analysis of LVGLS with polar mapping can reveal some diagnoses in echocardiogram examination that are undetectable through normal parameters, having been described as a fingerprint for some. One example is the apical sparing pattern in amyloidosis, which will be described below in a specific

Statement

chapter.²⁰ Such phenotypic characterization has been met with enthusiasm since it facilitates diagnosis of rare pathologies. However, if strain data are not combined with the patient's clinical history and morphological and hemodynamic aspects, diagnostic error can result. See examples of apical sparing in Figure 2.1.

Strain's utility as a diagnostic and prognostic tool was consolidated through application in cardio-oncology. This is currently the only area of clinical practice in which it guides conduct (ie, variation from baseline values during chemotherapy). When a relative reduction $> 15\%$ occurs, cardiotoxicity with subclinical myocardial injury is considered to have occurred.²¹ In 2019, a group of societies developed criteria for the proper use of different imaging modalities to evaluate cardiac structures in non-valvular heart disease. Of their 81 recommendations, only 4 dealt with the adequate use of strain: 3 in cardio-oncology and 1 in hypertrophic cardiomyopathy (HCM).²² Although well-designed studies have not validated strain for other applications, it is widely used in large cardio-oncology centers and was reinforced in a recent update of the Brazilian Cardio-oncology Guidelines.²³

2.2. Which is Better, Strain or Ejection Fraction?

LVEF is one of the main echocardiographic parameters for assessing ventricular function in daily practice, since the data are easy to interpret and are widely accessible through basic

ultrasound equipment. This parameter has been extensively validated for heart disease, having being used as a patient inclusion criterion in large therapeutic-intervention studies, as well as a parameter for evaluating and monitoring the results.²⁴ The prognostic value of LVEF has been well established in chronic HF,²⁵ and the European Society of Cardiology's current recommendation is for HF to be classified according to the following LVEF values: **1)** HFpEF: EF $\geq 50\%$; **2)** HF with a moderately reduced EF (40-49%); and **3)** HFrEF: EF $< 40\%$.²⁶

LVEF is an important quantitative parameter for defining specific strategies in HF, eg, it is used to indicate cardiac resynchronization therapy in patients with refractory HF (LVEF $\leq 35\%$) or to detect cardiotoxicity in cancer patients who are using anthracyclines ($\geq 10\%$ drop in LVEF compared to baseline and values below the lower limit of normality).²⁷ However, its accuracy is limited when estimated with the 2D Simpson method due to high interobserver variability, which can reach up to 13%.²⁸ Unlike the 2D Simpson method, 3D echocardiography is not based on geometric assumptions and directly measures cavity volumes and LVEF. Its results are quite comparable to those obtained by cardiac MRI. Since it involves automatic algorithms and a lower susceptibility to variation in the acquisition windows (orientation of the apical slices), 3D echocardiography has less intra- and interobserver variability than the 2D method (0.4 [SD, 4.5%]),²⁹ making it a good alternative for monitoring patients who have ventricular dysfunction or are at risk of myocardial damage.

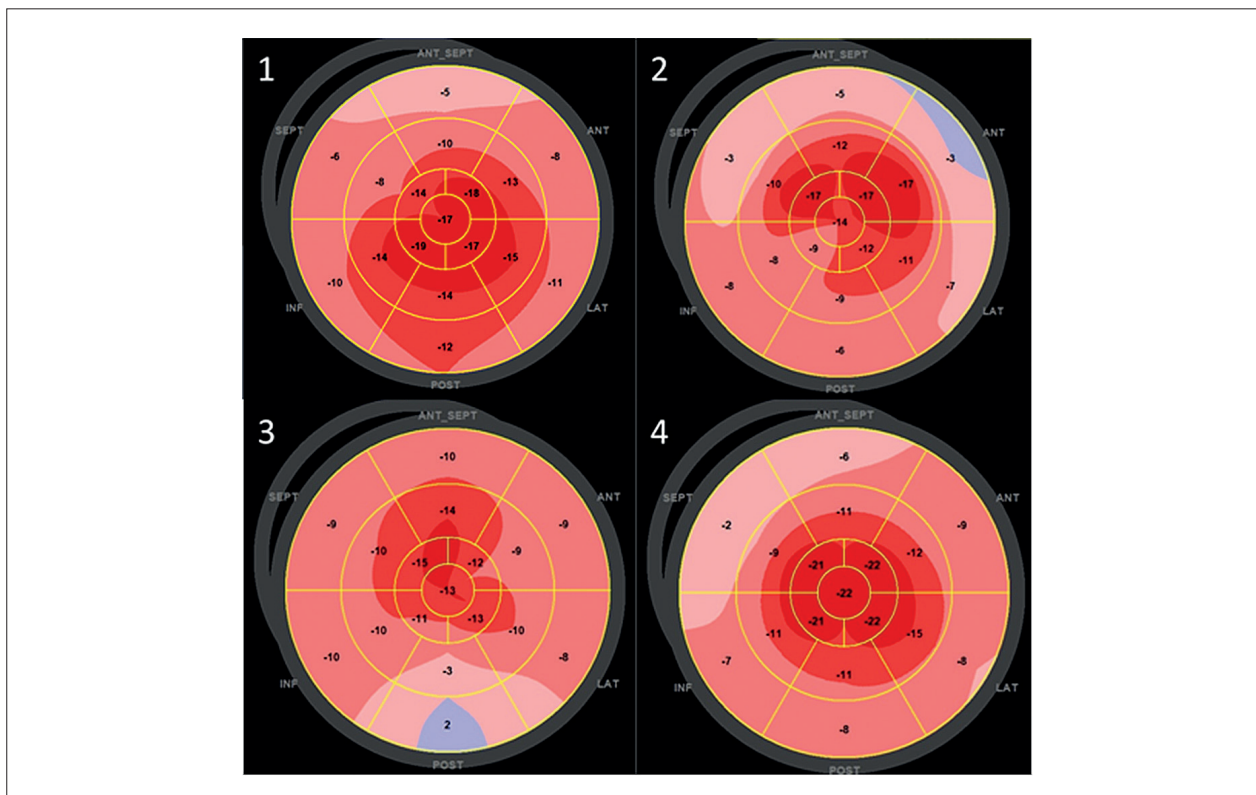


Figure 2.1 – Global longitudinal strain with apical sparing patterns in different heart diseases. 1: Anthracycline cardiotoxicity; 2: Non-compacted myocardium; 3: Hypothyroidism; 4: Transthyretin amyloidosis.

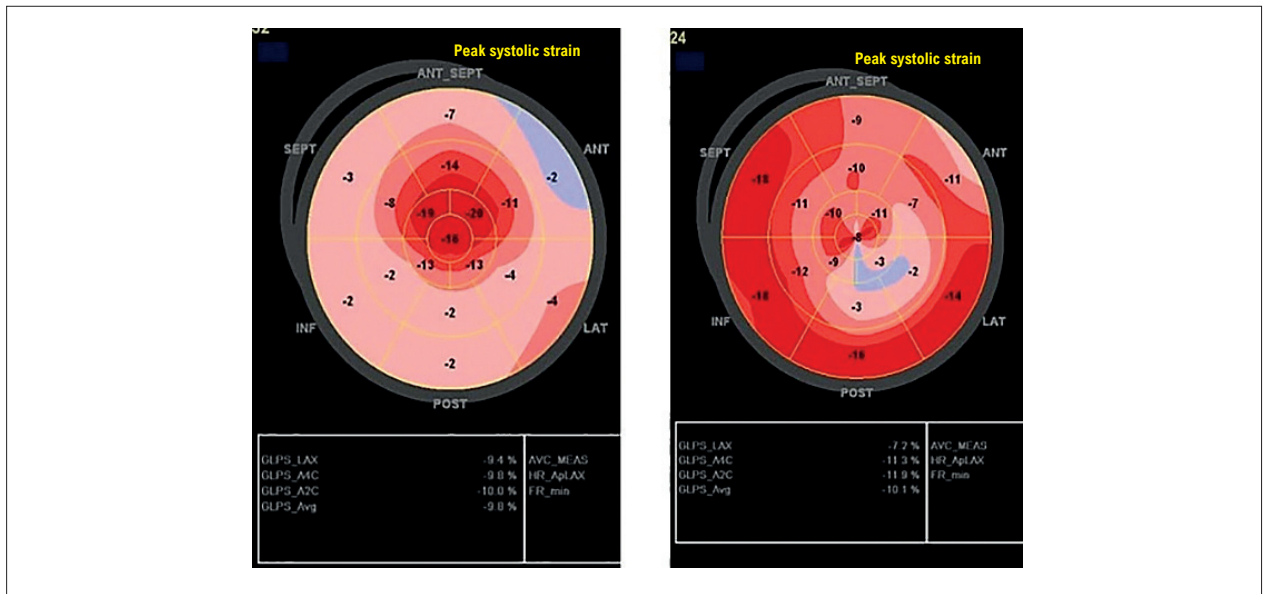


Figure 2.2 – Strain pattern in polar mapping: A: Typical amyloidosis pattern (apical sparing); B: Typical hypertrophic cardiomyopathy pattern with apical predominance (lower strain predominates in the apex, where hypertrophy was more pronounced in 2D assessment).

Myocardial deformation assessment techniques, such as strain, consider the 3 directions of myocardial fiber contraction: longitudinal, radial, and circumferential. LVEF is primarily determined by the radial and circumferential components, which result in thickening of the myocardial walls and reduction of the ventricular cavity in systole. However, LVEF (ie, the “ejective” function) is not the only determinant of ventricular performance: it also depends on adequate LV end-diastolic volume for normal systolic volume. This is why patients with cardiomyopathies involving phenotypic expression of concentric parietal hypertrophy (eg, infiltrative or hypertrophic) can have normal LVEF and low cardiac output. These patients clinically present as HFpEF and, despite normal LVEF, generally have a worse prognosis than patients with normal LVEF and preserved cardiac output due to changes in contractile function detectable only by GLS.³⁰

In fact, longitudinal deformation is the earliest myocardial contractility component to change in most cardiomyopathies and may signal the process at an initial and subclinical stage (prior to reduced LVEF), when therapeutic or cardioprotective measures could have better results. GLS may even be altered in genetic diseases that are not phenotypically expressed, such as Friedreich’s ataxia, which presents with normal mass and LVEF, and might even predict reduced LVEF and its prognosis.³¹

The prognostic value of GLS has been demonstrated in patients with HF, facilitating the prognostic effect of LVEF, especially in patients with EF > 35%.³² For this reason, Potter et al. suggested a new classification of ventricular function, complimenting LVEF with LVGLS to facilitate clinical decision-making and prognostic evaluation, especially in patients with LVEF > 53% (HFpEF).¹⁰

2.3. General Recommendations for Reporting Strain Results and Normality Values

To simplify description in echocardiography reports, the type of strain (which defines the contraction or relaxation movements) should be indicated, as well as its absolute values (mainly in sequential comparative studies) to prevent mistaken interpretations of worsening strain. The patient’s vital signs (blood pressure and heart rate) should also be included, due to preload and afterload changes that influence the overall strain value, in addition to the brand of ultrasound equipment and software version, due to varying normality parameters between the manufacturers.^{33,34} Table 2.1 lists essential information to be included in a complete strain report.⁹

Normal strain reference values^{9,35-39} must be included in the report. Table 2.2 describes simplified average normality values for different strain types, as well as the degree of use in clinical practice. Unlike LVEF, strain normality values have not yet been consistently assimilated in clinical cardiology and, thus, they must be included in the report as a reference.

2.4. Conclusion

Although current evidence for incorporating strain into daily clinical practice is robust, there are still several challenges to doing so in Brazil, such as unequal access to echocardiogram services with analysis software and a lack of national population data. We used values extrapolated from a population with a very different sociodemographic profile, with application adapted for the Brazilian population. The Brazilian Cardiology Society’s Department of Cardiovascular Imaging is promoting a multicentric work (already in progress), when echocardiographic data from healthy Brazilians is being analyzed. Strain adds to normal echocardiogram values, increasing prognostic robustness, enabling the diagnosis of cardiomyopathies (especially those presenting with increased myocardial thickness) and subclinical myocardial injury.

Statement

Table 2.1 – Essential elements for describing strain in echocardiography reports

Relevant Strain Information	Description
Vital signs	Blood pressure and heart rate ¹⁶
Strain type	Longitudinal, circumferential, and radial
Absolute strain value	For describing chamber function
Cardiac chamber	LV, RV, or LA
Polar map pattern (Figure 2.2)	Any typical patterns, such as amyloidosis or hypertrophic cardiomyopathy ⁴⁰
Variation (%) in sequential exams	Proven use in cardio-oncology. $\Delta\%$ = baseline strain examination (current/baseline) ²¹
Equipment and software version	Normal strain values vary according to equipment brand and version ³⁷

$\Delta\%$: percentage (delta) change; LA: left atrium; LV: left ventricle; RV: right ventricle.

Tabela 2.2 – General normality values for different strain and cardiac chamber modalities and applicaiton in clinical practice

Chamber/strain type	Normality value (absolute value)	Application in clinical practice
LV		
Longitudinal (negative)	18% ^{35,39} 20% ³⁵	++++
Radial (positive)	40% ³⁵	+
Circumferential (negative)	20%	+
RV		
Longitudinal free wall (negative)	20% ^{35,36}	+++
LA (varies with age, positive)		
Reservoir (most common)	39% ^{38,39}	+++
Conduit	23% ³⁸	+
Pump	17% ^{38,41}	+

LA: left atrium; LV: left ventricle; RV: right ventricle. ++++ Commonly used; +++ Used; ++ Limited use in clinical practice; + Limited use in clinical practice and not included in echocardiography equipment software.

3. Strain in Cardio-oncology

Cancer treatment-related cardiac dysfunction is an important cause of morbidity and mortality.^{42,43} This complication can interrupt treatment and compromise healing and/or adequate cancer control.^{44,45} HF due to the cardiotoxicity of chemotherapy drugs often has a worse prognosis than many neoplasms, with a 2-year mortality of up to 60%.⁴² Early identification of cardiotoxicity and cardioprotective intervention could affect prognosis in such cases.^{46,47} However, normal diagnostic methods, such as the 2D LVEF, have low sensitivity.^{48,49} Thus, earlier markers, such as strain analysis, could be of great importance.

Diagnostic imaging methods play a fundamental role in such circumstances, and echocardiography has been the

most common tool due to its anatomical correspondence, non-invasive nature, easy access, low cost, and lack of ionizing radiation.²⁷ Two-dimensional LVEF, the most common parameter for diagnosing cardiotoxicity, is calculated using Simpson's method.²¹ However, 3D echocardiography, when available, is the technique of choice for monitoring LVEF in cancer patients. Its main advantages include greater accuracy in recognizing LVEF values below the lower limit of normality and greater reproducibility than the 2D technique, with accuracy similar to cardiac MRI. However, its low availability, high cost, and learning curve prevent more widespread use.^{27,50}

Cancer treatment-related ventricular dysfunction is defined as a > 10% absolute drop in LVEF to < 50%, with or without HF symptoms. This echocardiographic examination should be repeated within 2-3 weeks to assess the effects of preload and afterload on LVEF.

Despite being an important and established prognostic factor, LVEF has low sensitivity for diagnosing cardiotoxicity. LVEF is dependent on certain factors, such as cardiac preload, image quality, and examiner experience. It can underestimate real cardiac damage, since compensatory hemodynamic mechanisms allow adequate LV systolic performance despite myocyte dysfunction.⁴⁸ Thus, reduced LVEF often occurs at a very late stage, when therapeutic intervention does not lead to functional recovery in most cases.^{46,48,49}

When cardiotoxicity is detected and treated early, patients have a greater chance of recovering ventricular function,^{46,51} and myocardial strain analysis can play an important role in this. Determining strain through 2D speckle-tracking has emerged as a sensitive and reproducible means of analyzing systolic function and LV contractility; this method has been validated in both in vitro and in vivo models.^{52,53} A growing number of publications have shown that myocardial strain analysis through 2D speckle-tracking is useful for early and subclinical detection of chemotherapy-induced cardiotoxicity, especially regarding relative decreases in GLS.^{23,54-57}

GLS analysis is recommended for patients who undergo potentially cardiotoxic chemotherapy treatment. A \geq 12% decrease in GLS in relation to baseline suggests a subclinical diagnosis of cardiotoxicity.^{21,27} Without baseline (pre-chemotherapy) values for comparison, expert opinion suggests an absolute strain value of < 17% as a marker of subclinical cardiotoxicity, provided there is no other underlying myocardial disease. GLS reductions < 8% from baseline are considered non-significant. Figure 3.1 presents an example of subclinical cardiotoxicity suggested by relative GLS reduction.

Figure 3.2 presents an algorithm for echocardiographic follow-up in cancer patients based on LVEF and GLS. Figures 3.3 and 3.4 present echocardiographic monitoring data in patients treated with anthracyclines and trastuzumab, respectively.

SUCCOUR was the first prospective multicenter trial to show the prognostic impact of GLS-based cardioprotection compared to LVEF (3D echocardiography)-based

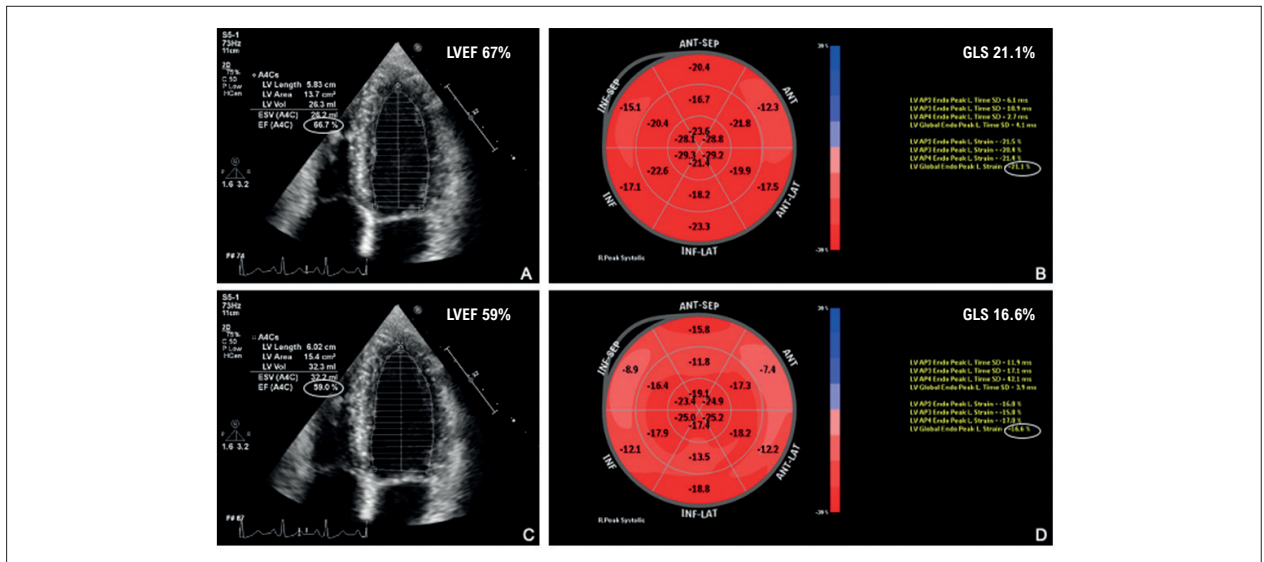


Figure 3.1 – Example of subclinical cardiotoxicity in a patient with breast cancer. Analysis of LVEF through Simpson’s method and GLS with bull’s eye mapping. A and B: pre-chemotherapy evaluation; B and C: evaluation after a cumulative dose of 240 mg/m² of doxorubicin. Although there was no significant reduction in LVEF, there was a 22% relative decrease in GLS. LVEF: left ventricular ejection fraction; GLS: global longitudinal strain.

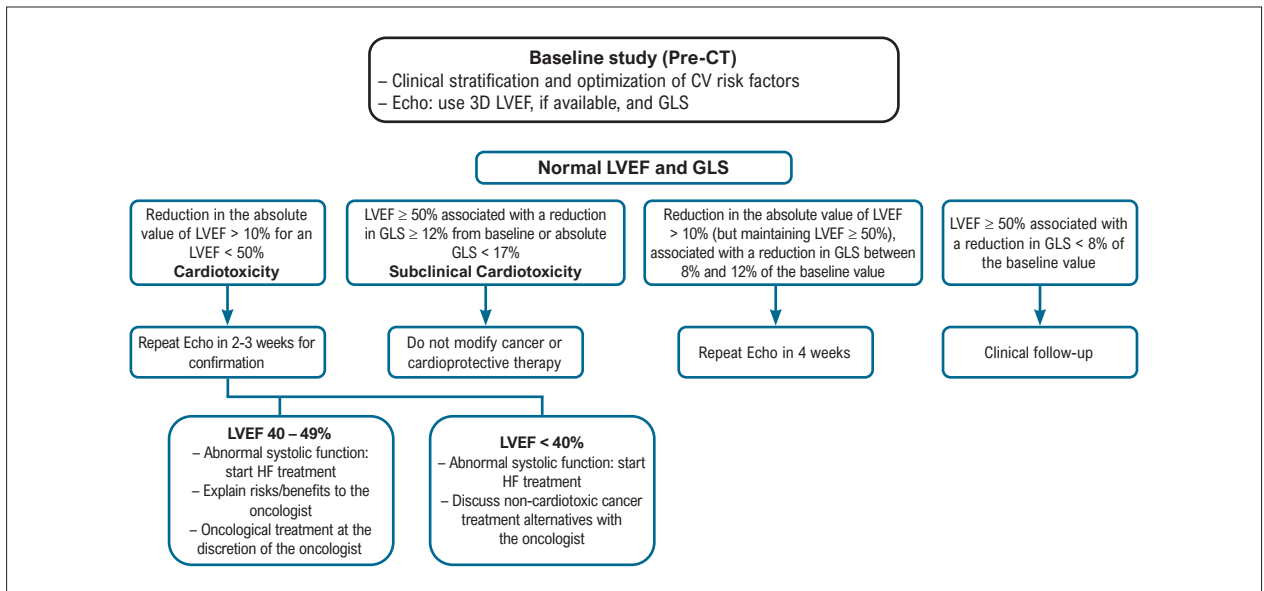


Figure 3.2 – Algorithm for evaluating cancer patients during chemotherapy treatment, based on LVEF and GLS. ACE: angiotensin-converting enzyme; CV: cardiovascular; CT: chemotherapy Echo: echocardiography; GLS: global longitudinal strain; HF: heart failure; LVEF: left ventricular ejection fraction.

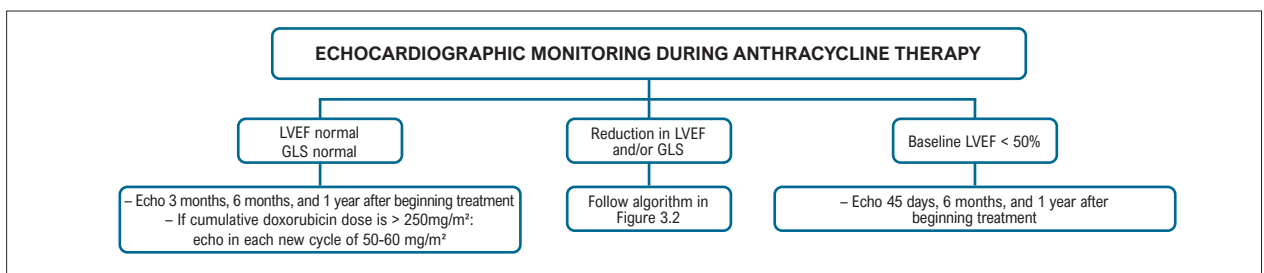


Figure 3.3 – Echocardiographic monitoring during anthracycline therapy. Echo: echocardiography; GLS: global longitudinal strain; LVEF: left ventricular ejection fraction.

Statement

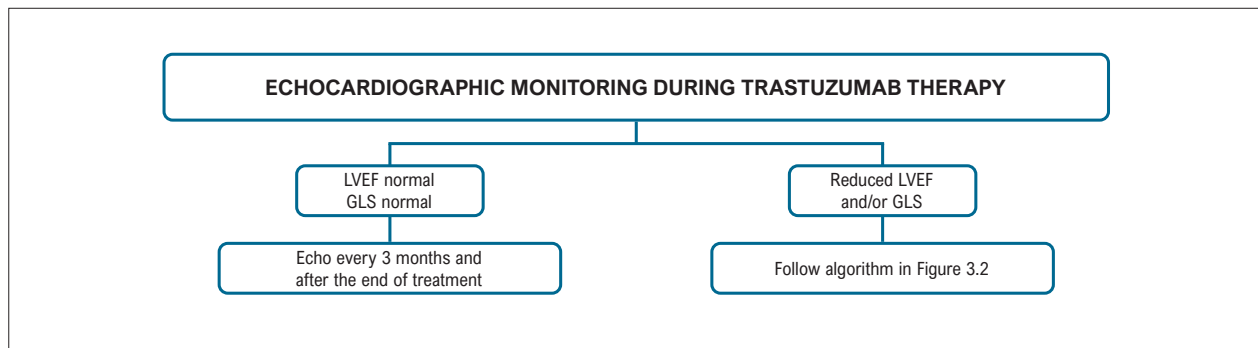


Figure 3.4 – Echocardiographic monitoring during trastuzumab therapy. Echo: echocardiography. GLS: global longitudinal strain; LVEF: left ventricular ejection fraction.

Table 3.1 – Relevant Clinical and Oncological Information in Echocardiography Reports

Time between chemotherapy drug infusion and echocardiography (pre- or post-)
Heart rate
Blood pressure
Volume status (description of the diameter and variation of the inferior vena cava)
Comparison with baseline, especially left ventricular ejection fraction and GLS: if there is a relative decrease, report the percentage)
Equipment/software used for GLS analysis

GLS: global longitudinal strain.

cardioprotection. In patients receiving anthracycline-based chemotherapy (ie, at high risk of cardiotoxicity), cardioprotective intervention (ACE inhibitors and beta-blockers) based on a $\geq 12\%$ reduction in GLS relative to baseline resulted in smaller LVEF reductions and a lower incidence of cancer treatment-related cardiac dysfunction over 1 year of follow-up.⁵⁸

Compared to 2D speckle tracking, calculating strain through 3D tracking has shown technical advantages regarding accuracy, reproducibility, and applicability in different contexts.⁵⁹⁻⁶² Recently, small studies have demonstrated the impact of 3D speckle-tracking on early recognition of chemotherapy-related mechanical changes.⁶³⁻⁶⁶ However, larger studies with longer follow-up are needed to assess this technique's prognostic value.

Nevertheless, GLS analysis has certain limitations, among which we highlight measurement variability among equipment manufacturers. Thus, measurements must always be performed on the same devices. Like LVEF, GLS is influenced by preload and afterload effects, ventricular geometry, tissue changes (eg, infarction and myocarditis) and conduction disorders. Finally, certain clinical and oncological information is essential and must be clear in the echocardiography report for accurate interpretation, as shown in the Table 3.1.

4. Strain in Diastolic Dysfunction

4.1. Introduction

DD is considered an early marker of myocardial damage and, even when asymptomatic, it has high mortality rates. As DD increases, LV filling pressures and HFpEF increase.^{67,68} The latter accounts for more than 50% of HF hospitalizations, with mortality rates comparable to those of HFrEF.⁶⁹ Unlike HFpEF, preclinical DD may be reversible. However, its pathophysiology is complex and, despite involving several parameters, the currently recommended algorithm is not very sensitive for subclinical stages.^{70,71}

Indeterminate cases are also frequent since these parameters do not always change simultaneously or linearly.⁷⁰ Non-diastolic factors can also contribute to HFpEF, leading to varied phenotypic expression depending on the predominant pathophysiological mechanism.⁷² Tools that assess LV and left atrial (LA) mechanics by measuring strain can overcome these diagnostic challenges.^{73,74} The role of RV mechanics in this context is still under investigation.⁷⁵

4.2. Left Ventricle Strain

Several studies have shown that myocardial strain parameters evaluated through speckle tracking, especially LVGLS, have a better correlation with LV relaxation and more accurately predict filling pressures and exercise intolerance than those derived from tissue Doppler.⁷⁶⁻⁷⁸ Reduced LVGLS helps detect DD at earlier stages and also predicts cardiovascular events in HFpEF.^{17,79-82} In light of this evidence, reduced LVGLS ($<16\%$) has already been included as a diagnostic criterion in a new algorithm in recent HFpEF guidelines.⁸³

4.3. Left Atrial Strain

LA strain allows for a more detailed analysis of LA function and its various components (reservoir, conduit, and pump function).⁷⁰ Changes in LA strain express ventriculoatrial coupling and result from chronic exposure to elevated LV pressure, and reductions in LA compliance and relaxation,^{41,84,85} which may precede morphological remodeling.⁸⁶⁻⁸⁸ Although reductions in all LA strain

components has been described,^{86,89,90} the reservoir LA strain is the most robust parameter, changing linearly with DD progression.⁹¹⁻⁹³ Morris et al, among other authors, demonstrated that reduced reservoir LA strain (< 23%) increased DD detection and correlated with filling pressures and clinical outcomes.⁹³⁻⁹⁹

Due to the growing evidence, LVGLS and LA reservoir strain could be integrated into the current DD algorithm, as proposed in the Central Figure. This strategy may help reclassify indeterminate cases and increase accuracy in identifying earlier stages of DD, especially in individuals with cardiovascular risk factors or unexplained dyspnea.⁹⁷

Standardization of strain methodology has helped minimize variability between manufacturers, which is still a limitation.^{7,92,100,101} New prospective multicenter studies are expected to determine whether modifying these indices with treatment can improve DD and HFpEF prognosis.

4.4. Conclusion

LVGLS and LA reservoir strain are subclinical disease markers that can be incorporated into current recommendations to refine the diagnosis, staging, and prognosis of DD. Considering the complex nature of such assessments, using artificial intelligence to validate and implement algorithms would be beneficial.

5. Strain in Cardiomyopathies

5.1. Introduction

Generally speaking, cardiomyopathies are disorders of the heart muscle. Strictly speaking, they are not associated with certain conditions known to be aggressive to the myocardium, such as coronary artery disease, arterial hypertension, valvular heart disease, and congenital heart disease. They can be divided into the following groups: dilated, hypertrophic, restrictive, arrhythmogenic cardiomyopathy, and “unclassified”.¹⁰²

5.2. Dilated Cardiomyopathy

Dilated cardiomyopathy is a disease that, by definition, affects myocardial tissue and leads to a progressive reduction in systolic function and dilation of the LV cavity. Clinically, individuals may present signs and symptoms of HF, requiring treatment, hospitalization, and finally, heart transplantation.¹⁰²⁻¹⁰⁷

Echocardiography, part of the first-line diagnostic arsenal, plays an extremely important role in diagnosis and prognosis. Its main objectives are to determine the volume of the cardiac chambers and assess LV systolic performance. This usually involves estimating the EF, which should be done according to Simpson’s method. Strain assessment is an additional echocardiographic tool that can enrich this process. It allows detection of subtle, subclinical abnormalities in the early stages of disease.

Abduch et al. found excellent correlation between volumetric parameters obtained by 3D echocardiography and strain assessment in patients with dilated cardiomyopathy.¹⁰⁸ Since the clinical course of dilated cardiomyopathy leads to more pronounced phases of LV systolic impairment, there will be greater reductions in strain and strain rate in the longitudinal, radial, and circumferential components Figure 5.1.¹⁰⁹ LV torsion also follows this downward trend with disease progression. Additionally, in very advanced stages, the rotations may also be inverted, ie, basal segments rotating counterclockwise and apical segments rotating clockwise.¹¹⁰⁻¹¹²

GLS is an independent predictor of all-cause mortality in patients with HFrEF, especially men without AF.¹¹³ In patients with recovered LVEF, abnormal GLS predicts the likelihood of decreased LVEF during follow-up, whereas normal GLS predicts the likelihood of stable LVEF during recovery.¹¹⁴

5.3. Arrhythmogenic Cardiomyopathy

Arrhythmogenic cardiomyopathy is histologically characterized by fibrofatty infiltration in the myocardial tissue. Although this infiltration generally occurs in

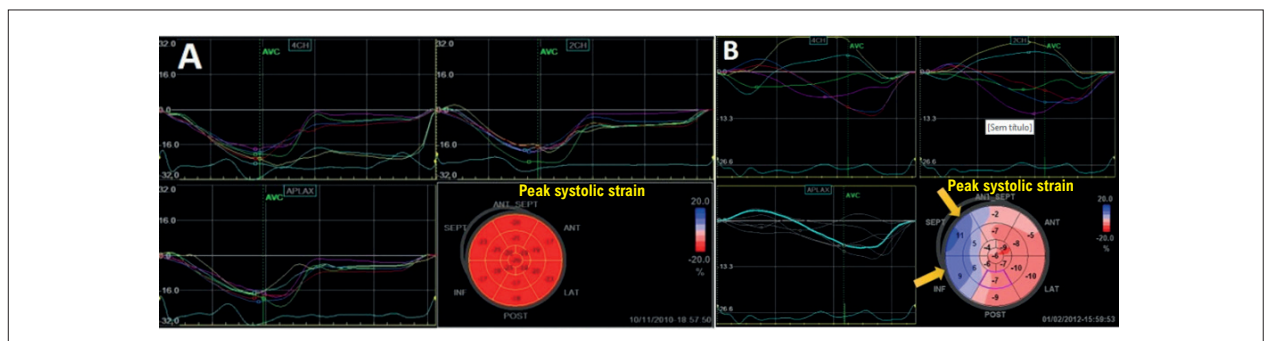


Figure 5.1 – A) Example of normal left ventricle global longitudinal strain. Note the negative deflections of the curves, which are relatively homogeneous in the 3 views. In the lower right is the parametric bull’s eye mapping, with all fields in more intense red, indicating good global strain; **B)** Example of strain in an individual with dilated cardiomyopathy due to Chagas disease. Note the reduced amplitude of the curves, which are also very heterogeneous. The septal and inferior wall strain curves have a positive deflection, ie, indicating distension or dyskinesia, which in the bull’s eye map appears blue (yellow arrows), in addition to pink areas, which indicate low strain values (GLS = -5.6%).

Statement

the entrance, exit, and apex of the RV (the “dysplasia triangle”), the LV can also be affected concomitantly or even exclusively.¹¹⁵⁻¹¹⁷

Macroscopically, the ventricular wall tends to thin and forms microaneurysms, progressing to systolic impairment and cavity dilation. The gold standard diagnostic method is cardiac MRI, although echocardiography is the initial examination. RV free wall strain assessment can help determine systolic impairment in this cavity.

In 2007 Prakasa et al. were the first to analyze strain in RV dysplasia/cardiomyopathy, finding a consistent difference in strain values between diseased (10% [SD 6%]) and healthy individuals (28% [SD 11%], $P = 0.001$).¹¹⁸

RV free wall LS is associated with the rate of structural progression in patients with arrhythmogenic cardiomyopathy. It can be a useful marker for determining which patients require closer follow-up and treatment. Patients with RV strain $< 20\%$ have a higher risk of structural progression (odds ratio: 18.4; 95% CI, 2.7-125.8; $P = 0.003$).¹¹⁹

Patients with arrhythmogenic cardiomyopathy have reduced right atrial (RA) strain in all diastole phases, even when the RA volume is normal. RA strain, obtained during the reservoir and pump phases, is associated with a greater risk of cardiovascular events.¹²⁰

5.4. Hypertrophic Cardiomyopathy

HCM, an autosomal dominant disease, is the most common heart disease of genetic etiology. It is characterized by increased ventricular myocardial thickness of different morphologies (concentric, apical, or septal, hypertrophy of the LV free wall and RV) and is related to increased morbidity and mortality in affected patients.¹²¹⁻¹²³

Echocardiography is the most common imaging method for morphological and hemodynamic diagnosis. About 25% of these patients have an LV outflow tract gradient > 30 mm Hg at rest, which can be quantified by continuous Doppler.¹²⁴ The gradient, which may be dynamic in these patients, can be better evaluated echocardiographically either using the Valsalva maneuver or through physical or pharmacological stress with dobutamine.¹²⁵ A high intraventricular gradient in HCM may be a determinant of decreased myocardial deformation and torsion mechanisms, as well as LA strain.¹²⁶

Myocardial strain measured through speckle-tracking helps clarify regional and global cardiac mechanics in HCM and can detect early changes in systolic function, fibrosis, and a greater risk of arrhythmia, even in patients with normal systolic function.¹²⁶⁻¹³⁰ Polar mapping helps differentiate phenocopies that lead to increased thickness and reduced longitudinal myocardial strain at the site of hypertrophy^{20,131,132} (Figure 5.2).

Hiemstra et al. found that indexed LA volume and LVGLS were independent prognostic factors for adverse outcomes, such as sudden death and heart transplantation, as well as independent GLS values $> 10\%$.¹³³ Although RV global longitudinal strain (RVGLS) may be altered in HCM

patients due to structural heart disease, its prognostic significance is unknown.^{133,134}

5.5. Endomyocardial Fibrosis

Endomyocardial fibrosis is the most common restrictive cardiomyopathy in tropical climates, affecting approximately 10 million people worldwide. It is characterized by subendocardial fibrosis of the apices and inflow tracts of one or both ventricles. Its etiology, which is still unknown, may be related to hypereosinophilia, parasitic infestations, or protein malnutrition, especially in populations of low socioeconomic status.

Echocardiography will show ventricles of normal or reduced size with “mushroom” or “V” ventricular morphology due to fibrosis, which may be associated with apical endocardial thrombosis, hyperkinesis of the basal portion of the LV (Merlon sign), greatly increased atrial volume, often preserved ventricular systolic function, and DD.¹³⁵⁻¹³⁷

Although few studies have assessed endomyocardial fibrosis using 3D echocardiography with speckle-tracking, they have found reduced GLS, especially with more severe apical involvement.^{137,138}

5.6. Noncompacted Myocardium

Noncompacted myocardial tissue is characterized by prominent trabeculae and deep intertrabecular recesses due to incomplete compaction during embryonic life. This can lead to a clinical picture of HF, arrhythmias, and thromboembolic events. Existing in sporadic and familial forms, the latter are related to sarcomere protein mutations. Myocardial strain indices allow a proper



Figure 5.2 – A) Two-dimensional image demonstrating non-obstructive asymmetric septal hypertrophy, with an interventricular septum measuring 23 mm and a posterior wall measuring 11 mm; B) normal global longitudinal strain (GLS) of the LV (20%), with parametric bull's eye mapping segments with good myocardial strain are darker red, while pink indicates lower strain values in the septal segments (8%); C) 4-chamber view, with lower myocardial strain in the middle and basal inferoseptal segments; D) note the reduced amplitude of the curves representing septal segments, also shown in pink in the bull's eye map, representing lower strain values (8%).

regional analysis of ventricular function in patients with noncompacted myocardium and help differentiate it from other forms of HCM.

An Indian study compared the myocardial strain in 12 patients with noncompacted myocardium, 18 patients with HCM, and 18 healthy controls. Both patient groups had reduced LS, although it was lower in the apical region in the noncompacted myocardium group than the HCM group (12.18 [SD, 6.25] vs 18.37 [SD, 3.67]; $p < 0.05$), suggesting that this region was more involved in myocardial noncompaction. Furthermore, an apical-basal gradient in LS was observed in noncompacted myocardium but not HCM.¹³⁹ DD was found in both patient groups. Another study found greater LS in a LV non-contraction group than a non-specific dilated cardiomyopathies group, reporting that the base-apex mid-wall gradient of strain is a useful index for differentiating these diseases (sensitivity: 88.4 %; specificity: 66.7%).¹⁴⁰

In normal hearts, the base rotates clockwise during systole, while the apex rotates counterclockwise, with torsion being the apical minus basal rotation. A study found that 50% of patients with noncompacted myocardium have rigid body rotation, with clockwise rotation of the apex and base, although others have found prevalences of 53.3% and 83%.^{141,142} A study of 28 children with noncompacted myocardium found that 39% had rigid body rotation. This group had lower LS, but not LVEF than those without rigid body rotation, which may have prognostic value.¹⁴³ These authors also suggested that rigid body rotation may be related to dysfunction of the compacted subepicardial apical layer and unrelated to trabeculae distribution. Another study of 101 children with noncompacted myocardium found that the adverse outcome group had lower longitudinal, radial, and circumferential strain, which suggests that this disease affects the heart globally rather than just the non-compacted region.¹⁴⁴

6. Strain in Valvular Heart Disease

Due to its combined analysis of changes in anatomy and valve function, transthoracic Doppler echocardiography is the first-line method for diagnosing valvular heart disease and classifying its severity.¹⁴⁵ This method helps define the best intervention type and time point for treating valvular heart diseases.

Classically, treatment is based on symptoms and complicating factors,¹⁴⁵ with LV dysfunction considered the most important complicating factor.¹⁴⁵ LV function is usually determined through echocardiographic LVEF measurement.¹⁴⁶

However, there is evidence that LV strain can identify ventricular dysfunction before EF decreases. Perhaps mitral regurgitation can best represent this paradox, since in this condition the high preload and low afterload mean that EF does not adequately represent LV systolic function. For this reason, the definition of LV dysfunction in this condition is quite conservative in clinical guidelines.^{145,147-149} However, some studies have indicated that even with these parameters, clinical outcomes after surgical correction

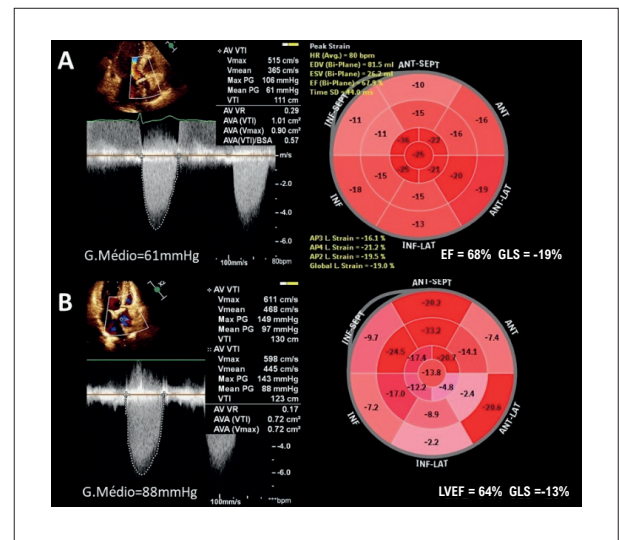


Figure 6.1 – Two patients with classic severe high-flow aortic valve stenosis with normal left ventricular ejection fraction (LVEF) but very different global longitudinal strain (GLS) values. (A) Mean aortic transvalve gradient = 61 mm Hg, with normal EF and GLS. (B) Mean aortic transvalve gradient = 88 mm Hg, with normal EF and reduced GLS.

of mitral regurgitation may not be satisfactory, especially regarding EF reduction and the presence of HF.¹⁵⁰⁻¹⁵¹ Thus, studies have shown that even in patients with an EF $> 60\%$ and an LV end-systolic diameter < 40 mm, reduced GLS ($\leq 19\%$) is associated with a postoperative EF $< 50\%$.¹⁵²⁻¹⁵⁴ GLS $< 18.1\%$, has also been associated with higher mortality and more cardiovascular events in a prospectively followed cohort of mitral regurgitation patients who underwent corrective surgery.¹⁵⁵

In aortic insufficiency, valvular heart disease severity has been correlated with decreased LV strain.¹⁵⁶ Furthermore, in patients with asymptomatic severe chronic aortic insufficiency and preserved EF, GLS $< 19\%$ was associated with higher mortality over time, which was corrected through valve replacement.¹⁵⁷ In the same group, postoperatively, GLS $< 19\%$ or a $> 5\%$ drop in GLS was correlated with higher mortality.¹⁵⁸

In severe aortic stenosis, EF $< 50\%$ and/or symptoms have been the standard factors for indicating treatment.^{145,147-149} However, waiting for the LVEF to drop $< 50\%$ before indicating aortic surgery can lead to unsatisfactory clinical outcomes.¹⁵⁹ Thus, a robust parameter for detecting subclinical myocardial dysfunction, such as GLS, would be a valuable tool in risk stratification (Figure 6.1). While LVEF cannot be used to distinguish between degrees of aortic stenosis, GLS decreases linearly with disease progression,¹⁶⁰ leading to a higher risk of adverse clinical outcomes, even in asymptomatic patients.¹⁶¹

Several studies have examined the prognostic value of GLS for predicting mortality and cardiovascular events in asymptomatic individuals with aortic stenosis and preserved LVEF to determine which ones should receive early valve intervention.¹⁶²⁻¹⁶⁴ In a meta-analysis of these studies, GLS

Statement

< 14.7% was the cut-off for higher mortality risk (sensitivity 60% and specificity 70%; area under the curve [AUC] = 0.68).¹⁶⁵ GLS < 14.7% was found in approximately one-third of the patients with moderate-to-severe aortic stenosis and preserved LVEF, resulting in a 2.6 times higher mortality risk. Of note, the relationship between GLS and mortality was significant in patients with LVEF 50%-59% as well as in those with LVEF \geq 60%. In contrast, GLS > 18% was associated with an excellent clinical outcome (97% [SD, 1%]; 2-year survival). Therefore, together with other clinical and echocardiographic data, reduced GLS, despite preserved LVEF, must be considered a strong prognostic predictor in clinical decision making about asymptomatic severe aortic stenosis.

7. Strain in Ischemic Heart Disease

7.1. Introduction

Echocardiography is an excellent tool in emergency departments for diagnosing acute coronary syndrome and its complications, providing information about the patient's short- and long-term prognosis. Its role is well defined in risk stratification for stable coronary artery disease and in myocardial viability assessment.

Two-dimensional echocardiography with strain assessment through 2D speckle tracking can add information without greatly extending the examination time. It accurately assesses subendocardial ischemia through LS in acute and chronic events.

This chapter will review all indications for longitudinal, circumferential, and radial strain in ischemic heart diseases, as well as other data involved in calculating strain, such as mechanical dispersion. Table 7.1 shows the main indications for strain assessment in ischemic heart disease.

7.2. Strain in Acute Coronary Syndrome

Two-dimensional strain assessment has good sensitivity for detecting myocardial ischemia. It is considered more reproducible than LVEF and its accuracy has been confirmed in cardiac MRI.^{52,166} Subendocardial fiber is more sensitive to the initial stages of ischemia, with the longitudinal component predominating in this type.¹⁶⁷ GLS is reduced in acute myocardial infarction (AMI) and correlates with the extent of the infarction, EF, adverse events, and response to reperfusion strategies.¹⁶⁸⁻¹⁷²

Patients with small infarcts have reduced global and radial strain, while circumferential and twist strain remain preserved. However, circumferential strain is compromised in transmural infarction.¹⁷³

Identifying the extent of transmural infarction is important, since it is associated with poor prognosis and adverse events. Subendocardial and non-transmural infarcts are associated with recovery after revascularization (Figure 7.1).¹⁷⁴

A strain value of 15% correlates with segmental changes (76% sensitivity and 95% specificity).¹⁶⁸ At a cutoff of 16.5%, radial strain differentiates transmural from non-transmural

infarctions (70% sensitivity and 71.2% specificity), while circumferential strain < 11% differentiates transmural from non-transmural infarctions (70% sensitivity and 71.2% specificity),¹⁷⁵ and 4.5% regional LS distinguishes transmural from non-transmural infarctions (81.2% sensitivity and 81.6% specificity).^{176,177}

Another important diagnostic benefit of GLS is that it can help determine the culprit artery in non-ST-elevation acute coronary syndromes. In a cohort of 58 patients, 33 with significant coronary artery disease (lesion > 50% determined through coronary angiography) who underwent strain analysis prior to the procedure, a cut-off of 19.7% could detect acute coronary disease (sensitivity 81%, specificity 88%, AUC = 0.92). A cut-off of 21% could exclude significant coronary stenosis in 100% of the patients. Regional LS was calculated as the mean systolic peak strain of each segment in the region of the studied vessel. If a cut-off of 21% were applied to the sample, 16 patients would have been spared from coronary angiography.^{178,179}

Table 7.1 – Main applications of strain assessment in ischemic heart disease

Strain indications in ischemic heart disease
Assessing segmental and global change
Differentiating subendocardial and transmural infarcts (longitudinal, radial, and circumferential change)
Determining the culprit artery according to "bull's eye" mapping
Assessing improvement in global and segmental strain after myocardial revascularization
Improving detection of coronary artery disease
Predicting outcomes and remodeling after acute myocardial infarction
Predicting outcomes, such as hospitalization for heart failure and all-cause mortality
Identifying patients at risk of arrhythmia

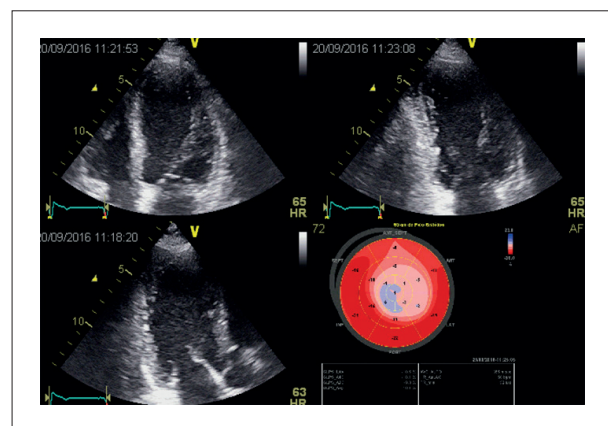


Figure 7.1 – Two-dimensional bull's eye mapping showing strain in the apical region of the left ventricle; the reduced segmental values are compatible with injury in the anterior descending artery.

Strain analysis can help detect acute coronary occlusion in patients without ST elevation who may benefit from early reperfusion therapy. One study evaluated 150 patients who underwent an echocardiographic examination prior to referral for coronary angiography, finding that 33 had an acute coronary occlusion. Although strain $< 14\%$ identified acute coronary occlusion with 85% sensitivity and 70% specificity, more robust studies are needed to validate the technique.¹⁸⁰

Strain analysis has emerged as a new technique for detecting subclinical segmental and global changes. Alongside enzymatic tests, electrocardiography, and risk scores, it enhances the prognostic evaluation of patients with acute coronary disease. This quick examination can be performed at bedside prior to coronary angiography, especially by trained echocardiographers. The above-mentioned studies on non-ST-elevation acute coronary syndromes indicate the technique for assessing segmental alterations and global ventricular function, differentiating small and transmural infarctions, determining the likely culprit artery, and for evaluating percutaneous revascularization outcomes. It can also be used to assess myocardial viability after an AMI.^{181,182}

7.3. Strain in Chronic Coronary Syndromes

The subendocardial region, in which the fibers are oriented longitudinally, is the most susceptible area to ischemia. Thus, assessing LS with 2D speckle-tracking could be a better method of detecting ischemia in this region than conventional echocardiography.¹⁸³

Interaction between normal and abnormal myocardium generates typical regional myocardial strain patterns, indicating that myocardial contraction and myocardial strain are not interchangeable parameters.^{16,184}

Since it assesses longitudinal LV function, GLS may be much more sensitive than LVEF for early detection of myocardial ischemia, although its specificity is not better than changes in wall mobility.^{185,186}

The variability of regional strain measurements in speckle tracking is relatively high, which makes these assessments less suitable for routine use. However, GLS measurements have proven reproducible and robust, probably due to being largely automated.¹⁸⁷ The other change is regional heterogeneity of myocardial activation, which affects the temporal sequence of myocardial contraction and relaxation.

In ischemia, not only is the amplitude of contraction reduced, but the beginning and duration of fiber contraction change, which leads to characteristic shortening or thickening of the myocardium after aortic valve closure.¹⁸⁷ This "post-systolic shortening" is characteristic of ischemia, although it can also occur in any type of regional dysfunction (scarring, dyssynchrony, etc.).^{187,188} Post-systolic shortening can be understood as a signal to delay relaxation so that the ischemic region can shorten while the LV pressure reduces and the surrounding tissue relaxes.¹⁶ In healthy hearts, less post-systolic shortening with normal systolic function is a frequent finding (30%-40% of myocardial segments) and

can be found mainly at the apex and base of the inferior, septal, and anteroseptal walls.^{16,189} In the context of ischemic cardiomyopathy, temporal evaluation of the GLS curve pattern is important, since ischemic segments can often have preserved peak systolic values but are temporally delayed in relation to non-ischemic segments.

It should be pointed out that regional LS measurements do not necessarily align visually with contraction changes, which involve radial thickening and endocardial movement into the cavity.¹⁶

GLS can help detect coronary artery disease in patients with stable angina (stenosis $\geq 70\%$), having reduced values in the presence of coronary artery disease (17.1 [SD 2.5%] vs 18.8 [SD 2.6%]; $p < 0.001$), especially when associated with exercise testing. It can also determine which artery has likely been affected.¹⁸³ LS and (especially) strain rate can detect segmental changes in the late post-myocardial infarction period with higher sensitivity and accuracy.¹⁸⁹

In stratifying post-AMI patients, GLS $< 15\%$ prior to hospital discharge was an independent predictor of LV dilation in 3-6 months of follow-up, in addition to indicating the size of the infarct area.¹⁹⁰ In the same context, GLS $< 14\%$ was an independent predictor of cardiovascular death and hospitalization due to HF.¹⁹¹ In stable chronic patients, GLS $< 11.5\%$ was a predictor of all-cause mortality and the combined outcome (all-cause mortality and hospitalization for HF).¹⁹²

Heterogenous regional myocardial contraction can also be assessed by mechanical dispersion, which is the standard deviation of the time to maximum myocardial shortening across all LV segments. This index has a predictive value for ventricular tachyarrhythmia in post-infarction patients. Mechanical dispersion was higher in patients with recurrent arrhythmias after AMI than in those without them (85 [SD, 29] ms vs 56 [SD, 13] ms, $p < 0.001$).¹⁹³

7.4. Right Ventricular Strain in Ischemic Heart Disease

RV function is compromised in approximately one-third of inferior wall infarctions, and its involvement has been described as an important predictor of hospital mortality and major complications. Assessing RV function is challenging due to its structural complexity. RV free wall strain has been shown to predict proximal right coronary artery occlusion in patients with inferior wall AMIs (RV free wall strain $< 14.5\%$, AUC = 0.81; $p < 0.001$).¹⁹⁴

In the stable phase of chronic ischemic disease, RV free wall strain is altered in patients with right coronary stenosis (lesions $> 50\%$) and can be used to detect subclinical dysfunction.¹⁹⁵

8. Strain Assessment in Systemic Diseases (Amyloidosis and Fabry Disease)

8.1. Strain Assessment in Cardiac Amyloidosis

Amyloidosis is a systemic disease caused by extracellular deposition of insoluble amyloid fibrils in tissue. Cardiac

Statement

involvement is an important prognostic factor and has a great impact on quality of life, occurring more commonly in light chain amyloidosis and transthyretin amyloidosis.¹⁹⁶

Echocardiography is a first-line method for diagnosis and prognostic evaluation of cardiac amyloidosis (CA) and other infiltrative heart diseases. Most classic echocardiography findings and more specific signs of CA only occur at very advanced stages.³⁰ Clinical conditions such as HFpEF and ventricular hypertrophy may be warning signs for CA.¹⁹⁷

8.1.1. Myocardial Strain Assessment in the Diagnosis of Cardiac Amyloidosis

The consistent LVGLS changes in patients with CA are directly related to the degree of amyloid infiltration, which is quantified in MRI through the degree of delayed gadolinium enhancement and extracellular volume calculated in T1 imaging.³⁰ A relative apical sparing pattern of LS has been described in the literature, characterized by a basal-apical gradient (“cherry-on-top” pattern) (Figure 8.1).

Phelan et al., originally calculated relative apical sparing with the following equation: mean apical LS/(mean LS of the middle segments + mean LS of the basal segments). Values > 1.0 had good accuracy in diagnosing CA and differentiating it from ventricular hypertrophy due to aortic stenosis and HCM (AUC: 0.94).²⁰

This regional LS pattern, with its basal-apical gradient, is indistinct in immunoglobulin light chain amyloidosis and transthyretin amyloidosis. It should be pointed out that the classic apical sparing pattern, although generally characteristic of CA, may be absent, as reported by Ternacle et al., who found that 52% of CA patients had “non-diagnostic” relative apical sparing (< 1.0).¹⁹⁸ In some cases, this could be explained by a low degree of amyloid infiltration in the myocardium in very early stages of the disease. LS > 2.1 in the basal and apical regions of the septum associated with a mitral inflow deceleration time < 200 ms also accurately differentiated CA from other diseases involving LV hypertrophy and a parietal phenotype, such as Fabry disease, Friedreich's ataxia, and LV hypertrophy related to systemic arterial hypertension.¹⁹⁹

An LVEF/GLS ratio > 4.1 accurately differentiated CA from HCM, performing better than relative apical sparing or LS in the basal and apical regions of the septum, regardless of CA type.²⁰⁰ RV myocardial strain is generally reduced in CA patients, and it may help differentiate CA from other causes of parietal hypertrophy (Figure 8.2). A relative apical sparing pattern has also been found, similar to what has been described in the LV.²⁰¹ Bellavia et al. demonstrated that RV changes can occur early in patients with immunoglobulin light chain amyloidosis, even in cases where LV parietal thickness is still normal.²⁰²

In CA, like other infiltrative cardiomyopathies, other myocardial strain components may be significantly compromised, such as circumferential strain,²⁰³ radial strain,²⁰⁴ and twist (Figure 8.3). In early-stage systemic amyloidosis with no evidence of CA, twist and untwist may be increased in compensation,²⁰⁵ with these parameters progressively

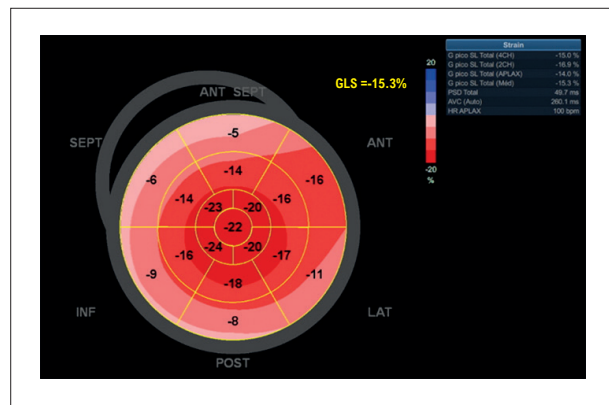


Figure 8.1 – Longitudinal 2D strain of the left ventricle in a patient with cardiac transthyretin amyloidosis, showing relative apical preservation (apical sparing pattern), with lower strain in the middle and basal segments and higher strain in the apical segments.

deteriorating during the clinical course of the disease.²⁰⁶ In advanced cases, the cardiac base and apex may rotate in the same direction, creating a pattern called “rigid body rotation”, in which the important contribution of cardiac torsion to ventricular mechanics is completely lost.

LA strain often undergoes significant change in CA, due partially to LV DD but also to direct amyloid fibril infiltration in the atrial wall (Figure 8.4). In a recent study by Aimo et al., only peak atrial LS (in addition to classic echocardiographic variables and cardiac biomarkers) was independently associated with CA diagnosis.²⁰⁷ It was also found that advanced atrial infiltration could cause severe dysfunction and loss of mechanical efficiency, leading to atrial electromechanical dissociation.²⁰⁸ In a large cohort, Bandera et al. found atrial electromechanical dissociation (determined by LS analysis) in 22.1% of the patients in sinus rhythm, which was a determining factor for poor prognosis compared to patients in sinus rhythm with preserved atrial mechanical function.²⁰⁹ In a Mayo Clinic series of 156 CA patients, intracardiac thrombi were detected by transesophageal echocardiography in 27%,²¹⁰ which has been reproduced in other studies, with thrombi occurring even in patients in sinus rhythm (Figure 8.5).^{211,212}

Three-dimensional strain assessment can help demonstrate changes in all components of myocardial strain in patients with CA. Vitarelli et al. found that LV peak basal rotation and RV and LV basal LS could accurately distinguish CA from other ventricular hypertrophies.²¹³ In 3D echocardiography LS, Baccouche et al.²¹⁴ found the same apical sparing pattern, with a characteristic basal-apical gradient.

Myocardial work (MW) has also been assessed in patients with CA. Clemmensen et al. found that patients with CA had a lower left ventricular myocardial work (LVMW) index than the control group, with more pronounced changes in basal segments and when undergoing stress echocardiography. The LVMW index from rest to peak exercise increased 1974 mm Hg% in controls (95% CI, 1699-2250 mm Hg%; $P < 0.0001$) but only 496 mm Hg% in CA patients (95% CI, 156-835 mm Hg%; $P < 0.01$).²¹⁵

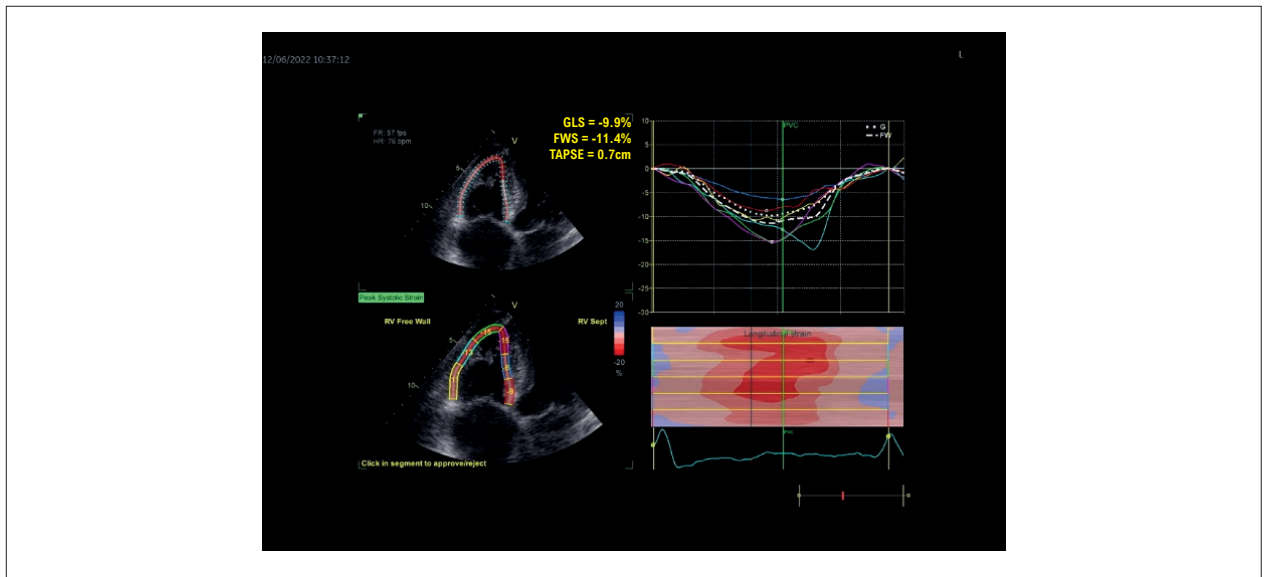


Figure 8.2 – Longitudinal 2D strain assessment in the right ventricle of a patient with cardiac transthyretin amyloidosis, showing a lower absolute global value (RVGLS = 9.9%) and an absolute reduction in mean free wall strain (FWS) (11.4%), with lower values in middle and basal segments and higher values in apical segments. TAPSE: tricuspid annular plane systolic excursion.

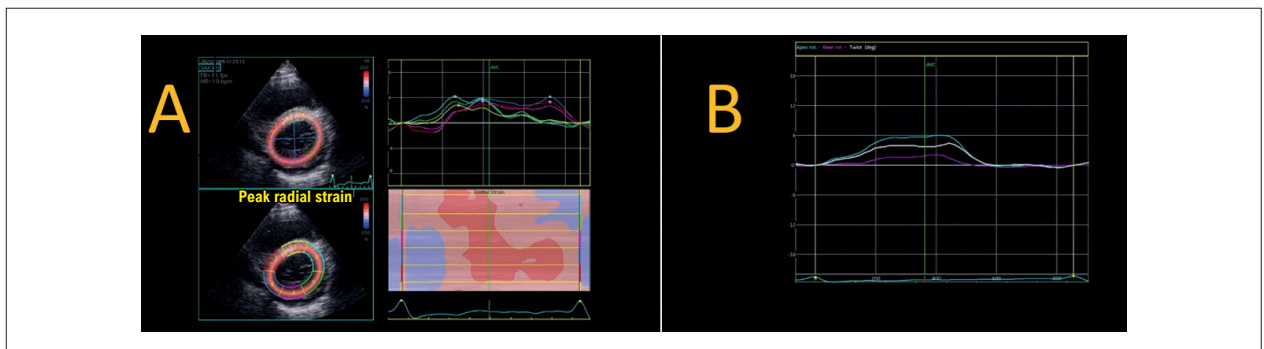


Figure 8.3 – Transthyretin amyloidosis. Significantly lower absolute left ventricular (LV) radial strain values in all basal segments in 2D assessment (A). There is also a change in circumferential strain, resulting in significantly reduced “twist” (4°) and LV torsion (B).

The use of strain to assess clinical course and monitor response to specific CA treatments is very promising. Giblin et al. retrospectively evaluated 45 patients with cardiac transthyretin amyloidosis at 1 year of follow-up, comparing LS and MW values between groups of patients treated or not with Tafamidis.²¹⁶ In untreated patients, they found greater deterioration in GLS ($p = 0.02$), LVMW index, and MW efficiency ($p = 0.04$), with no significant differences between groups in circumferential strain, radial strain, or twist.

Myocardial deformation parameters have also been extensively studied as prognostic indices in CA due to their ability to provide quantitative data, as well as to their high sensitivity and reproducibility. At a mean follow-up of 11 months Ternacle et al. found that mean apical LS (cut-off: -14.5%), elevated N-terminal pro-B-type natriuretic peptide, and New York Heart Association functional class III

or IV were independent predictors of major cardiovascular events.¹⁹⁸ In another study, relative apical sparing index was independently associated with a composite outcome of death or heart transplantation within 5 years (hazard ratio [HR] 2.45; $p = 0.003$), maintaining its predictive value even in the multivariate analysis ($p = 0.018$).²¹⁷

A large study by Buss et al. of 206 patients with systemic light chain amyloidosis found that Doppler-based LS and GLS were strongly associated with N-terminal pro-B-type natriuretic peptide levels and survival (best cut-off: -11.78%); in the multivariate analysis, only DD and GLS remained as independent predictors of survival.²¹⁸

A recent study by Liu et al. included 40 patients with multiple myeloma with preserved EF before beginning bortezomib treatment, measuring baseline GLS and MW parameters. Global MW efficiency was significantly associated with adverse cardiac events after 6 months

Statement

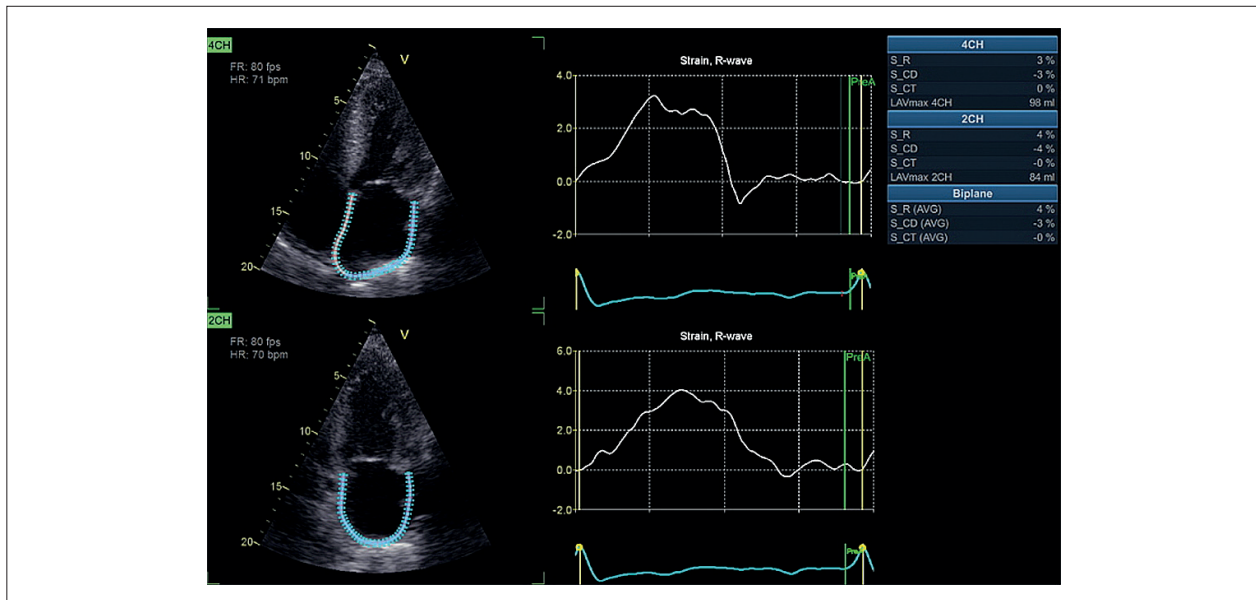


Figure 8.4 – Immunoglobulin light chain amyloidosis. Two-dimensional left atrial (LA) strain, with 4-chamber and 2-chamber apical windows, showing an important reduction in LA strain (reservoir strain = 4%).

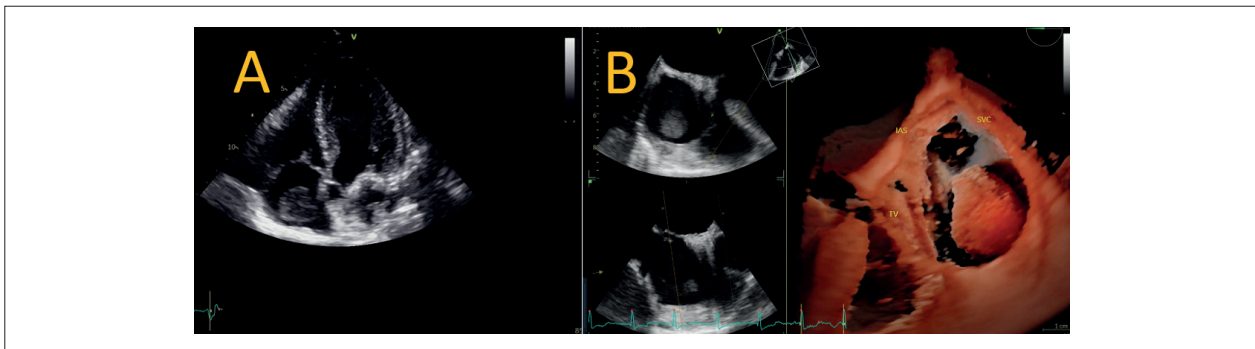


Figure 8.5 – Transthyretin amyloidosis. The 2D apical window shows: (A) a large mobile mass inside the right atrium in a patient with sinus rhythm; (B) a 3D-rendered transesophageal echocardiography image showing a large mass (thrombus) adhered to the right atrial appendage. IAS: interatrial septum; SVC: superior vena cava; TV: tricuspid valve.

of chemotherapy (AUC = 0.896; 95% CI: 0.758-0.970; $p < 0.05$).²¹⁹ RVLS has also been associated with CA prognosis. In a study of 136 patients with CA, Huntjens et al. found that strain values in all cavities were significantly associated with survival in median follow-up of 5 years.²²⁰ Peak LALS and mean RV free wall strain continued to be independently associated with prognosis in the multivariate analysis. As an independent variable, peak LALS had the most robust association with survival ($p < 0.001$), while the greatest prognostic value was obtained by combining LALS, GLS, and mean RV free wall strain ($p < 0.001$).

8.2. Fabry Disease

Fabry disease (or Anderson-Fabry disease) is the most common glycogen storage disease, affecting 1 in 50,000 individuals.²²¹ Being an X-linked recessive disease, it is more common in men; women are carriers without alpha-

galactose activity. The condition leads to a progressive accumulation of globotriaosylceramide in the kidneys, heart, and nerves. Clinically, patients present with skin changes (angiokeratomas), peripheral neuropathy, renal failure, and HF due to restrictive cardiomyopathy with increased myocardial thickness. Although these clinical manifestations can occur in childhood, they are more common after the third decade of life.²²²

Morphological analysis shows characteristically increased LV thickness, which may progress to a reduced compliance and HFpEF due to restrictive cardiomyopathy. Other interesting findings that may be considered red flags are papillary muscle hypertrophy, double contour sign, and dynamic obstruction of the LV outflow tract.²²³ This similar phenotype to HCM is described in 6% of men²²⁴ and 12% of women diagnosed in later age.²²⁵ On the other hand, bull's eye parametric analysis of LVLS plays

an important role in differentiating cardiomyopathies that involve increased myocardial thickness, especially in asymmetric LV hypertrophy with an etiological possibility of HCM, amyloidosis (mainly transthyretin), Fabry disease, or hypertensive heart disease in older patients.

HCM typically involves lower segmental values and greater thickness, while amyloid cardiomyopathy produces an apical sparing pattern and has a greater effect on the middle and basal regions of the LV. On the other hand, hypertensive heart disease can present with slightly reduced GLS. Curiously, Fabry disease involves a unique pattern in which, despite an asymmetrical increase in ventricular thickness, the basal portion of the inferolateral wall is most affected by LS (Figure 8.6); a progressive decreasing pattern occurs in untreated disease. There is a good correlation between LVLS assessment and delayed-enhanced cardiac MRI in different stages of the disease.²²² In addition, a study compared Fabry disease patients without myocardial alterations to a healthy control group, finding significantly lower myocardial values for LV, RV, LA in the Fabry group than the control group (18.1 [SD, 4.0], 21.4 [SD, 4.9], and 29.7 [SD, 9.9] vs 21.6 [SD, 2.2], 25.2 [SD, 4.0], and 44.8 [SD, 11.1%], respectively, $P < 0.001$). Interestingly, in addition to these differences, strain changes correlated well with symptom severity.²²⁶

Treatment is currently available for Fabry disease, and morphological changes in the heart, such as reduced thickness, can appear after 1 year of treatment.^{227,228} Thus, improved LVLS is expected to occur earlier, even before ventricular mass reduction. However, therapeutic response and GLS patterns throughout treatment should still be investigated.

Myocardial strain assessment is an important tool for diagnosing ventricular hypertrophies of unknown etiology, mainly within a coherent clinical context and a good echocardiographic window, including follow-up of family members without access to genetic assessment or therapeutic response (Figure 8.6).

9. Strain in Hypertension

9.1. Introduction

This section discusses the main advantages and disadvantages of strain assessment in hypertension, with and without criteria for hypertensive cardiomyopathy (ie, LV hypertrophy), and its current clinical value.

9.2. Hypertension without Left Ventricular Hypertrophy Criteria

During its clinical course, hypertension causes changes in myocardial contractility, which appear as reduced LS in response to afterload and high wall systolic stress. These changes have proven prognostic significance. Reduced GLS reflects subclinical myocardial dysfunction even before the onset of LV hypertrophy or EF reduction (detected through traditional measurement methods); strain is the only measurement to change in stage I hypertension.²²⁹⁻²³⁹ GLS reduction initially occurs in the basal region of the interventricular septum, extending to the basal and middle regions of other walls, which is likely because of overload in the interventricular septum due to systolic wall stress in the early stages of hypertension (Figure 9.1).^{240,241} The longitudinal fibers of the subendocardial layer are affected early in this phase, along with the mesocardium, but not the epicardium, as suggested in some studies.²⁴²

Another study found that LS change in the epicardial layer was the only variable that could predict cardiovascular events, indicating that it may correspond to the most severe and chronic type of damage.²⁴³ However, the majority of currently available devices cannot analyze myocardial layers separately. On the other hand, radial and circumferential strain, which are based on overall myocardial thickness, tend to remain unchanged or even increase in a probable attempt to mechanically compensate for lower GLS,^{60,236} with a change in circumferential component indicating more severe myocardial dysfunction.²⁴⁴

The main explanations for reduced GLS are an increase in the synthesis of collagen, culminating in fibrosis, which

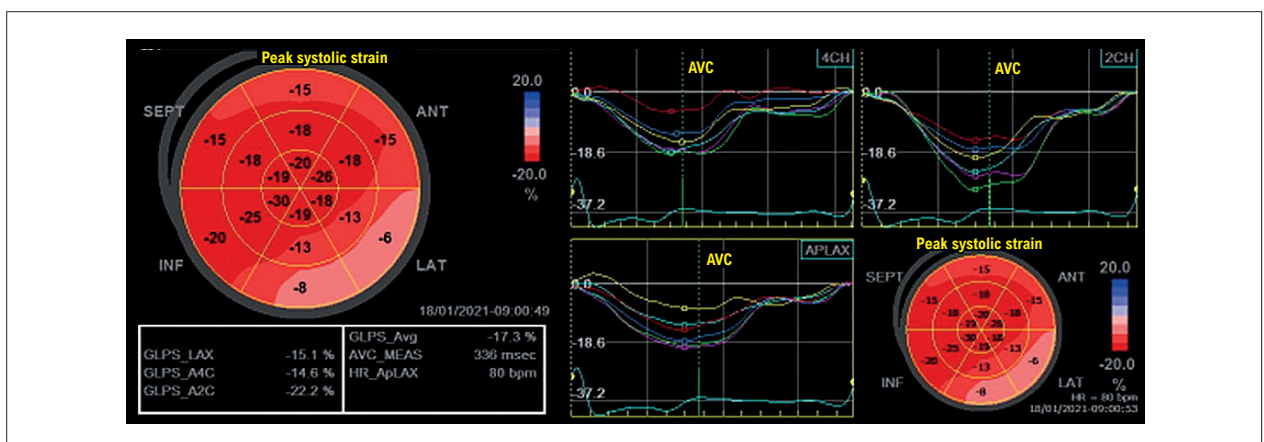


Figure 8.6 – Global longitudinal strain in a patient with Fabry disease: bull's eye map shows the lowest values in the basal portions of the left ventricle inferolateral wall. AVC: aortic valve closure.

Statement

is a strong marker of myocardial dysfunction. Reduced GLS correlates not only with plasma markers of fibrosis, such as elevated tissue metalloproteinase inhibitor, but with fibrosis detected through delayed gadolinium-enhanced MRI in hypertensive patients.^{231,234,238,239} Decreased GLS has also been observed in patients with masked and white-coat hypertension,^{245,246} being correlated with conventional echocardiographic markers of DD,²⁴⁰ as well as greater long-term deterioration in individuals who discontinue antihypertensive treatment.²⁴⁷

9.3. Hypertension with Left Ventricular Hypertrophy Criteria

The myocardial consequences of chronic hypertension include myocyte hypertrophy, myocardial fibrosis, and medial thickening of the intramyocardial coronary arteries.²⁴⁸ Consequently, hypertension and changes in myocardial remodeling are risk factors for major cardiac events, such as HF and premature death. Thus, the purpose of strain analysis in these cases is to detect subtle changes in systolic function, even before conventionally determined EF is compromised, thus facilitating the selection of HFpEF cases for treatment.

LV remodeling may affect various types of strain. In concentric hypertrophy, for example, GLS values can progressively decrease according to geometric type, from concentric remodeling to eccentric hypertrophy with LV dilation.²⁴⁹⁻²⁵¹ Although most studies find preserved global circumferential strain and global radial strain values,²⁵² some series have found them to be reduced²⁴⁹ and that they tend to remain normal in the epicardial layers in individuals with hypertension and LV hypertrophy.²⁵⁰ Torsion and twisting behavior can also vary, with normal or reduced values according to the ventricular geometry.^{249,253} In 3D analysis of hypertensive patients, GLS tends to deteriorate according to the degree of hypertrophy and LV cavity diameter.^{62,250}

In addition to the correlation between reduced GLS and different patterns of LV hypertrophy, strain assessment can clarify the cause of hypertrophy, since it is more often reduced in HCM than LV hypertrophy due to hypertension.²⁵⁴

9.4. Clinical Treatment

GLS decreases concomitantly with functional class²⁴¹ and increases with long-term treatment, as found in 3-year follow-up after antihypertensive treatment²⁵⁵ and described in case reports of emergency antihypertensive treatment.²⁵⁶ Reduced GLS is also correlated with abnormal blood pressure in patients undergoing treatment, even after adjusting for other clinical variables, such as age, diabetes, and LV mass index.²⁵⁷

9.5. Conclusion

There is enough evidence to recommend strain assessment for patients with hypertension, regardless of LV hypertrophy, both to identify subclinical structural alterations and to identify the best treatment for HFpEF conditions. On the other hand, more robust studies are needed to guide systematic assessment in this population

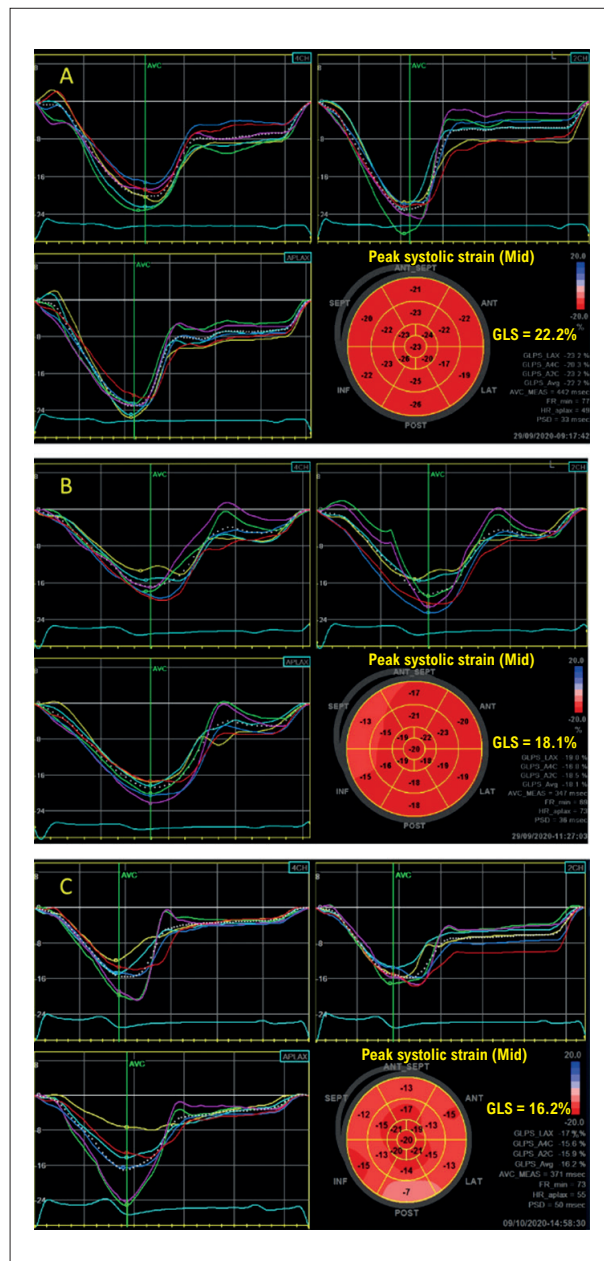


Figure 9.1 – Examples of global longitudinal strain polar mapping with peak systolic strain curves obtained in 4, 2 and 3 chambers. (A) healthy non-hypertensive patient with preserved GLS; (B) hypertensive patient without LV hypertrophy whose GLS is at the lower limit of normality (note altered myocardial strain in the basal septum); (C) hypertensive patient with LV hypertrophy and reduced GLS (note greater change in myocardial strain in basal and middle segments than apical segments).

10. Strain in Athletes

Regular intense physical activity results in a series of profound adaptive electrical, structural, and functional changes, usually referred to as athlete's heart.²⁵⁸ Analysis of this condition is important for a better understanding of the mechanisms of cardiac adaptation and how to improve training to optimize performance. Analysis can

also differentiate pathologies with similar morphological characteristics to those induced by training.

High-performance athletes with large LV volumes are considered to be on the healthy physiological spectrum of athlete's heart. Some studies have reported slightly lower GLS in resting athletes than sedentary people, while others report the opposite.^{259,260} However, most studies have found no significant difference between these groups.²⁶¹ This variation may be related to the effects of different factors such as preload and afterload, myocardial mass, and sinus bradycardia. Thus, reduced GLS values in athletes with normal or supranormal LV diastolic function may help distinguish between cardiac pathologies and secondary adaptations to exercise. Absolute values $\geq 18\%$ are still considered within normal limits. Much greater reductions in these indexes are found in patients with HCM and systemic arterial hypertension.²⁶² However, global circumferential strain and radial strain were found to differ significantly between athletes and controls.²⁶¹ Bull's-eye mapping can help differentiate athlete's heart from other diseases involving hypertrophy.²⁶³

When athletes are categorized according to exercise type and intensity (static vs dynamic), differences arise predominantly in mechanical aspects of the LV. A recent study showed that cardiac torsion was greater in low dynamic/high static (weightlifting, martial arts) athletes and in low static/high dynamic (marathon, soccer) athletes than controls. In contrast, torsion was lower in high dynamic/moderate static (swimming, water polo) athletes than controls, which could be explained by changes in apical, but not basal, rotation. Peak untwisting was higher in low dynamic/high static athletes and lower in high dynamic/high static athletes.²⁶¹ Studies using speckle tracking to quantify myocardial strain have shown that competitive endurance athletes have normal or increased strain values.²⁶⁴⁻²⁶⁸

In the RV, tissue Doppler and speckle tracking myocardial strain indices may be slightly lower in the basal and middle segments of the RV free wall (notably in endurance athletes) than controls.²⁶⁹ It is still unclear whether this reduction is an adaptive response to exercise or a subclinical change due to myocardial injury.²⁷⁰ Some authors assume that it can be explained by curvature changes between the apex and base of the RV, resulting in a strain difference between segments.

Speckle tracking studies of atrial function in athletes are still in their infancy and show conflicting results. One study found that LA contraction assessed by GLS significantly decreased after training.²⁷¹ Another study found no differences in atrial strain between athletes and sedentary controls.²⁷²

Strain measurement is also important in diastolic function assessment. Dynamic exercise leads to more effective ventricular relaxation and biventricular dilation, while static exercise may be related to increased myocardial thickness and LV concentric hypertrophy, which could lead to some degree of diastolic impairment.²⁷³ In addition, illicit performance-enhancing drugs can lead

to deterioration of ventricular, systolic, and/or diastolic function, and speckle tracking echocardiography can detect these alterations early.²⁷⁴

Thus, when evaluating ventricular function in professional and/or amateur athletes, all available tools in the echocardiography arsenal are to be used. Strain analysis can detect incipient changes in systolic function, long before contractility changes or EF reductions can be detected in 2D assessment.

When evaluating athletes, speckle tracking echocardiography has shown great promise as a complement to routine 2D echocardiography. Unlike sedentary individuals, absolute GLS values $> 16\%$ in this population can be considered normal; lower values should raise suspicion of pathology, especially when combined with signs such as significant ventricular hypertrophy or dilation.²⁷⁵

11. Strain in Stress Echocardiography

Table 11.1 shows the main applications of strain in stress echocardiography.

A more complete review article on stress echocardiography will soon be published in this journal.

12. Strain in Congenital Heart Disease

Some studies have demonstrated the high prognostic value of speckle tracking strain assessment, reinforcing its usefulness for both congenital and acquired pathologies.⁹ However, myocardial strain is subject to physiological variations due to age, sex, heart rate, preload, blood pressure, and body surface area, as well as the analysis software.²⁹⁶ Continuous effort has been made to determine normal strain values for universal reference in pediatrics so that myocardial strain assessment of can be included in the clinical routine.²⁹⁷⁻²⁹⁹

Tables 12.1 to 12.3 present the myocardial strain values found in the literature for normal children and those with congenital heart diseases, while Table 12.4 shows the recommended cut-off values. A more complete review article on the subject is forthcoming in this journal.

13. Right Ventricle Strain

13.1. Introduction

The RV plays an important role in the pathophysiology of cardiopulmonary disease. A large amount of evidence has shown that RV dysfunction is an important independent marker of morbidity and mortality in clinical conditions such as HF, valvular heart disease, pulmonary hypertension, pulmonary embolism, and ischemic heart disease, as well as in congenital heart disease in adults.³⁰⁸⁻³¹³

Cardiac MRI is the gold standard non-invasive test for RV volume, EF, and structural assessment. However, its main limitations are its high cost, longer image acquisition time, and poor availability in most centers.³¹⁴ Two-dimensional echocardiography is the most common initial test for structural and functional evaluation of the RV due to its wide availability,

Statement

Table 11.1 – Strain applications in stress echocardiography

Clinical scenario	Concept
Ischemia detection ^{189,276-280}	<ul style="list-style-type: none"> Regional LS detects endocardial ischemia. CS can help differentiate transmural and non-transmural infarctions. Increased time to peak LS can help detect ischemia. Post-systolic shortening (sensitive but not specific for detecting ischemia). Systolic RLS (lower dependence on load and heart rate than strain). Diastolic strain parameters.
Feasibility assessment ²⁸¹⁻²⁸⁵	<ul style="list-style-type: none"> LS and RLS increase the accuracy of viability detection in MI patients treated with TCA and low doses of dobutamine. LS is the best predictor of functional improvement after CABG. Lack of response to dobutamine accurately predicts lack of improvement after CABG. Differentiation between stunned and hibernating myocardium (lower LS and RLS and post-systolic shortening).
Aortic stenosis ^{286,287}	<ul style="list-style-type: none"> GLS in the evaluation of low-flow/low-gradient aortic stenosis. Patients with GLS > 10% after dobutamine use have longer survival. Stress GLS is more accurate than resting GLS.
Hypertensive cardiomyopathy ²⁸⁸	<ul style="list-style-type: none"> LS and RS deficits are more evident during stress than rest in the initial phases, allowing prevention measures.
Diabetic cardiomyopathy ^{289,290}	<ul style="list-style-type: none"> Lower RLS in middle and basal segments during DSE. Early decreased myocardial velocities in asymptomatic patients with insulin resistance during DSE.
Cardiomyopathies ^{132,291-293}	<ul style="list-style-type: none"> Lower systolic functional reserve detected in LS and RS after stress. No improvement in diastolic function parameters. Increased time-to-peak in HCM with important dyssynchrony. Low RVLS values in arrhythmogenic dysplasia do not significantly improve with stress.
Athlete's heart ^{294,295}	<ul style="list-style-type: none"> Slightly lower LS values with preserved or supranormal myocardial reserve. Stress GLS helps differentiate athlete's heart from cardiomyopathy.

CABG: coronary artery bypass grafting; CS: circumferential strain; DSE: dobutamine stress echocardiography; GLS: global longitudinal strain; HCM: hypertrophic cardiomyopathy; LS: longitudinal strain; MI: myocardial infarction; RLS: regional longitudinal strain; RS: radial strain; RV: right ventricle; TCA: transluminal coronary angioplasty.

Table 12.1 – Normal left ventricular strain values according to age group²⁹⁸

Age in years	Peak systolic GLS	Peak strain in apical 4-chamber view	Peak circumferential systolic global strain	Peak circumferential systolic strain at the papillary muscle level	Peak radial global systolic strain	Peak radial systolic strain at the papillary muscle level
0-1	18.7% (20.8, 16.7)	19.4% (22.2, 16.6)	—	18.2% (22.6, 13.7)	—	44.4% (36.6, 52.1)
2-9	21.7% (23.0, 20.5)	21.0% (21.8, 20.2)	24.5% (27.2, 21.7)	20.3% (21.4, 19.1)	48.0% (33.3, 62.8)	50.8% (47.4, 54.1)
10-13	20% (20.8, 19.1)	20.5% (21.7, 19.2)	21.9% (26.5, 17.4)	21.5% (23.1, 19.8)	43.7% (33.0, 54.5)	52.1% (48.5, 55.8)
14-21	19.9% (20.6, 19.2)	19.9% (21.2, 18.6)	16.4% (23.3, 9.6)	16.4% (23.3, 9.6)	44.0% (41.6, 46.4)	46.4% (39.7, 53.1)
Overall	20.2% (20.8, 19.6)	20.4% (21.1, 19.8)	22.3% (19.9, 24.6)	20.4% (21.1, 19.8)	45.2% (38.8, 51.7)	49.4% (47.2, 51.6)

GLS: global longitudinal strain. Values expressed as mean and 95% CI.

low cost, non-invasiveness, and shorter image acquisition time. However, 2D RV assessment is challenging due to the complex structure of the cavity, its unfavorable position in the thoracic wall, and intense myocardial trabeculation, which prevents better visualization of the endocardium due to its thinner walls and high dependence on loading conditions in the most common systolic function indices.³¹⁵

Several echocardiographic parameters are used to indicate RV systolic function in clinical practice. Recently, 2D speckle-tracking was introduced into clinical practice as an objective indicator of regional and global myocardial contractility, initially for LV and more recently for RV evaluation. Research has highlighted the advantages of this new methodology over conventional echocardiographic parameters.³¹⁶

Table 12.2 – Normal right ventricular strain values according to age group³⁰⁰

	31 days-24 months	2-5 years	5-11 years	11-18 years
GLS RV %	25.4 (3.9)	25.9 (4.0)	25.8 (4.7)	25.4 (4.1)

GLS: global longitudinal strain; RV: right ventricle. Values expressed as mean (SD)

Table 12.3 – Valores normais de strain atrial direito e esquerdo, segundo as faixas etária³⁰¹

Measure	31 days-24 months	2-5 years	5-11 years	11-18 years
LA strain (R)%	52.8 (10.1)	55.7 (10.7)	58.1 (10)	57.6 (10.5)
LA strain (C)%	14.2 (6.6)	12.7 (6.1)	14.0 (6.7)	15.1 (7.0)
RA strain (R)%	47.1 (9.6)	49.6 (10.2)	51.6 (10.7)	52.0 (10.6)
RA strain (C)%	11.5 (6.0)	11.9 (5.9)	11.8 (6.3)	12.8 (5.8)

C: atrial contraction phase; LA: left atrium; R: reservoir phase; RA atrium. Values expressed as mean (SD)

Table 12.4 – A selection of studies evaluating the use of strain in idiopathic pulmonary hypertension and congenital heart disease

	Authors	Parameter	Cut-off	Findings	Sn/Sp
Idiopathic pulmonary hypertension	Muntean et al. ³⁰²	mid-segment FW RV strain	18.5%	Predictor of clinical worsening	Sn: 91.7%, Sp: 30.8% AUC=0.88, SD 0.06
Ebstein's anomaly	Kühn et al. ³⁰³	RVGLS (6 segments)	20.15%	Diagnosis of RV dysfunction (EF < 50% in MRI)	Sn: 77% Sp: 46%
Systemic RV (PO TGA Senning/Mustard)	Lipczyńska et al. ³⁰⁴	RVGLS (6 segments)	14.2%	Diagnosis of RV Dysfunction (EF < 45% in MRI)	Sn: 83%, Sp: 90% AUC= 0.882
Systemic RV (CTGA)	Kowalik et al. ³⁰⁵	RVGLS (6 segments)		Diagnosis of RV dysfunction (EF < 45% in MRI)	Sn: 77.3% Sp: 72.7%
PO AOLCA	Castaldi et al. ³⁰⁶	LV peak segmental strain	14.8%	Predictor of fibrosis in MRI	Sn: 92.5% Sp: 93.7%
Univentricular physiology (PO Fontan)	Park et al. ³⁰⁷	Circumferential strain rate	-1.0s ⁻¹	Predictor of hospital stay >14 days after TCC anastomosis	Sn: 72% Sp: 60%

AOLCA: anomalous origin of the left coronary artery; AUC: area under the curve; TCC: total cavopulmonary connection; CTGA: corrected transposition of the great arteries; EF: ejection fraction; FW: free wall; GLS: global longitudinal strain; MRI: magnetic resonance; PO: postoperative; RV: right ventricle; Sn: sensitivity; Sp: specificity.

13.2. Anatomical and Functional Characteristics of the Right Ventricle

Table 13.1 shows the main characteristics that differentiate the ventricles.³¹⁷⁻³¹⁹ LV and RV function are closely related (a phenomenon called systolic ventricular interaction) since they share obliquely arranged muscle fibers in the interventricular septum. These have a mechanical advantage over the transverse fibers of the RV free wall.³⁶ The continuity of these muscle fibers allows the RV free wall to be pulled during LV contraction, with an estimated 20%-40% of RV stroke volume and systolic pressure due to LV contraction.^{318,319}

13.3. Right Ventricle and Echocardiographic Parameters in Systolic Function Assessment

Several indices are routinely used to assess RV systolic function, such as fractional area change, tricuspid annular plane systolic excursion, tricuspid annular peak systolic velocity, and myocardial performance index. Each has its advantages and limitations, varying feasibility and reproducibility, and debatable diagnostic and prognostic efficacy.^{35,36} At present,

no single method is considered a good indicator of RV systolic function. However, due to the orientation of the predominant longitudinal muscle fibers from the tricuspid annulus to the apex, preference is given to indices that explore movement along the longitudinal axis when assessing regional or global RV longitudinal function.⁹²

Two-dimensional speckle tracking echocardiography is an imaging modality that evaluates myocardial deformation, an intrinsic property of the myocardium, in the 3 directions (longitudinal, circumferential, and radial). The longitudinal direction is the most common due to its good reproducibility, relevant prognostic information, validation in an experimental study⁷⁵ and in clinical cardiac MRI studies of various cardiovascular diseases.³²⁰⁻³²³ Thus, RV 2D speckle-tracking can be considered a good marker of systolic function, with prognostic value in several cardiovascular diseases.^{75,324-330}

13.4. Acquisition and Limitations

Determining RVGLS through 2D speckle tracking requires a modified apical 4-chamber window focused on

Statement

the RV, with the transducer displaced more laterally and towards the right shoulder, which allows better visualization of the free wall and more reproducible measurements (Figure 13.1). It is important to optimize the orientation, depth, and gain to maximize the size of the RV, and to view its apex throughout the entire cardiac cycle.³⁶ During image acquisition, the transducer should not be positioned anteriorly or posteriorly (avoiding the aortic valve and coronary sinus, respectively), showing only the interatrial septum.³³¹ Once adequate visualization is obtained, the device should be set to record 3 cardiac cycles and acquire images at 50-80 frames per second. This rate can be obtained through indirect adjustments, such as image depth, resolution, and the ultrasound beam size, as well as by direct adjustment of the echocardiography device.

Some software still requires the beginning and end of the RV ejection time to be defined, using pulsed Doppler echocardiography in the RV outflow tract.

The region of interest is defined by the endocardial border, which includes the RV free wall and interventricular septum. It should not include the pericardium and its width should not be too narrow, since this could lead to erroneous results. The baseline reference points must be positioned correctly; suboptimal positioning, eg, on the atrial side of the tricuspid annulus, could result in reduced LS values.³³² The region of interest can be manually plotted or generated automatically; if generated automatically, the user must have permission to check and edit it manually as needed.⁹² After a tracking quality check and final operator approval, the regional strain values are displayed.

Table 13.1 – Anatomical and functional characteristics of the ventricles

	Right ventricle	Left ventricle
Structure	Inlet, trabecular region, infundibulum.	No infundibulum and limited trabeculation.
Form	Multiple muscle bands Triangular in the coronal plane Crescent in the transverse plane	Elliptical
Predominant myocardial fiber orientation	Subepicardium: circumferential Subendocardium: longitudinal	Subepicardium: oblique Mesocardium: circumferential Subendocardium: longitudinal
Arrangement of fibers in the free wall	Transverse predominance	Olique predominance
Arrangement of fibers in the IVS	Obliquely, extending to the outflow tract	Obliquely
Contribution of IVS thickening in the transverse axis and shortening in the longitudinal axis in systole	+++	+++
Contraction pattern	Mainly longitudinal from base to apex	Subepicardium and Subendocardium: longitudinal shortening in opposite directions. Mesocardium: circumferential direction
Mass (g/m ²)	26 (SD, 5)	87 (SD, 12)
Wall thickness (mm)	2-5	7-11

IVS: Interventricular septum

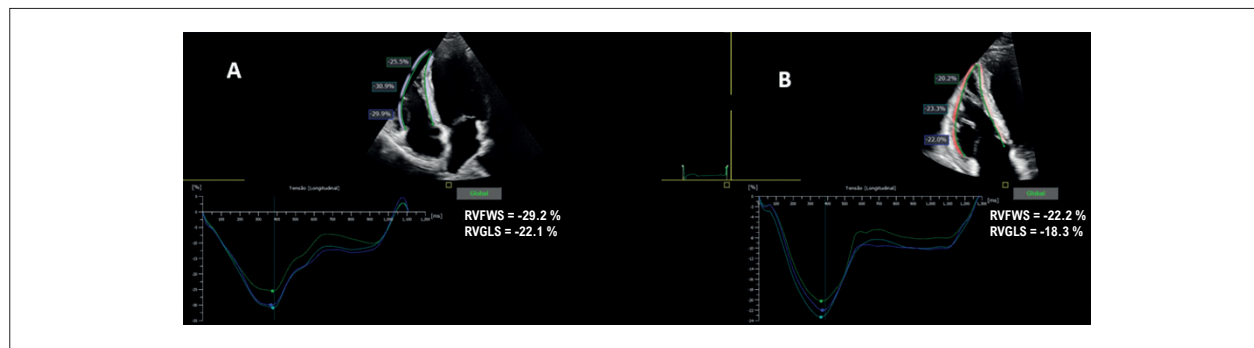


Figure 13.1 – Imaging protocol for right ventricular (RV) strain measurement through speckle tracking echocardiography in an apical 4-chamber view: A) apical 4-chamber window (inappropriate acquisition method); B) apical 4-chamber window focused on the RV (adequate acquisition method). RVFWS: RV free wall strain; RVGLS: RV global longitudinal strain.

According to current recommendations, the highest value reached during systole (peak systolic strain) should be used, with Doppler tracking of the pulmonary valve used to determine the end-diastole and end-systole.⁹² Whenever possible, appropriate software should be used, since the automatic detection algorithm of RV segments reduces the need for operator intervention, thus contributing to reproducible results.

The RV free wall is divided into basal, middle, and apical segments. The interventricular septum is similarly segmented. RV free wall LS is the mean strain value of all 3 segments, while RVGLS is the mean strain value of the free wall segments and the interventricular septum. RV free wall LS is more common in practice and clinical research, since LV function can interfere with RVGLS through the interventricular septum, leading to lower absolute values.³³³ RV free wall LS must be reported as a standard parameter, with RVGLS being optional.⁹²

As limitations, in addition to inadequate acoustic windows, experimental studies and mathematical models have shown that the magnitude of myocardial strain is influenced by heart rate, in addition to preload and afterload. In preserved systolic function, studies have confirmed that strain can increase with higher preload and heart rate and can decrease when they are lower.^{16,334}

13.5. Indications/Normal Values

The association between RV systolic dysfunction and poor prognosis in several cardiovascular diseases has been well-established, and RVGLS is an independent prognostic marker in pulmonary hypertension, HF, ischemic heart disease, and other cardiomyopathies; according to cardiac MRI, it is better correlated with right ventricular ejection fraction in than traditional parameters.^{35,320-23,334-336}

RVGLS is lower in patients with pulmonary hypertension, showing good correlation with invasive hemodynamic parameters of RV performance.³³⁷ Furthermore, RVGLS has been found to be an independent predictor of all-cause mortality and pulmonary hypertension-related events. Aiming to assess the prognostic value of RVGLS in these patients, a recent meta-analysis found that a 19% relative reduction in RVGLS is associated with an increased risk of pulmonary hypertension-related events, while a 22% relative reduction is associated with a higher risk of all-cause mortality.³²⁴ Figure 13.2 shows an example of RV strain in a patient with primary pulmonary hypertension.

In patients with HF, RVGLS has high sensitivity and accuracy for diagnosing RV systolic dysfunction.³³⁸ A recent study found that absolute values < 14.8% are associated with adverse events, such as mortality, heart transplantation, and hospitalization, regardless of LVEF or LV DD.¹⁹ In addition, RVGLS and RV free wall LS could detect subtle RV systolic function abnormalities in patients with HF and reduced LVEF, and to a lesser extent in those with HF and preserved LVEF.³²⁹ In patients eligible for LV assist device implantation, RVGLS is useful for stratifying the risk of RV failure. With a sensitivity of 68% and a specificity of 76%, an absolute RVGLS value < 9.6% can identify

patients with post-procedure RV failure (ie, requiring an RV assist device or inotrope therapy > 14 days).³³⁹ In heart transplant patients, a combination of LVGLS and RV free wall LS measurements can help exclude acute cellular rejection and reduce the number of routine biopsies.³⁴⁰ Figures 13.3 and 13.4 show examples of VR strain in a patient with a ventricular assist device and a heart transplant patient, respectively.

In acute myocardial infarction, cardiac MRI RVGLS has the best correlation with right ventricular ejection fraction.³⁴¹ It has been shown to be an independent predictor of death, reinfarction, and hospitalization due to HF, which confirms its fundamental role in assessing this population.³⁴² A separate section will discuss the assessment of patients with arrhythmogenic RV dysplasia.

The role of RV systolic dysfunction has recently been investigated in other cardiomyopathies. In one study

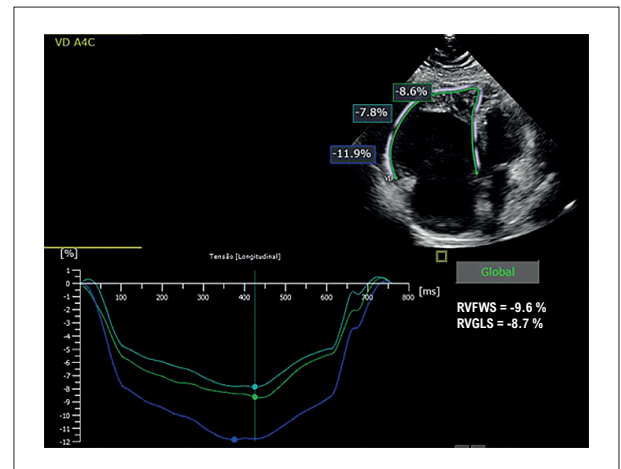


Figure 13.2 – Example of right ventricular (RV) strain in a patient with primary pulmonary hypertension. TomTec software. RVFWS: RV free wall strain; RVGLS: RV global longitudinal strain.

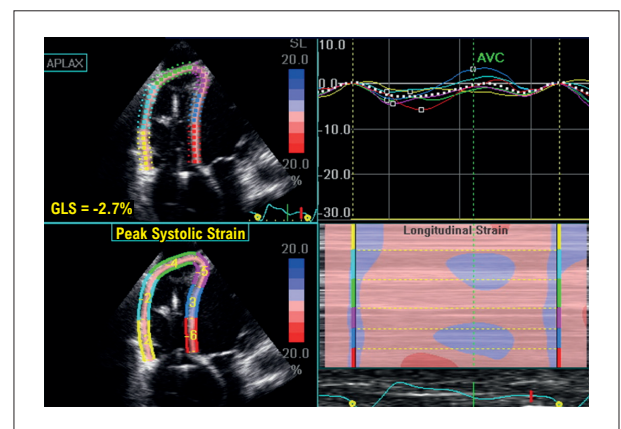


Figure 13.3 – Example of right ventricular strain in a patient using a ventricular assist device. GE EchoPAC software. AVC: aortic valve closure; GLS: global longitudinal strain.

Statement

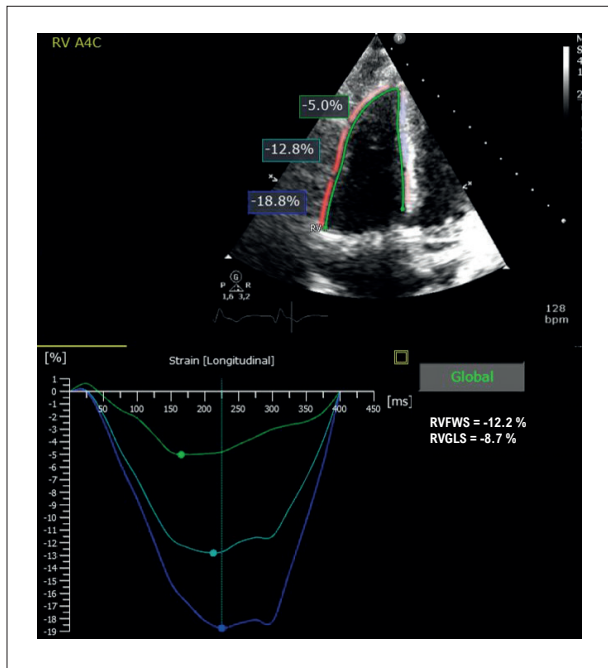


Figure 13.4 – Example of right ventricular strain in a heart transplant patient. TomTec Software. RVFWS: right ventricular free wall strain; RV4CS: right ventricular global longitudinal strain.

lower RVGLS values were found in an HCM group than in healthy controls,³⁴³ while another reported that RVGLS can differentiate HCM and hypertrophy secondary to hypertension with high sensitivity and specificity.³⁴⁴

The valvular heart disease with the greatest effect on the RV is mitral stenosis, frequently changing its conventional assessment parameters. The pattern of change in RVGLS is segmental, with significantly lower values in the interventricular septum and RV basal free wall, and normal values in the middle and apical free wall.^{345,346} Among patients with significant functional tricuspid regurgitation, RV free wall LS identified more individuals with RV dysfunction (84.9%) than fractional area change (48.5%) and tricuspid annular plane systolic excursion (71.7%). Furthermore, RV free wall LS was independently associated with all-cause mortality and had higher prognostic value when combined with traditional RV assessment parameters.³²⁸

Due to the lack of studies, there is no consensus about normal RV strain values. According to the most recent American Society of Echocardiography/European Association of Cardiovascular Imaging recommendations for echocardiographic cardiac chamber quantification in adults, RVGLS and RV free wall LS values below 20% are considered abnormal.³⁵ However, this requires caution since different equipment types use different software programs, particular reference values, and differences in mapping level (endocardial, epicardial, or the entire myocardial wall).

Table 13.2 summarizes the main recommendations for GLS in RV assessment.

Table 13.2 – Indications for global longitudinal strain in RV assessment

- Pulmonary hypertension (including patients with acute or chronic pulmonary embolism)
- Heart failure with reduced or preserved ejection fraction
- Acute myocardial infarction
- Cardiomyopathies (ADRV, HCM, DCM)
- Valvular heart disease (mitral stenosis, functional tricuspid regurgitation)
- Candidates for ventricular assist device implantation
- Heart transplant

ADRV: arrhythmogenic dysplasia of the right ventricle; DCM: dilated cardiomyopathy; HCM: hypertrophic cardiomyopathy.

14. Left and Right Atrial Strain

14.1. Left Atrial Strain Assessment Techniques

Strain analysis involves the 3 components of LA function: reservoir, conduit, and contractile. Strain rate is also used, although less commonly, ie, the peak strain rate during the reservoir phase, the conduit phase, and atrial contraction.^{92,347}

Four- and 2-chamber apical images are optimized for the LA and taken at a high frame rate, usually 40-80 frames per second. A specific cardiac cycle is selected and point-to-point tracking is performed manually from the endocardial border of the mitral annulus to the opposite mitral annulus, extrapolating the entrance of the pulmonary veins and the left atrial appendage. The software creates the region of interest, which is adjusted to 3 mm in width and must include the endocardial and epicardial borders. If the tracking quality fails in ≥ 2 segments after manual adjustment, this incidence must be excluded from the analysis. Finally, the software calculates the GLS for each of the above-mentioned apical windows.

LA strain analysis can involve 2 different reference points: the beginning of the P-wave in the electrocardiogram² or the R-wave peak of the QRS complex.³⁴⁸ The first method allows easier recognition of LA strain components, requiring the sum of the absolute values of LA conduit strain and LA contractile strain to obtain LA reservoir strain. The second method directly provides the LA reservoir strain value, which has the best prognostic value, while the other components are obtained from the graph. The most recommended and common method is to use the R-wave as a reference, since it has the smallest volume in the LA, and LA reservoir strain is thus more easily obtained.⁹²

14.2. Normality Values

There is great heterogeneity in the literature regarding normality values for LA strain. A meta-analysis by Pathan et al. is the best evidence at the moment, which found the following mean values for LA reservoir strain, LA conduit strain, and LA contractile strain, respectively: 39.4% (95% CI:

38%–40.8%); 23% (95% CI: 20.7%–25.2%) and 17.4% (95% CI: 16.0%–19.0%).³⁷

14.3. Clinical Applicability of Left Atrial Strain

LA strain assessment has shown greater prognostic value than volumetric measurement alone in several clinical contexts³⁴⁹ (Figure 14.1).

14.3.1. Left Atrial Strain and Diastolic Function in Heart Failure

LA strain is decreased in HFrEF and has prognostic value for all-cause mortality or rehospitalization for HF,³⁵⁰ good correlation with functional capacity³⁵¹ and LV filling pressures,³⁵² and is a good predictor of response to myocardial resynchronization therapy.³⁵³ In HFpEF, LA strain plays an important role in diagnosis³⁵⁴ and prognosis,^{73,355} and can predict the risk of AF.⁹⁸

In about 20% of HFpEF cases, LV diastolic function may have an indeterminate pattern.⁹³ LA strain can recategorize these patients,⁹⁰ since the 3 atrial function components have shown good accuracy in determining increased LA pressure.⁸⁹

14.3.2. Atrial Fibrillation

In AF, the LA reservoir and conduit functions decrease and contractile function is absent. LA strain can predict new AF in several pathologies, such as HFrEF,³⁵⁶ mitral stenosis,³⁵⁷ and Chagas disease³⁵⁸, as well as after pacemaker implantation,³⁵⁹ in addition to predicting AF recurrence after cardioversion³⁶⁰ or ablation.³⁶¹⁻³⁶³ AT function assessment through strain could become part of the decision-making process for AF ablation. LA reservoir strain is also associated with ischemic stroke independent of CHA₂DS₂-VASc score, age, or anticoagulant use.³⁶⁴

14.3.3. Valvular Heart Disease

LA strain may signal greater severity and an unfavorable course in mitral and aortic valve disease.^{365,366} In severe primary mitral regurgitation, LA reservoir strain can predict hospitalization for HF or all-cause mortality, regardless of whether surgical intervention is recommended.^{367,368}

14.3.4. Coronary Artery Disease

Coronary artery disease is associated with atrial dysfunction through 2 main mechanisms: LV DD and direct LA ischemia.³⁶⁹ LA strain may have important prognostic value in acute coronary syndrome, correlating with greater severity³⁷⁰ and unfavorable outcomes.³⁷¹

14.4. Right Atrial Strain

Although data on RA strain is lacking, a recent study of 101 healthy volunteers found the following values using the QRS complex as a reference: reservoir 37.6% (SD 6.9), conduit 26.0% (SD 7.1), and contraction 11.6% (SD 4.4).³⁷ Assessing RA function is a target of interest in congenital heart diseases,^{301,373} tricuspid valve disease, and pulmonary hypertension.³⁷⁴

15. Assessing Left Ventricular Torsion

15.1. Introduction

LV function is determined through complex interactions between tissue anatomy, myocardial contractility, and hemodynamics. The muscle fibers of the LV myocardial wall are oriented in different directions. In the subendocardial region, they are almost parallel to the wall and move in a right-handed rotation (right-handed helix), which gradually changes in subepicardial fibers to 60–70°, leading to a left-handed rotation (left-handed helix).^{375,376}

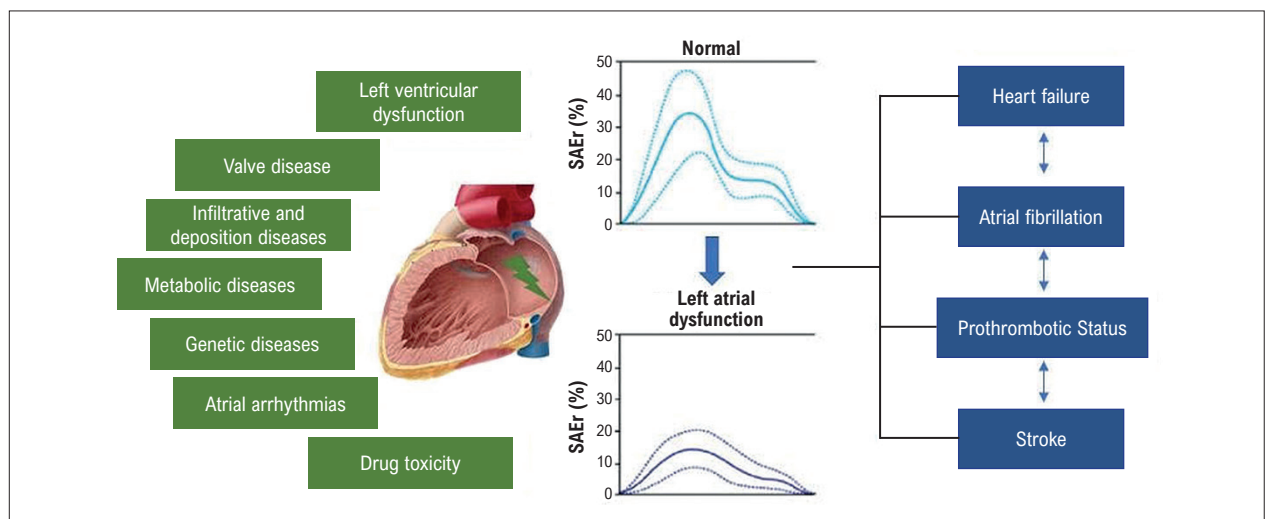


Figure 14.1 – Strain assessment of mechanisms involved in left atrial dysfunction.

Statement

Subepicardial fiber contraction causes the apex of the LV to rotate counterclockwise and its base to rotate clockwise. Conversely, subendocardial fiber contraction causes the apex and base of the LV to rotate in opposite directions. Given the greater rotation radius of the epicardial layer, the direction of the subepicardial fibers prevails in the general direction of rotation when both layers contract simultaneously. This results in global counterclockwise rotation near the apex and clockwise rotation near the base during ventricular ejection,³⁷⁷ as shown in Figure 15.1.

This twisting motion in the LV contributes to an even distribution of fiber shortening and stress along all walls, thus producing a relatively high EF (~60%) despite limited shortening (~20%).³⁷⁸ The twisting and shearing of the subendocardial fibers during ventricular ejection results in the storage of potential energy, which is subsequently used to unwind the coiled fibers during diastole, thus untwisting the helices, which together produce diastolic suction.^{379,380} Preload and afterload conditions and contractility alter the extent of ventricular torsion.³⁸¹ Increased preload or contractility increases LV torsion, while increased afterload has the opposite effect.

Several imaging techniques can be used to quantify the mechanics of ventricular torsion: echocardiography (tissue Doppler, 2D and 3D speckle tracking, velocity vector imaging, cardiac MRI (tissue tagging), and sonomicrometry. Currently, there is no gold standard for assessing LV torsion mechanics, and the above-mentioned imaging modalities have good agreement.³⁸² Due to its safety, availability, and cost-effectiveness, echocardiography is the most commonly used imaging modality.

15.2. Definitions and Nomenclature

Twist, twist rate, untwist, and untwist rate are the common terms for describing the systolic rotation and reverse diastolic rotation of the base and apex of the LV as seen from the apex. These terms are defined in Tables 15.1 and 15.2.

15.3. Step-by-step Assessment of Ventricular Torsion by Speckle Tracking Echocardiography

To evaluate the rotation mechanism, parasternal short-axis images of the LV are obtained at the basal (mitral valve) and apical levels (below the papillary muscles) (Figure 15.2). It is important to obtain apical images in which RV does not appear or only part of the LV appears, typically 1 or 2 intercostal spaces below the usual position. Most evaluation errors occur due to inappropriate selection of basal and apical planes and region of interest adjustment.

By convention, when rotation is clockwise, tracking begins below the baseline, and when rotation is counterclockwise, tracking begins above the baseline. (Figure 15.3). The normal global twist value is 9.7° (SD, 4.1°), although there are few reference values in the literature for torsion, which is estimated at $1.35^\circ/\text{cm}$ (SD $0.54^\circ/\text{cm}$).³⁸³

15.4. Clinical Applications

LV torsion parameters have generally been used to assess changes in ventricular mechanics in pathologies

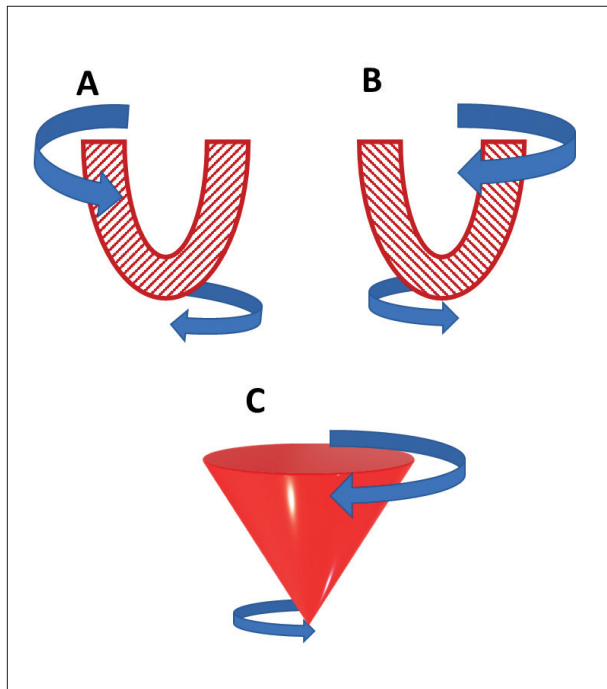


Figure 15.1 – Rotation direction of subendocardial fibers: (A) subepicardial fibers (B) overall LV rotation with (C) simultaneous contraction of the fibers. Adapted from Stöhr et al.³⁸⁴

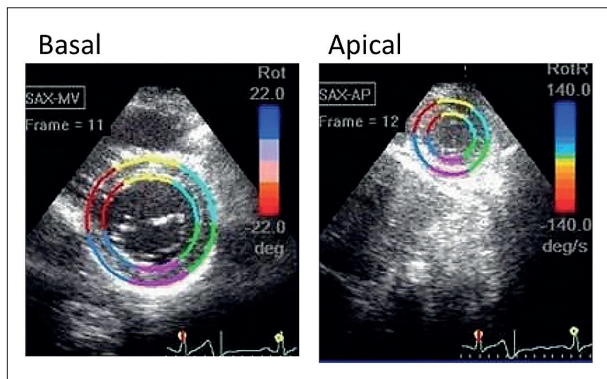


Figure 15.2 – Image acquisition plan for basal and apical rotation measurement (Images courtesy of Dr. Marcio Lima).

with reduced LVEF (ischemic and dilated cardiomyopathy) or preserved LVEF (HFpEF, hypertension, HCM, aortic stenosis, aortic insufficiency, and mitral insufficiency), as well as to assess subclinical myocardial dysfunction due to chemotherapy.

Twist and torsion measurements, although good parameters for global systolic function analysis, are limited in terms of reproducibility, which is mainly due to the lack of anatomical parameters for the apical section. The findings on ventricular twist and torsion changes are not specific, but they could contribute to a better understanding of the pathophysiology of different cardiomyopathies, helping differentiate them (Table 15.3).

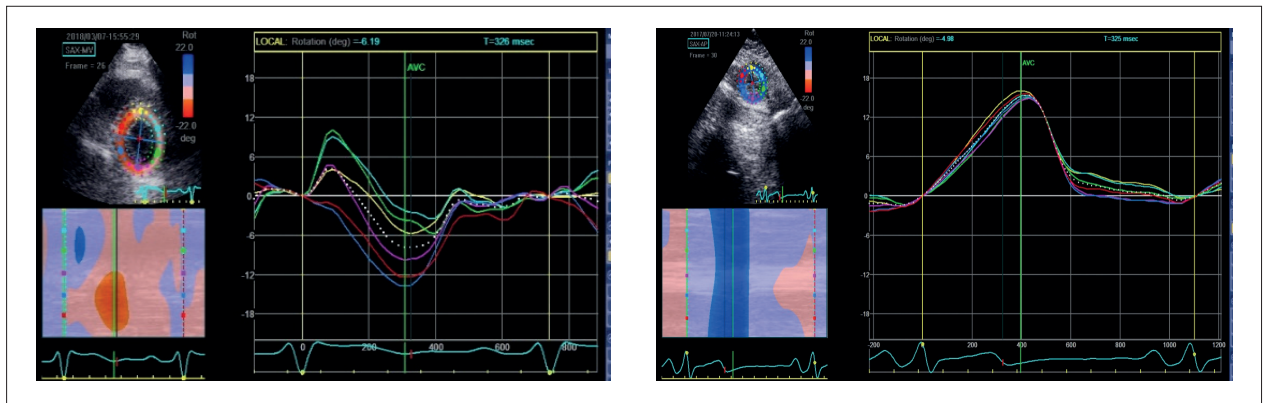


Figure 15.3 – Clockwise (below baseline) and counterclockwise (above baseline) rotation (Images courtesy of Dr. Marcio Lima).

Table 15.1 – Definitions and parameters used to assess left ventricular twist during systole

Parameter	Definition
Apical rotation (°)	Peak counterclockwise systolic rotation of the apical LV region (measured in degrees)
Apical rotation rate (°/s)	Peak counterclockwise apical rotation speed (measured in degrees/second)
Basal rotation (°)	Peak clockwise systolic rotation of the basal region of the LV (measured in degrees)
Basal rotation rate (°/s)	Peak basal clockwise rotation velocity (measured in degrees/second)
LV twist (°)	Peak difference of LV apex and base systolic rotation (measured in degrees)
LV torsion (°/cm)	Normalized twist: ratio of the twist angle and the distance between the base and apex in systole (measured in degrees/centimeter)
Twist rate (°/s)	Peak LV twist speed (measured in degrees/second)

(o): degrees; (o/s): degrees per second; (°/cm): degrees per centimeter. LV = left ventricle.

Table 15.2 – Definitions and parameters used to assess left ventricular twist mechanism in diastole

Parameter	Definition
Apical reverse rotation (°)	Peak clockwise diastolic rotation of the apical LV region (measured in degrees)
Apical reverse rotation rate (°/s)	Peak velocity of clockwise apical reverse rotation (measured in degrees/second)
Basal reverse rotation (°)	Peak diastolic counterclockwise rotation of the basal region of the LV (measured in degrees)
Basal reverse rotation rate (°/s)	Peak basal rotation speed (measured in degrees/second)
Untwist (°)	Difference in peak reverse diastolic rotation of the apex and base of the LV (measured in degrees)
Untwist Rate (°/s)	Peak LV untwist speed (measured in degrees/second)

(o): degrees; (o/s): degrees per second; LV = left ventricle.

Table 15.3 – Left ventricular twist in different cardiovascular diseases

Cardiovascular disease	LV twist	Findings
Ischemic cardiomyopathy	Decreased	Twist decreases depending on the location and extent of ischemia.
Dilated cardiomyopathy	Decreased	Twist decreases proportionally to decreased ejection fraction
Hypertrophic cardiomyopathy	Increased	Twist increases especially if the LV outflow tract is obstructed
Aortic stenosis	Increased	Increased twist in cases of increased LV afterload.

16. Strain in Ventricular Dyssynchrony Analysis

16.1. Introduction

Due to its expressive reduction of morbidity and mortality, cardiac resynchronization therapy (CRT) is indicated in national and international guidelines. CRT is a class I recommendation for symptomatic dilated cardiomyopathy patients who are undergoing optimized clinical treatment and have a left bundle branch block (LBBB) pattern in electrocardiography, QRS duration ≥ 150 ms, and LVEF $< 35\%$ (evidence level A).³⁸⁵

Due to a lack of data about echocardiographic synchrony assessment, these guidelines consider LBBB ≥ 150 ms as

Statement

a marker of dyssynchrony. However, echocardiography is also limited as a dyssynchrony marker. Thus, at present, echocardiographic dyssynchrony assessment for CRT selection must be performed in an individualized and judicious manner by an adequately trained examiner and interpreted together with the patient's clinical data. It is also important to remember that not only can echocardiography assess cardiac synchrony but it can help select the best site for LV electrode implantation, as well as determine response and reverse remodeling. More recent findings indicate that it can identify ventricular arrhythmia risk.³⁸⁵

16.2. Dyssynchrony Assessment when Selecting Patients for Cardiac Resynchronization Therapy

Assessing mechanical dyssynchrony and efficiency through strain alone is insufficient to indicate CRT. However, even with a precise recommendation, the chance of success (ie, improvement in clinical, functional, and/or imaging variables) is approximately 60%–70%. The CRT response rate can be estimated and even improved through echocardiography. In this context, myocardial strain measurement stands out.

Initial analysis of dyssynchrony through radial strain describes the time difference between maximum radial strain of the middle anteroseptal and inferolateral segments. Values > 130 ms indicate patients with a higher response rate,³⁸⁶ as shown in Figure 16.1.

In addition to radial dyssynchrony, independent predictors of long-term prognosis include an inhomogeneous pattern of septal rebound stretch in speckle-tracking and LV reverse remodeling with a higher value in LBBB and apical rocking detected by visual analysis. This pattern reflects incoordinated contraction, which results in reduced myocardial performance. Recent studies have indicated that septal rebound stretch assessment can improve patient selection for CRT, especially patients without defined LBBB.³⁸⁷ The pattern consists of 3 aspects of LS in the inferoseptal and anterolateral (frequently basal) segments: 1) peak opposition of the septal curves (negative) and lateral curves (positive); 2) peak negative septal strain in up to 70% of the ejection time; 3) peak negative strain in the lateral wall after aortic valve closure,³⁸⁸ as shown in Figure 16.2.

Global LVMW efficiency analysis has recently shown promise in CRT. Global LVMW efficiency can be quantified non-invasively through myocardial strain curves and blood pressure measurements. Lower global LVMW efficiency values have been independently associated with better long-term prognosis.³⁸⁹ Figure 16.3 shows changes in strain, MW, and myocardial efficiency in a patient who underwent successful CRT.

16.3. Myocardial Viability Assessment

Another application of myocardial strain in the CRT context is the correlation between myocardial fibrosis and reduced strain values. Reduced global radial strain values correlate with a greater degree of fibrosis (detected in cardiac MRI), thus identifying patients with a lower chance of ventricular function recovery. Reduced LS in patients with ischemic heart disease can also be used for this purpose.

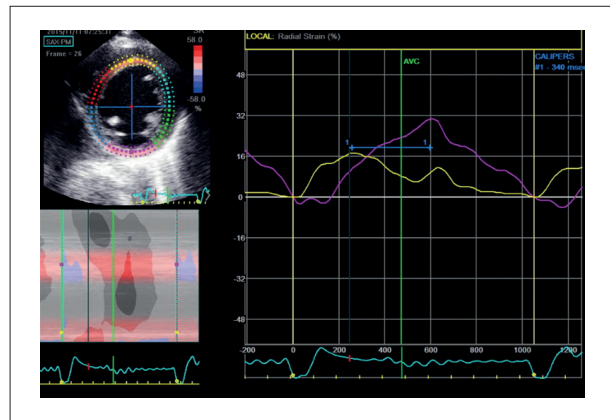


Figure 16.1 – Radial strain image showing curves for the middle segments of the anteroseptal and inferolateral walls. The interval > 130 ms correlates with a higher CRT response rate, in this case 340 ms.

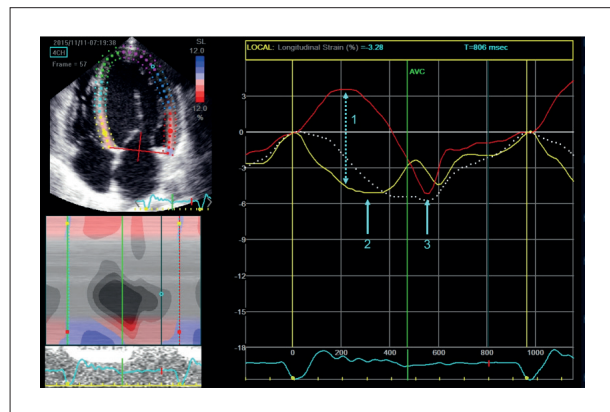


Figure 16.2– Longitudinal strain image with inferoseptal (yellow) and anterolateral (red) basal segment curves with typical left bundle branch block pattern: 1) initial opposition of the peak of the septal (negative) and lateral (positive) curves; 2) negative septal strain peak in ≤ 70% of the ejection time, with shortening interrupted during systole, ie, prior to aortic valve closure (AVC) resulting in systolic stretching; 3) negative strain peak in the lateral wall after AVC.

16.4. Electrode Implantation Site

Equally important as total LV fibrosis, compromised values at the LV electrode implantation site have been associated with lower CRT response. Studies have shown that positioning the LV electrode in the segment with the greatest delay in mechanical contraction results in higher CRT success rates. Speckle tracking can identify the segment that should be stimulated. In the TARGET study, LV electrode placement guided by 2D speckle-tracking resulted in better clinical response and lower rates of mortality and hospitalization for HF.^{390,391}

16.5. Prognostic Assessment after CRT

Post-CRT dyssynchrony analysis through LS is a strong predictor of ventricular arrhythmias. Speckle-tracking findings of persistent or increased mechanical scattering 6 months after CRT are associated with worse prognosis. Furthermore, CRT

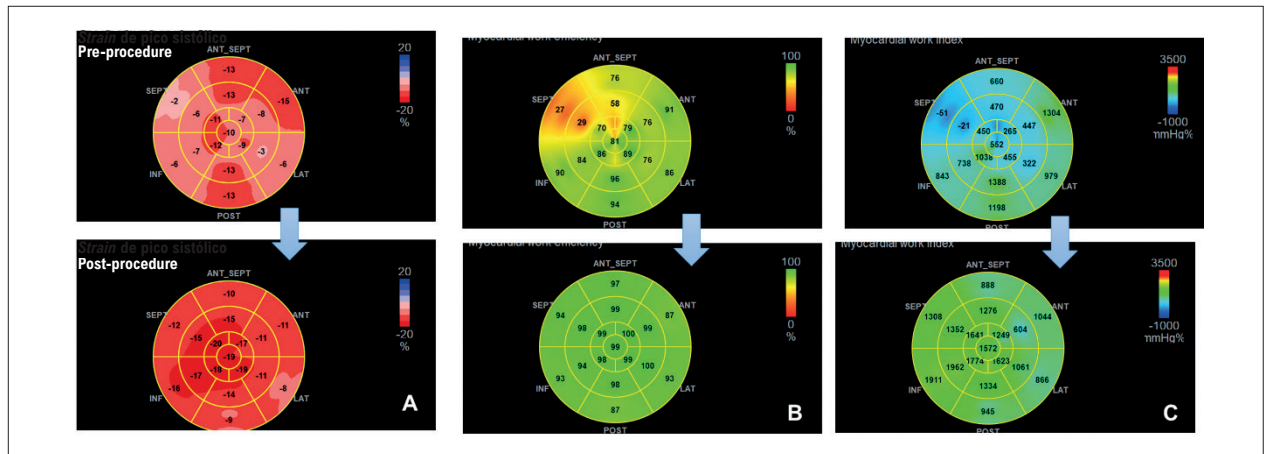


Figure 16.3 – Pre- and post-procedure polar maps of (A) longitudinal strain, (B) myocardial work, and (C) myocardial efficiency in a patient who underwent successful resynchronization therapy.

response (reverse remodeling) depends on improvement in both longitudinal and circumferential function after CRT.³⁹²

16.6. Adjustment of Resynchronization Parameters

About 30% of patients who undergo CRT are considered non-responders due to a lack of clinical and/or functional improvement, including a lack of reverse remodeling (evidenced by lower ventricular dimensions and higher EF).³⁹³ In these patients, adjustments to the atrioventricular, interventricular, and left intraventricular intervals may improve CRT response. Some studies have shown that speckle-tracking can guide adjustment of CRT parameters, leading to significant improvement in functional class and EF in non-responders.³⁹⁴

17. Myocardial Work

17.1. Introduction

Having recently emerged as an echocardiographic tool to increase information about ventricular function, MW adds the effects of LV afterload to LS measurement. After the experimental work of Suga et al. in 1979,³⁹⁵ which demonstrated that the area under the pressure-volume curve, invasively acquired with an intraventricular conductance catheter, reflected regional MW and oxygen consumption per beat, interest has grown in non-invasive imaging methods to make such analysis feasible.^{396,397}

In 2012, Russell et al.³⁹⁸ validated a non-invasive method of analyzing the LV pressure-strain loop, integrating systolic blood pressure at the time of speckle tracking LS assessment, which after interpretation by the software, calculates pressure-strain loops globally and per segment (Figure 17.1). The AUC represents MW, which is highly correlated with direct intraventricular measurements. MW also reflects regional myocardial oxygen metabolism comparably to positron emission tomography with 18F- fluorodeoxyglucose.³⁹⁹⁻⁴⁰¹

Modest increases in blood pressure can reduce GLS by up to 9%, which could be misinterpreted as reduced

contractility, when in fact MW remains preserved, reflecting only increased afterload. Thus, MW is considered an advance in the understanding of ventricular mechanics.^{398,402} The main differences between MW and the LV strain are shown in Table 17.1.

17.2. Calculating Myocardial Work

To obtain accurate and reproducible results, appropriate MW calculation techniques must be used for image acquisition, as well as post-processing and parameter analysis. This technology is currently only available in workstations or devices embedded with GE software (GE Healthcare, Horten, Norway). Analyses can be performed directly on the device or post-processed in workstations using previously acquired images.

The image acquisition protocol for calculating MW follows the same technical prerequisites for GLS analysis, which will be discussed in a subsequent chapter. After 2D strain is assessed using images acquired in the 3 apical

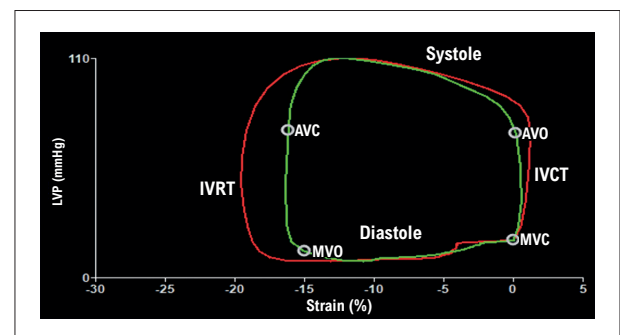


Figure 17.1 – Left ventricular pressure-strain loop. Red: global pressure-strain loop. Green: pressure-strain loop for the basal segment of the inferolateral wall. AVC: aortic valve closure; AVO: aortic valve opening; IVCT: isovolumetric contraction time; IVRT: isovolumetric relaxation time LVP: left ventricular pressure estimated by systolic blood pressure; MVC: mitral valve closure; MVO: mitral valve opening.

Statement

Table 17.1 – Main differences between myocardial work and left ventricular strain

	Strain	Myocardial work
AFI use	yes	yes
Measure	AVO-AVC	IVCT + ET + IVRT
Integrated with blood pressure	no	yes
Value	%	mmHg%
Incorporates postload	no	yes
Measures efficiency	no	yes
Estimates myocardial oxygen consumption	no	yes

AFI: automated functional imaging AVO: Aortic valve opening; AVC: AV closure; IVCT: isovolumetric contraction time; ET: ejection time; IVRT: isovolumetric relaxation time.

projections through automated functional imaging, MW can be evaluated by the software (Figure 17.2). Blood pressure values measured non-invasively at the time of the examination must be manually entered into the patient identification form during the examination or later into the MW calculation form itself (Figure 17.3). These non-invasive blood pressure measurements will be automatically input into the pressure-strain loop.

For temporal indexing of the values, the events of the cardiac cycle must be marked, identifying the opening and closing of the mitral and aortic valves. This can be performed through spectral Doppler or 2D analysis of mitral and aortic flow through an apical 3-chamber projection, which shows the opening and closing of both valves (Figure 17.4). These points can also be marked on the MW calculation screen, modifying apical 3-chamber image frame-by-frame, selecting the exact moment of each event (Figure 17.5). After checking the images and markings, the software performs the calculations and displays a polar (bull's-eye) map beside GLS and peak strain values for each segment. A polar map with the MW index for each segment appears on the right side, with global MW index and MW efficiency values below it. When the “work efficiency” key is selected, the software shows the global MW efficiency values for each segment on the polar map (Figure 17.6). Selecting the “advanced” key generates curves and graphs of the LV pressure-strain loops throughout the cardiac cycle, in addition to a bar graph showing the proportions of constructive and wasted MW (Figure 17.7).

The following parameters are provided by the software:

1. Global MW index: total work in the area under the pressure-strain curve, calculated from the closing to the opening of the mitral valve. A bull's eye map with segmental and global MW values is provided (Figure 17.6).
2. Constructive MW: work that contributes to LV ejection during systole, obtained by shortening during systole plus myocyte elongation during isovolumetric relaxation (Figure 17.7).
3. Wasted MW: work that does not contribute to LV ejection, obtained by myocyte elongation (rather than shortening) during systole plus shortening during the isovolumetric relaxation phase (post-systolic shortening) (Figure 17.7).
4. MW efficiency (MW efficiency/global MW efficiency): the result of the following formula: constructive MW / (constructive MW + wasted MW); efficiency is rated as 0-100% (Figure 17.6).

17.3. Normality Values

Due to the recent validation of MW and its variables for clinical use, multicenter trials with an adequate number of patients have not yet been conducted to produce definitive normality values.

Manganaro et al. recently analyzed data from the NORRE study to establish normal reference limits for MW. This prospective European multicenter study included 226 patients from 22 echocardiography laboratories, providing reference values for most 2D and 3D echocardiographic data.⁴⁰³ The mean or median (SD) and/or CI of MW variables were, respectively, 1896 (SD, 308) mm Hg% (CI: 1292-2505) for global MW index, 2232 (SD, 331) mm Hg% (CI: 1582-2881) for constructive MW, 79 mm Hg% (CI: 53-122) for wasted MW, and 96% (CI: 94-97), for global MW efficiency.⁴⁰³

Another study found higher global MW index and constructive MW values in women > 40 years of age, with a strong correlation between a higher global MW index and constructive MW values and higher systolic blood pressure.⁴⁰⁴

17.4. Potential Clinical Use

A major limitation to more widespread use of MW is that the software is only produced by GE Healthcare. In addition, MW is calculated using manual systolic pressure measurements in afterload. Care should be taken in clinical situations involving additional afterload or increased systolic blood pressure, such as aortic stenosis, obstructive HCM, and some congenital heart diseases. Despite its promise as new tool, current scientific knowledge about MW assessment is still in the research phase.

Certain publications on MW in clinical practice are gaining notoriety, one of which involves patient selection for myocardial resynchronization. Although LBBB analysis can sometimes be difficult to interpret (Figure 17.8), visual and quantitative analysis of MW has made it easier to recognize cases of QRS widening without an associated mechanical dyssynchrony (Figure 17.9). In addition to visual analysis, the ability of constructive MW to identify CRT responders has been recognized as equivalent to contractile reserve.⁴⁰⁵ Another interesting way to identify patients who benefit from CRT is through wasted septal work.⁴⁰⁶ Thus, MW assessment in patients with LBBB can improve stratification through visual analysis, as well as quantify constructive and wasted work.

Another interesting field for MW assessment is obstructive coronary disease. MW can detect obstructive coronary disease at rest better than LVGLS, even in patients with preserved EF and no segmental contractility changes.⁴⁰⁷ MW can also

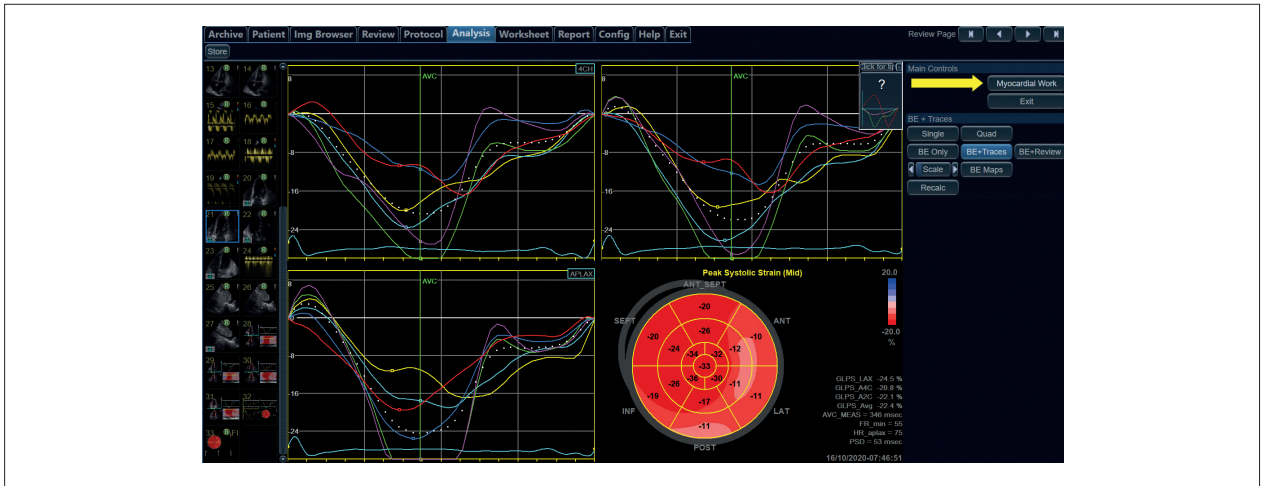


Figure 17.2 – After assessing 2D LV longitudinal strain with the automated functional imaging method and processing the 3 apical windows, the software offers to calculate myocardial work (yellow arrow).

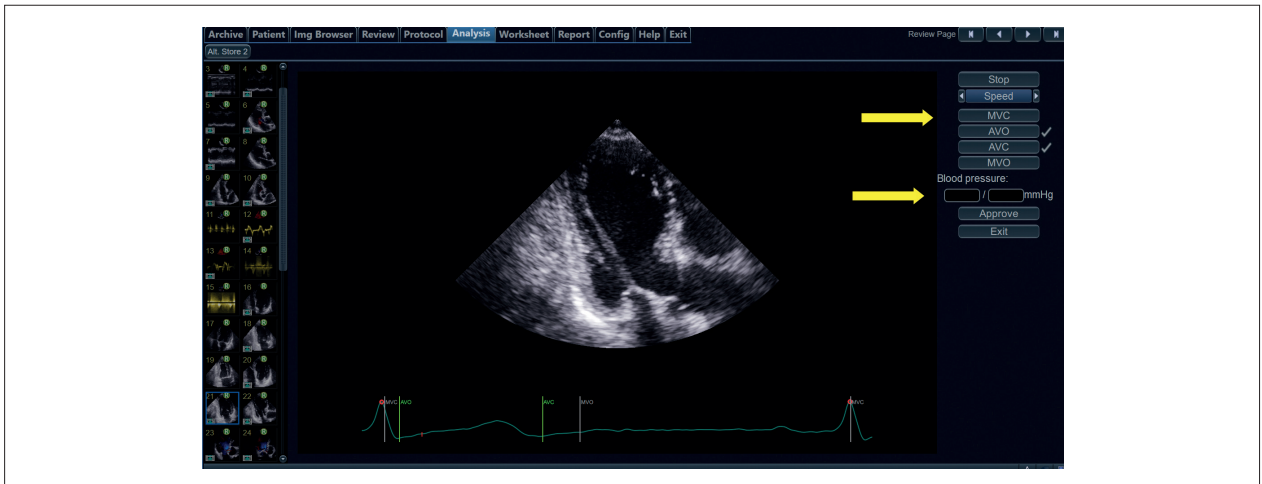


Figure 17.3 – Initial screen of myocardial work calculation. In this step, non-invasively measured blood pressure values can be inserted (bottom arrow), and cardiac events, such as the opening and closing of the mitral and aortic valves can be reassessed or marked (top arrow).

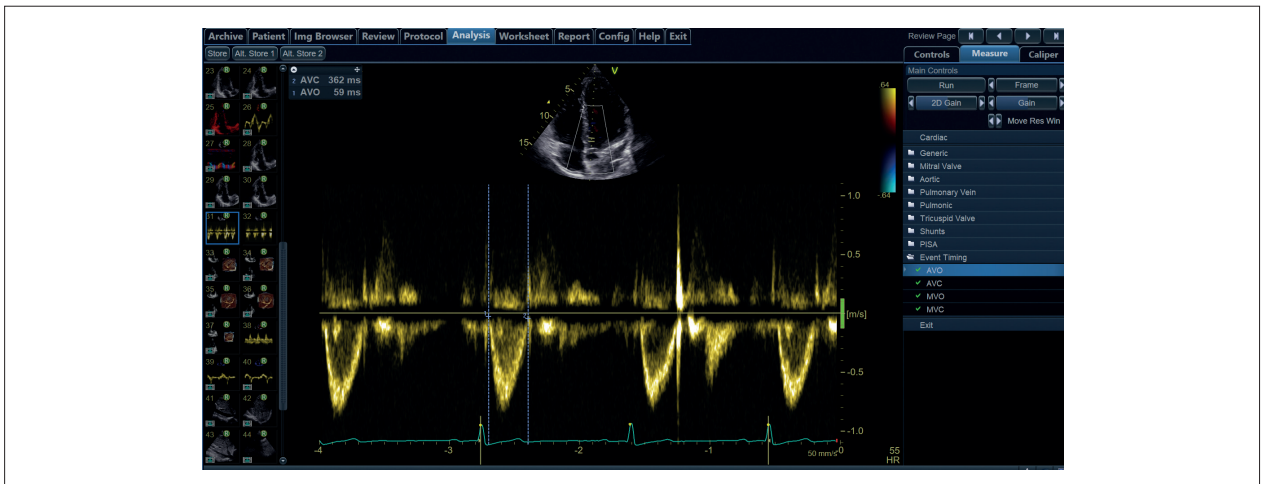


Figure 17.4 – Marking cardiac events through spectral Doppler: A) marking mitral valve opening (MVO) and mitral valve closing (MVC) according to mitral inflow; B) marking aortic valve opening (AVO) and aortic valve closing (AVC) through LV outflow.

Statement



Figure 17.5 – Cardiac events can also be marked on the myocardial work calculation screen, modifying apical 3-chamber images frame by frame and selecting the exact moment of each event in the right sidebar menu (arrows).

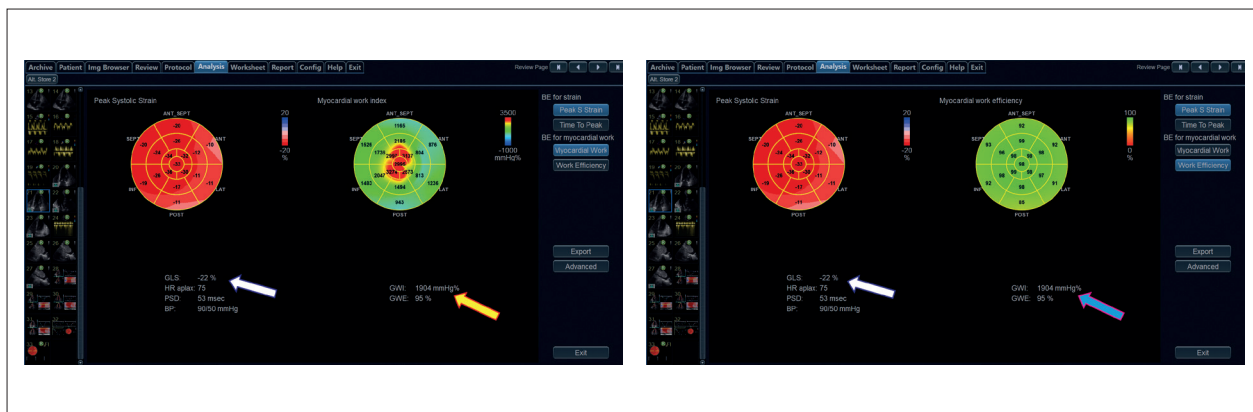


Figure 17.6 – After approval of the obtained data, appropriately marking events and pressure filling, the software displays the global and segmental longitudinal strain values on the left (white arrows) and polar maps with myocardial work index values (A: yellow arrow) and myocardial work efficiency (B: blue arrow).

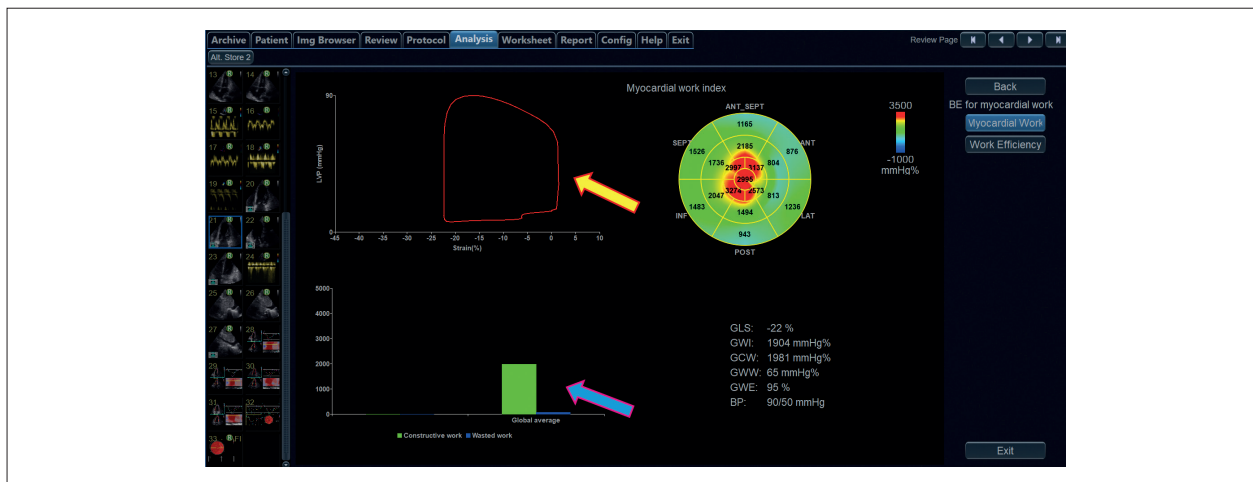


Figure 17.7 – Selecting the “advanced” key shows analyses by curves and graphs, showing the LV pressure-strain loops throughout the cardiac cycle (yellow arrow), in addition to a bar chart showing the proportions of constructive and wasted MW (blue arrow).



Figure 17.8 – Two cases with similar left bundle branch block morphologies.

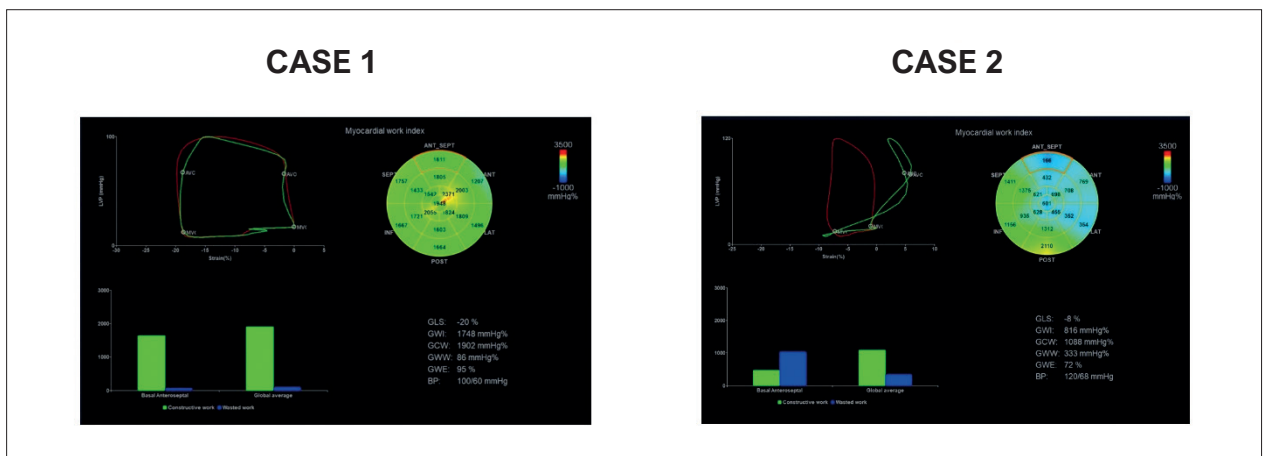


Figure 17.9 – Case 1 has no changes in myocardial mechanics: myocardial work in the pressure-strain loop (green line) is similar to the global value (red line). In case 2, “true” left bundle branch block; in the same septal portion, the green line assumes a figure-8 shape.

identify AMI patients at greater risk of complications and predict recovery,⁴⁰⁸ as well as predict long-term complications in patients with ST-elevation MI.⁴⁰⁹

In addition to these clinical situations, MW has shown promise for dilated cardiomyopathy, HCM, amyloidosis, and other conditions. Certainly, with greater software availability and more evidence in the literature, MW will quickly be incorporated into clinical practice.

18. Three-dimensional Strain Assessment: What can be Added

18.1. Introduction

Three-dimensional myocardial strain assessment through speckle tracking has numerous advantages over 2D assessment. Considering that the LV myocardium consists of 3 layers of fibers arranged in different directions (longitudinal,

circumferential, and transverse), the speckles have a non-linear trajectory, escaping the image’s 2D plane during part of the cardiac cycle. Although multiple longitudinal and transverse images of the LV myocardium may be acquired in 2D assessment, the speckles are interpolated. Thus the method is not as accurate as 3D, which allows monitoring throughout the cardiac cycle in multiple dimensions, being unaffected by extraplanar myocardial torsion or apical shortening.⁴¹⁰

In the RV, global analysis of myocardial chambers is only possible through 3D methodology, whereas only the septum and/or free wall can be assessed in 2D. Furthermore, 3D strain assessment is more reliable and physiological, since different components of myocardial strain are analyzed simultaneously through a single dataset or cardiac cycle. Thus, 3D strain is a quantitative, objective, comprehensive, and reproducible assessment of myocardial mechanical function. However, it strongly depends on a good

Statement

acoustic window and a regular heart rhythm, which limit the routine and systematic incorporation of 3D strain.⁴¹¹ Clinical application is also limited by differences in the algorithms for monitoring the speckles and cut-off points for myocardial strain, which are not standardized across software platforms.^{412,413}

Since 3D strain measurements obtained through different equipment and software manufacturers are not interchangeable, the baseline and follow-up imaging, as well as the analyses, must be performed using the same equipment, and the results must be interpreted in light of the equipment's specific normality values.^{410,412} Normality reference values also vary between 2D and 3D methodologies, with only a modest correlation between LS values. Finally, further clinical research is needed to determine the accuracy and prognostic value of 3D strain assessment.

18.2. Left Ventricular Strain

Three-dimensional speckle-tracking is superior to 2D speckle tracking in that it is not limited to a single slice and that it allows analysis of vectorized data in 3 orthogonal planes. Two-dimensional strain assessment requires a very high temporal resolution (34-50 volumes per second) due to the short duration of the speckles (ie, a few milliseconds) in the slice, which does not occur in 3D. Additionally, the ideal in 3D speckle tracking is to acquire 6 beats at the highest line density and 44 volumes per second at a frequency of 2-4 MHz (which is more accurate than MRI). Acquisition of single volumes is not recommended, since higher temporal resolution decreases image and tracking quality by reducing line density.⁴¹⁴

The general feasibility of 3D speckle-tracking is approximately 85% due to the following limitations: unfavorable acoustic windows, cardiac arrhythmias (preventing acquisition of multiple beats), incomplete visualization of the apical segments of the LV and RV, speckle-tracking problems in follow-up (distance from the transducer), and determining normal values and clinical prognosis.

18.3. Right Ventricular Strain

The analysis of RV contraction is especially important to understand the mechanism of this chamber in the face of congenital and acquired diseases. However, unlike the LV, estimating the RV is more difficult due to the complex shape that the RV presents and due to its thin wall. Despite this, MRI images and speckle tracking by echocardiography have been promising in right ventricular analysis. However, the values obtained by ST3D for the RV are still not well established.⁴¹⁵ Technical problems persist for the 3D strain analysis when the objective is to analyze the right chambers, since the software was created for the analysis of the LV and still is adapted for the RV on most machines. Although the 3D strain allows global analysis of the entire right myocardium, the three-dimensional technology for this chamber is still in progress, with no well-defined cutoff values for the 3D strain of the RV so far.

18.3.1. Full-volume 3D Acquisition and Analysis

Harmonic imaging ideally provides 4 triggered beats per capture. The depth must be adequate so that only the RV, its walls, and the tricuspid annulus fill the volume; the systolic peak strain is generally used for analysis.

18.4. Left Atrial Strain

In 3D strain assessment of the LA (as well as the ventricles), ultrasound can acquire volumetric data in real time and can measure all strain components. However, 3D tracking is a great challenge, and the temporal and spatial resolution of 3D is lower than 2D, which makes 3D analysis more complex and time consuming, since high image quality is required to determine 3D strain.

Another point under discussion is inter- and intraobserver variability in cardiac mechanics.⁴¹⁴ The reservoir, conduit, and pumping phases can be well analyzed in 2D strain, and the mean cut-off values for 2D strain in each of these phases have been relatively well defined. However, reference values for 3D strain have not yet been determined. When strain analysis becomes relevant, the main applications of this method in the LV are: HFpEF,⁷ intracavitary filling pressures,⁹⁵ atrial function among elite athletes,⁴¹⁶ and cardiomyopathies.⁴¹⁷ Nevertheless, 2D strain data have been better corroborated than 3D strain data; the incorporation of 3D strain in LA assessment will depend on future research.

19. The Role of Cardiac Resonance and Tomography in Strain Assessment

19.1. Introduction

Due to its high spatial and temporal resolution and non-invasiveness, cardiac MRI has become an important method of assessing global and segmental function in both ventricles. Strain assessment, an established and reliable method for measuring and quantifying regional and global contractile dysfunction, can detect subclinical cardiac dysfunction and, thus, is useful for assessing myocardial function. Echocardiography is currently the most available and least expensive method for assessing strain, but analysis may be impaired in patients with a limited acoustic window.

19.2. Strain Acquisition Methods by Cardiac Magnetic Resonance Imaging

Myocardial tagging, consisting of a preparation phase in which magnetic tags (black lines) are orthogonally superimposed on the myocardium at the beginning of a cine sequence, is the most validated technique for assessing strain in cardiac MRI.^{12,418} Alternatives to tagging that provide direct analysis of myocardial strain in cardiac MRI are cine strain encoding and cine displacement encoding with stimulated echoes.⁴¹⁹ Feature tracking (FT), a recently developed method, can quantify myocardial strain in traditional cine cardiac MRI images without additional acquisitions or lengthy analysis.^{420,421}

In all strain analysis techniques, the global circumferential and LS parameters have proven more reproducible and consistent than regional ones.⁴²² Further details about strain acquisition through cardiac MRI can be found in the references.^{12,418-422}

19.3. Determining Right Ventricle Strain Through Cardiac Magnetic Resonance Imaging

Myocardial strain measurement is an accurate and practical method for assessing RV function, since it is an earlier and more sensitive marker of contractile dysfunction than other methods, such as EF. Studies have demonstrated the potential of RV cardiac MRI strain to provide additional information and independent prognosis.⁴²³⁻⁴²⁸ A number of studies have analyzed RV strain in healthy individuals and control groups without heart disease.^{423,426,429,430}

The pathologies that most affect RV, such as congenital heart disease, pulmonary hypertension, and arrhythmogenic dysplasia, have the greatest applicability in RV strain analysis. One study used cardiac MRI FT in patients with corrected tetralogy of Fallot, finding lower strain values in these patients than controls, which were related to systolic function parameters (biventricular EF), as well as functional capacity in cardiopulmonary testing.⁴²⁵

Assessing global and segmental RV function is fundamental for multi-parametric diagnosis of arrhythmogenic dysplasia, and RV strain has proven an extremely useful tool in this regard.^{428,431} Global and segmental RV strain are significantly lower in patients with arrhythmogenic dysplasia, regardless of RV dimensions and function, and impaired RV strain may represent an early marker of the disease.⁴²⁸ Figure 19.1 presents examples of RV strain in a normal patient and a patient with pulmonary hypertension.

19.4. Determining Left Ventricular Strain Through Cardiac Magnetic Resonance Imaging

In healthy individuals, mean values for LV strain types (global circumferential strain, global radial strain, and GLS) have been determined over the past decade with cardiac MRI FT,⁴¹⁹⁻⁴²³ including a major meta-analysis.⁴²⁴ The largest and most recent studies on global circumferential strain and global radial strain by cardiac MRI FT analyzed the mean of 3 short-axis slices. In most cases, LVGLS was calculated using a 4-chamber slice, while more recent publications assessed the mean of 3 longitudinal slices. GLS and global circumferential strain values varied within a narrow range while global radial strain values had wider confidence intervals; it is speculated that planar movement and large personal variability could partially explain this phenomenon, although the real cause still remains uncertain.⁴²⁴

There is a strong relationship between myocardial strain and delayed myocardial enhancement, especially global circumferential strain, in addition to GLS derived from cardiac MRI FT. There is also good correlation between echocardiography-derived techniques and cardiac MRI.⁴²⁵

In dilated cardiomyopathy, markedly lower GLS is strongly associated with worse survival, even in patients with very low EF, regardless of functional class and other cardiac MRI

findings.⁴²⁶ Cardiac MRI FT can identify HFpEF and DD subgroups through altered GLS.⁴²⁷

The diagnostic value of cardiac MRI GLS and echocardiography GLS are similar when differentiating between constrictive pericarditis and restrictive cardiomyopathy, having a high discriminatory value. GLS values are significantly lower in restrictive cardiomyopathy, while they are close to normal in pericarditis.⁴²⁸ Longitudinal and circumferential strain are also altered in myocarditis.⁴²⁹

Studies on MRI strain and myocardial tagging have found a high capacity to determine amyloidosis carriers; this method could even be more sensitive than the post-contrast sequence itself.⁴³⁰ The lost base-apex gradient of circumferential strain seems to be an early finding of Fabry disease, since longitudinal and circumferential strain did not vary significantly from healthy controls.⁴³¹

According to cardiac MRI FT, patients with HCM have lower GLS, global radial strain, and global circumferential strain than healthy controls, with GLS and global radial strain being predictors of adverse events,⁴³² just as significantly higher GLS has been found in hypertension patients than HCM patients.⁴³³

Ischemic coronary disease diagnosis by cardiac MRI can be improved by adding FT analysis, allowing detection of small changes in circumferential strain after dobutamine stress; GLS may be useful for detecting infarctions and assessing viability.⁴³⁴ The 3 types of strain are reduced in patients who have suffered acute myocardial infarction with ST-segment elevation, being independent predictors of adverse cardiovascular events.⁴³⁵

Patients with severe aortic stenosis have lower GLS and global circumferential strain than healthy controls, despite the symptoms.⁴³⁶ In patients with bicuspid aortic valve and preserved EF, signs of DD have been observed through circumferential strain changes.⁴³⁷ Chemotherapy-induced cardiotoxicity results in GLS and global circumferential strain abnormalities long before LVEF is reduced.⁴³⁸

A recent study reported that cardiac MRI FT-derived GLS has a stronger association with mortality than a combination of LVEF and myocardial delayed enhancement. This has been the largest study to date to assess prognosis through cardiac MRI FT-derived GLS. After adjusting for classic risk factors, including LVEF and myocardial delayed enhancement, a 1% worsening in GLS was associated with an 89% higher mortality risk in both ischemic and non-ischemic patients.⁴³⁹

19.5. Determining Left Atrial Strain Through Cardiac Magnetic Resonance Imaging

LA function assessment has been increasingly recognized as a factor in a variety of cardiac pathologies. Change in LA function is normally associated with worse prognosis and precedes HF diagnosis. The LA functions as a reservoir for pulmonary vein drainage, serving as a conduit for flow to the LV due to a pressure difference due to mitral leaflets opening and contractile function, with atrial systole occurring at the end of LV diastole.⁴⁴⁰

Cardiac MRI FT-derived atrial strain analysis reliably quantifies LA longitudinal strain and strain rate. Using standard cine MRI images, it can differentiate between patients with

Statement

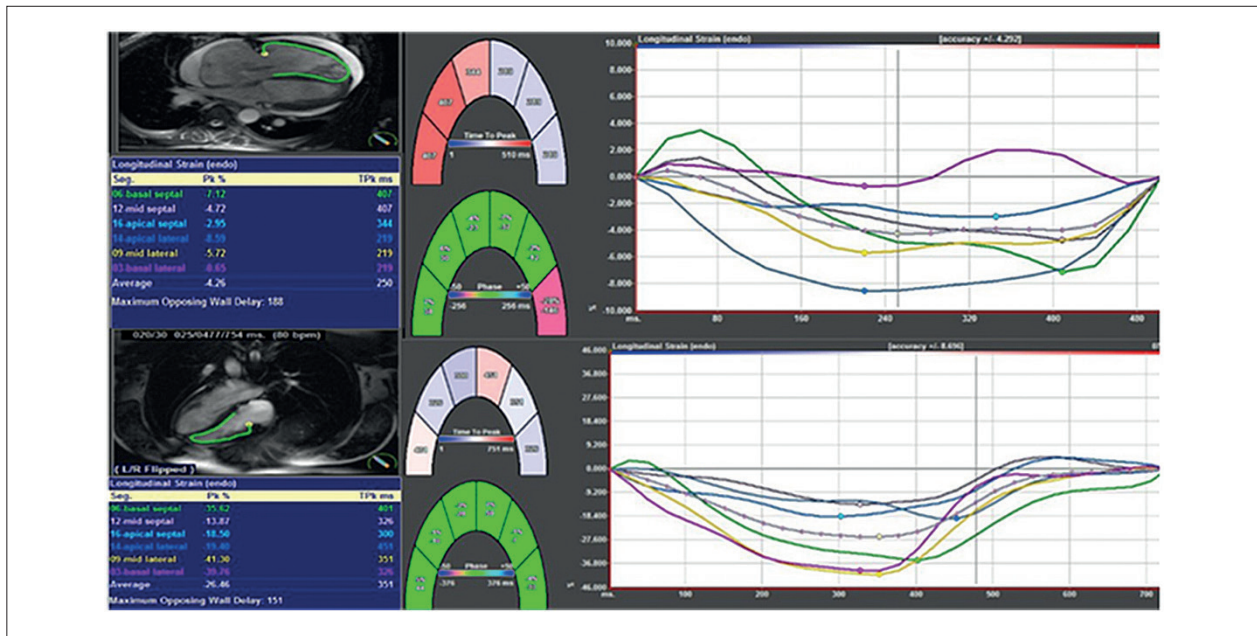


Figure 19.1 – Global longitudinal strain analysis through feature tracking in patients with (above) and without pulmonary hypertension (below). GLS was 4.26% and 26.46% in the patients with and without pulmonary hypertension, respectively.

altered LV relaxation and healthy patients, as shown in Table 19.1.⁴⁴¹ In a MESA substudy, global peak longitudinal atrial strain and LA volume indexes were independent predictors of HF onset, even after adjusting for LV mass and N-terminal pro-B-type natriuretic peptide.⁴⁴² LA phasic function has been found to be an independent risk predictor for mortality or hospitalization for HF, even after adjusting for LA volume and ventricular remodeling.⁴⁴³

19.6. Determining Strain Through Cardiac Tomography

Strain can be assessed through cardiac tomography FT using contrast and triggered acquisitions, functionally reconstructing the cardiac cycle. Although data are still scarce, this method has been tested in patients with significant aortic stenosis undergoing transcatheter aortic prosthesis implantation. Similar GLS values were found between cardiac tomography FT and echocardiography,^{444,445} including high intraobserver and intraclass reproducibility for cardiac tomography FT LVGLS, despite apparently underestimating the values.⁴⁴⁴

Another study explored the relationship between cardiac tomography FT-derived strain and ischemic heart disease in

patients with significant lesions in the left anterior descending artery. Lower LS was observed in segments related to the anterior descending artery, despite normal diastolic and systolic volumes and EF.⁴⁴⁶

Currently, strain assessment through cardiac MRI and cardiac tomography is limited due to availability issues and the high cost of post-processing software. However, like strain assessed through echocardiography, its application has been well established, facilitating early diagnosis of dysfunction in various cardiomyopathies.

Table 19.1 – Left Atrial Strain

Type	HFpEF	HCM	Normal
Reservoir	16.3 ± 5.8	22.1 ± 5.5	29.1 ± 5.3
Conduit	11.9 ± 4.0	10.4 ± 3.9	21.3 ± 5.1
Pump	4.5 ± 2.9	11.7 ± 4.0	7.8 ± 2.5

HCM: Hypertrophic cardiomyopathy; HFpEF: Heart failure with preserved ejection fraction.

References

- Loizou CP, Pattichis CS, D'Hooge J. Handbook of Speckle Filtering and Tracking in Cardiovascular Ultrasound Imaging and Video. London: The Institution of Engineering and Technology; 2018.
- Sutherland GR, Di Salvo G, Claus P, D'hooge J, Bijnens B. Strain and Strain Rate Imaging: A New Clinical Approach to Quantifying Regional Myocardial Function. J Am Soc Echocardiogr. 2004;17(7):788-802. doi: 10.1016/j.echo.2004.03.027.
- D'hooge J, Heimdal A, Jamal F, Kukulski T, Bijnens B, Rademakers F, et al. Regional Strain and Strain Rate Measurements by Cardiac Ultrasound: Principles, Implementation and Limitations. Eur J Echocardiogr. 2000;1(3):154-70. doi: 10.1053/euje.2000.0031.
- Tressino CG, Hortegal RA, Momesso M, Barretto RBM, Le Bihan D. Como eu Faço: Avaliação do Strain do Ventrículo Esquerdo. Arq Bras Cardiol: Imagem Cardiovasc. 2020;33(4):ecom15. doi: 10.47593/2675-312X/20203304ecom15.

5. Hortegal R, Abensur H. Strain Echocardiography in Patients with Diastolic Dysfunction and Preserved Ejection Fraction: Are We Ready? *Arq Bras Cardiol: Imagem Cardiovasc.* 2017;30(4):132-9. doi: 10.5935/2318-8219.20170034.
6. Bijmens B, Cikes M, Butakoff C, Sitges M, Crispi F. Myocardial Motion and Deformation: What Does It Tell Us and How Does It Relate to Function? *Fetal Diagn Ther.* 2012;32(1-2):5-16. doi: 10.1159/000335649.
7. Voigt JU, Pedrizzetti G, Lysyansky P, Marwick TH, Houle H, Baumann R, et al. Definitions for a Common Standard for 2D Speckle Tracking Echocardiography: Consensus Document of the EACVI/ASE/Industry Task Force to Standardize Deformation Imaging. *J Am Soc Echocardiogr.* 2015;28(2):183-93. doi: 10.1016/j.echo.2014.11.003.
8. Albuquerque PH, Del Castillo JM, Borba L, Ferro CM, Cabral C Jr; Everaldo A Filho, et al. Avaliação da Área de Risco Funcional pela Análise do Strain Miocárdico na Angina Instável. *Arq Bras Cardiol: Imagem Cardiovasc.* 2020;33(3):eabc73. doi: 10.5935/2318-8219.20200039.
9. Collier P, Phelan D, Klein A. A Test in Context: Myocardial Strain Measured by Speckle-Tracking Echocardiography. *J Am Coll Cardiol.* 2017;69(8):1043-56. doi: 10.1016/j.jacc.2016.12.012.
10. Potter E, Marwick TH. Assessment of Left Ventricular Function by Echocardiography: The Case for Routinely Adding Global Longitudinal Strain to Ejection Fraction. *JACC Cardiovasc Imaging.* 2018;11(2 Pt 1):260-74. doi: 10.1016/j.jcmg.2017.11.017.
11. Castel AL, Menet A, Ennezat PV, Delelis F, Le Goffic C, Binda C, et al. Global Longitudinal Strain Software Upgrade: Implications for Intervendor Consistency and Longitudinal Imaging Studies. *Arch Cardiovasc Dis.* 2016;109(1):22-30. doi: 10.1016/j.acvd.2015.08.006.
12. Tee M, Noble JA, Bluemke DA. Imaging Techniques for Cardiac Strain and Deformation: Comparison of Echocardiography, Cardiac Magnetic Resonance and Cardiac Computed Tomography. *Expert Rev Cardiovasc Ther.* 2013;11(2):221-31. doi: 10.1586/erc.12.182.
13. Farsalinos KE, Daraban AM, Ünlü S, Thomas JD, Badano LP, Voigt JU. Head-to-Head Comparison of Global Longitudinal Strain Measurements among Nine Different Vendors: The EACVI/ASE Inter-Vendor Comparison Study. *J Am Soc Echocardiogr.* 2015;28(10):1171-81. doi: 10.1016/j.echo.2015.06.011.
14. Mirea O, Pagourelas ED, Duchenne J, Bogaert J, Thomas JD, Badano LP, et al. Intervendor Differences in the Accuracy of Detecting Regional Functional Abnormalities: A Report From the EACVI-ASE Strain Standardization Task Force. *JACC Cardiovasc Imaging.* 2018;11(1):25-34. doi: 10.1016/j.jcmg.2017.02.014.
15. Sousa RD, Regis CDM, Silva IDS, Szewierenko P, Hortegal RA, Abensur H. Software for Post-Processing Analysis of Strain Curves: The D-Station. *Arq Bras Cardiol.* 2020;114(3):496-506. doi: 10.36660/abc.20180403.
16. Voigt JU, Cvijic M. 2- and 3-Dimensional Myocardial Strain in Cardiac Health and Disease. *JACC Cardiovasc Imaging.* 2019;12(9):1849-63. doi: 10.1016/j.jcmg.2019.01.044.
17. Buggey J, Alenezi F, Yoon HJ, Phelan M, DeVore AD, Khouri MC, et al. Left Ventricular Global Longitudinal Strain in Patients with Heart Failure with Preserved Ejection Fraction: Outcomes Following an Acute Heart Failure Hospitalization. *ESC Heart Fail.* 2017;4(4):432-39. doi: 10.1002/ehf2.12159.
18. Nahum J, Bensaid A, Dussault C, Macron L, Clémence D, Bouhemad B, et al. Impact of Longitudinal Myocardial Deformation on the Prognosis of Chronic Heart Failure Patients. *Circ Cardiovasc Imaging.* 2010;3(3):249-56. doi: 10.1161/CIRCIMAGING.109.910893.
19. Motoki H, Borowski AG, Shrestha K, Hu B, Kusunose K, Troughton RW, et al. Right Ventricular Global Longitudinal Strain Provides Prognostic Value Incremental to Left Ventricular Ejection Fraction in Patients with Heart Failure. *J Am Soc Echocardiogr.* 2014;27(7):726-32. doi: 10.1016/j.echo.2014.02.007.
20. Phelan D, Collier P, Thavendiranathan P, Popović ZB, Hanna M, Plana JC, et al. Relative Apical Sparing of longitudinal Strain Using Two-Dimensional Speckle-Tracking Echocardiography is Both Sensitive and Specific for the Diagnosis of Cardiac Amyloidosis. *Heart.* 2012;98(19):1442-8. doi: 10.1136/heartjnl-2012-302353.
21. Plana JC, Galderisi M, Barac A, Ewer MS, Ky B, Scherrer-Crosbie M, et al. Expert Consensus for Multimodality Imaging Evaluation of Adult Patients During and after Cancer Therapy: A Report from the American Society of Echocardiography and the European Association of Cardiovascular Imaging. *Eur Heart J Cardiovasc Imaging.* 2014;15(10):1063-93. doi: 10.1093/ehjci/jeu192.
22. Writing Group Members; Doherty JU, Kort S, Mehran R, Schoenhagen P, Soman P, et al. ACC/AATS/AHA/ASE/ASNC/HRS/SCAI/SCCT/SCMR/STS 2019 Appropriate Use Criteria for Multimodality Imaging in the Assessment of Cardiac Structure and Function in Nonvalvular Heart Disease: A Report of the American College of Cardiology Appropriate Use Criteria Task Force, American Association for Thoracic Surgery, American Heart Association, American Society of Echocardiography, American Society of Nuclear Cardiology, Heart Rhythm Society, Society for Cardiovascular Angiography and Interventions, Society of Cardiovascular Computed Tomography, Society for Cardiovascular Magnetic Resonance, and the Society of Thoracic Surgeons. *J Am Soc Echocardiogr.* 2019;32(5):553-79. doi: 10.1016/j.echo.2019.01.008.
23. Hajjar LA, Costa IBSDSD, Lopes MACQ, Hoff PMG, Diz MDPE, Fonseca SMR, et al. Brazilian Cardio-oncology Guideline - 2020. *Arq Bras Cardiol.* 2020;115(5):1006-43. doi: 10.36660/abc.20201006.
24. McMurray JJ, Packer M, Desai AS, Gong J, Lefkowitz MP, Rizkala AR, et al. Angiotensin-Nepriylsin Inhibition versus Enalapril in Heart Failure. *N Engl J Med.* 2014;371(11):993-1004. doi: 10.1056/NEJMoa1409077.
25. Pocock SJ, Ariti CA, McMurray JJ, Maggioni A, Køber L, Squire IB, et al. Predicting Survival in Heart Failure: A Risk Score Based on 39 372 Patients from 30 Studies. *Eur Heart J.* 2013;34(19):1404-13. doi: 10.1093/eurheartj/ehs337.
26. Ponikowski P, Voors AA, Anker SD, Bueno H, Cleland JG, Coats AJ, et al. 2016 ESC Guidelines for the Diagnosis and Treatment of Acute and Chronic Heart Failure: The Task Force for the Diagnosis and Treatment of Acute and Chronic Heart Failure of the European Society of Cardiology (ESC). Developed with the Special Contribution of the Heart Failure Association (HFA) of the ESC. *Eur J Heart Fail.* 2016;18(8):891-975. doi: 10.1002/ehf.592.
27. Zamorano JL, Lancellotti P, Muñoz DR, Aboyans V, Asteggiano R, Galderisi M, et al. 2016 ESC Position Paper on Cancer Treatments and Cardiovascular Toxicity Developed Under the Auspices of the ESC Committee for Practice Guidelines: The Task Force for Cancer Treatments and Cardiovascular Toxicity of the European Society of Cardiology (ESC). *Eur J Heart Fail.* 2017;19(1):9-42. doi: 10.1002/ehf.654.
28. Thavendiranathan P, Grant AD, Negishi T, Plana JC, Popović ZB, Marwick TH. Reproducibility of Echocardiographic Techniques for Sequential Assessment of Left Ventricular Ejection Fraction and Volumes: Application to Patients Undergoing Cancer Chemotherapy. *J Am Coll Cardiol.* 2013;61(1):77-84. doi: 10.1016/j.jacc.2012.09.035.
29. Thavendiranathan P, Liu S, Verhaert D, Calleja A, Nitinunu A, van Houten T, et al. Feasibility, Accuracy, and Reproducibility of Real-Time Full-Volume 3D Transthoracic Echocardiography to Measure LV Volumes and Systolic Function: A Fully Automated Endocardial Contouring Algorithm in Sinus Rhythm and Atrial Fibrillation. *JACC Cardiovasc Imaging.* 2012;5(3):239-51. doi: 10.1016/j.jcmg.2011.12.012.
30. Knight DS, Zumbo G, Barcella W, Steeden JA, Muthurangu V, Martinez-Naharro A, et al. Cardiac Structural and Functional Consequences of Amyloid Deposition by Cardiac Magnetic Resonance and Echocardiography and Their Prognostic Roles. *JACC Cardiovasc Imaging.* 2019;12(5):823-33. doi: 10.1016/j.jcmg.2018.02.016.
31. Dedobbeleer C, Rai M, Donal E, Pandolfo M, Unger P. Normal Left Ventricular Ejection Fraction and Mass but Subclinical Myocardial Dysfunction in Patients with Friedreich's Ataxia. *Eur Heart J Cardiovasc Imaging.* 2012;13(4):346-52. doi: 10.1093/ejchocard/jer267.

Statement

32. Stanton T, Leano R, Marwick TH. Prediction of All-Cause Mortality from Global Longitudinal Speckle Strain: Comparison with Ejection Fraction and Wall Motion Scoring. *Circ Cardiovasc Imaging*. 2009;2(5):356-64. doi: 10.1161/CIRCIMAGING.109.862334.
33. Smiseth OA, Torp H, Opdahl A, Haugaa KH, Urheim S. Myocardial Strain Imaging: How Useful is it in Clinical Decision Making? *Eur Heart J*. 2016;37(15):1196-207. doi: 10.1093/eurheartj/ehv529.
34. Ünü S, Mirea O, Duchenne J, Pagourelis ED, Bézy S, Thomas JD, et al. Comparison of Feasibility, Accuracy, and Reproducibility of Layer-Specific Global Longitudinal Strain Measurements among Five Different Vendors: A Report from the EACVI-ASE Strain Standardization Task Force. *J Am Soc Echocardiogr*. 2018;31(3):374-380.e1. doi: 10.1016/j.echo.2017.11.008.
35. Lang RM, Badano LP, Mor-Avi V, Afilalo J, Armstrong A, Ernande L, et al. Recommendations for Cardiac Chamber Quantification by Echocardiography in Adults: An Update from the American Society of Echocardiography and the European Association of Cardiovascular Imaging. *J Am Soc Echocardiogr*. 2015;28(1):1-39.e14. doi: 10.1016/j.echo.2014.10.003.
36. Longobardo L, Suma V, Jain R, Carerj S, Zito C, Zwicke DL, et al. Role of Two-Dimensional Speckle-Tracking Echocardiography Strain in the Assessment of Right Ventricular Systolic Function and Comparison with Conventional Parameters. *J Am Soc Echocardiogr*. 2017;30(10):937-946.e6. doi: 10.1016/j.echo.2017.06.016.
37. Pathan F, D'Elia N, Nolan MT, Marwick TH, Negishi K. Normal Ranges of Left Atrial Strain by Speckle-Tracking Echocardiography: A Systematic Review and Meta-Analysis. *J Am Soc Echocardiogr*. 2017;30(1):59-70.e8. doi: 10.1016/j.echo.2016.09.007.
38. Sugimoto T, Robinet S, Dulgheru R, Bernard A, Ilardi F, Contu L, et al. Echocardiographic Reference Ranges for Normal Left Atrial Function Parameters: Results from the EACVI NORRE Study. *Eur Heart J Cardiovasc Imaging*. 2018;19(6):630-8. doi: 10.1093/ehjci/jev018.
39. Oikonomou EK, Kokkinidis DG, Kampaktis PN, Amir EA, Marwick TH, Gupta D, et al. Assessment of Prognostic Value of Left Ventricular Global Longitudinal Strain for Early Prediction of Chemotherapy-Induced Cardiotoxicity: A Systematic Review and Meta-analysis. *JAMA Cardiol*. 2019;4(10):1007-18. doi: 10.1001/jamacardio.2019.2952.
40. Singh A, Voss WB, Lentz RW, Thomas JD, Akhter N. The Diagnostic and Prognostic Value of Echocardiographic Strain. *JAMA Cardiol*. 2019;4(6):580-8. doi: 10.1001/jamacardio.2019.1152.
41. Thomas L, Marwick TH, Popescu BA, Donal E, Badano LP. Left Atrial Structure and Function, and Left Ventricular Diastolic Dysfunction: JACC State-of-the-Art Review. *J Am Coll Cardiol*. 2019;73(15):1961-77. doi: 10.1016/j.jacc.2019.01.059.
42. Felker GM, Thompson RE, Hare JM, Hruban RH, Clemetson DE, Howard DL, et al. Underlying Causes and Long-Term Survival in Patients with Initially Unexplained Cardiomyopathy. *N Engl J Med*. 2000;342(15):1077-84. doi: 10.1056/NEJM200004133421502.
43. Hoening MJ, Botma A, Aleman BM, Baaijens MH, Bartelink H, Klijn JG, et al. Long-Term Risk of Cardiovascular Disease in 10-Year Survivors of Breast Cancer. *J Natl Cancer Inst*. 2007;99(5):365-75. doi: 10.1093/jnci/djk064.
44. Monsuez JJ, Charniot JC, Vignat N, Artigou JY. Cardiac Side-Effects of Cancer Chemotherapy. *Int J Cardiol*. 2010;144(1):3-15. doi: 10.1016/j.ijcard.2010.03.003.
45. Yeh ET, Tong AT, Lenihan DJ, Yusuf SW, Swafford J, Champion C, et al. Cardiovascular Complications of Cancer Therapy: Diagnosis, Pathogenesis, and Management. *Circulation*. 2004;109(25):3122-31. doi: 10.1161/01.CIR.0000133187.74800.B9.
46. Cardinale D, Colombo A, Lamantia G, Colombo N, Civelli M, De Giacomo G, et al. Anthracycline-Induced Cardiomyopathy: Clinical Relevance and Response to Pharmacologic Therapy. *J Am Coll Cardiol*. 2010;55(3):213-20. doi: 10.1016/j.jacc.2009.03.095.
47. Negishi K, Negishi T, Haluska BA, Hare JL, Plana JC, Marwick TH. Use of Speckle Strain to Assess Left Ventricular Responses to Cardiotoxic Chemotherapy and Cardioprotection. *Eur Heart J Cardiovasc Imaging*. 2014;15(3):324-31. doi: 10.1093/ehjci/jet159.
48. Ewer MS, Lenihan DJ. Left Ventricular Ejection Fraction and Cardiotoxicity: Is Our Ear Really to The Ground? *J Clin Oncol*. 2008;26(8):1201-3. doi: 10.1200/JCO.2007.14.8742.
49. Swain SM, Whaley FS, Ewer MS. Congestive Heart Failure in Patients Treated with Doxorubicin: A Retrospective Analysis of Three Trials. *Cancer*. 2003;97(11):2869-79. doi: 10.1002/cncr.11407.
50. Armstrong GT, Plana JC, Zhang N, Srivastava D, Green DM, Ness KK, et al. Screening Adult Survivors of Childhood Cancer for Cardiomyopathy: Comparison of Echocardiography and Cardiac Magnetic Resonance Imaging. *J Clin Oncol*. 2012;30(23):2876-84. doi: 10.1200/JCO.2011.40.3584.
51. Cardinale D, Colombo A, Bacchiani G, Tedeschi I, Meroni CA, Veglia F, et al. Early Detection of Anthracycline Cardiotoxicity and Improvement with Heart Failure Therapy. *Circulation*. 2015;131(22):1981-8. doi: 10.1161/CIRCULATIONAHA.114.013777.
52. Amundsen BH, Helle-Valle T, Edvardsen T, Torp H, Crosby J, Lyseggen E, et al. Noninvasive Myocardial Strain Measurement by Speckle Tracking Echocardiography: Validation Against Sonomicrometry and Tagged Magnetic Resonance Imaging. *J Am Coll Cardiol*. 2006;47(4):789-93. doi: 10.1016/j.jacc.2005.10.040.
53. Korinek J, Wang J, Sengupta PP, Miyazaki C, Kjaergaard J, McMahon E, et al. Two-Dimensional Strain--A Doppler-Independent Ultrasound Method for quantitation of Regional Deformation: Validation In Vitro and In Vivo. *J Am Soc Echocardiogr*. 2005;18(12):1247-53. doi: 10.1016/j.echo.2005.03.024.
54. Negishi K, Negishi T, Hare JL, Haluska BA, Plana JC, Marwick TH. Independent and Incremental Value of Deformation Indices for Prediction of Trastuzumab-Induced Cardiotoxicity. *J Am Soc Echocardiogr*. 2013;26(5):493-8. doi: 10.1016/j.echo.2013.02.008.
55. Sawaya H, Sebag IA, Plana JC, Januzzi JL, Ky B, Cohen V, et al. Early Detection and Prediction of Cardiotoxicity in Chemotherapy-Treated Patients. *Am J Cardiol*. 2011;107(9):1375-80. doi: 10.1016/j.amjcard.2011.01.006.
56. Sawaya H, Sebag IA, Plana JC, Januzzi JL, Ky B, Tan TC, et al. Assessment of Echocardiography and Biomarkers for the Extended Prediction of Cardiotoxicity in Patients Treated with Anthracyclines, Taxanes, and Trastuzumab. *Circ Cardiovasc Imaging*. 2012;5(5):596-603. doi: 10.1161/CIRCIMAGING.112.973321.
57. Thavendiranathan P, Poulin F, Lim KD, Plana JC, Woo A, Marwick TH. Use of Myocardial Strain Imaging by Echocardiography for the Early Detection of Cardiotoxicity in Patients During and after Cancer Chemotherapy: A Systematic Review. *J Am Coll Cardiol*. 2014;63(25 Pt A):2751-68. doi: 10.1016/j.jacc.2014.01.073.
58. Negishi T, Thavendiranathan P, Negishi K, Marwick TH; SUCCOUR investigators. Rationale and Design of the Strain Surveillance of Chemotherapy for Improving Cardiovascular Outcomes: The SUCCOUR Trial. *JACC Cardiovasc Imaging*. 2018;11(8):1098-105. doi: 10.1016/j.jcmg.2018.03.019.
59. Abate E, Hoogslag GE, Antoni ML, Nucifora G, Delgado V, Holman ER, et al. Value of Three-Dimensional Speckle-Tracking Longitudinal Strain for Predicting Improvement of Left Ventricular Function after Acute Myocardial Infarction. *Am J Cardiol*. 2012;110(7):961-7. doi: 10.1016/j.amjcard.2012.05.023.
60. Galderisi M, Esposito R, Schiano-Lomoriello V, Santoro A, Ippolito R, Schiattarella P, et al. Correlates of Global Area Strain in Native Hypertensive Patients: A Three-Dimensional Speckle-Tracking Echocardiography Study. *Eur Heart J Cardiovasc Imaging*. 2012;13(9):730-8. doi: 10.1093/ehjci/jes026.
61. Mor-Avi V, Sugeng L, Lang RM. Real-time 3-Dimensional Echocardiography: An Integral Component of the Routine Echocardiographic Examination in Adult Patients? *Circulation*. 2009;119(2):314-29. doi: 10.1161/CIRCULATIONAHA.107.751354.

62. Urbano-Moral JA, Arias-Godinez JA, Ahmad R, Malik R, Kiernan MS, DeNofrio D, et al. Evaluation of Myocardial Mechanics with Three-Dimensional Speckle Tracking Echocardiography in Heart Transplant Recipients: Comparison with Two-Dimensional Speckle Tracking and Relationship with Clinical Variables. *Eur Heart J Cardiovasc Imaging*. 2013;14(12):1167-73. doi: 10.1093/ehjci/jet065.
63. Miyoshi T, Tanaka H, Kaneko A, Tatsumi K, Matsumoto K, Minami H, et al. Left Ventricular Endocardial Dysfunction in Patients with Preserved Ejection Fraction after Receiving Anthracycline. *Echocardiography*. 2014;31(7):848-57. doi: 10.1111/echo.12473.
64. Santoro C, Arpino G, Esposito R, Lembo M, Paciolla I, Cardalesi C, et al. 2D and 3D Strain for Detection of Subclinical Anthracycline Cardiotoxicity in Breast Cancer Patients: A Balance with Feasibility. *Eur Heart J Cardiovasc Imaging*. 2017;18(8):930-6. doi: 10.1093/ehjci/jex033.
65. Tarr A, Stoebe S, Tuennemann J, Baka Z, Pfeiffer D, Varga A, et al. Early Detection of Cardiotoxicity by 2D and 3D Deformation Imaging in Patients Receiving Chemotherapy. *Echo Res Pract*. 2015;2(3):81-8. doi: 10.1530/ERP-14-0084.
66. Piveta RB, Rodrigues ACT, Vieira MLC, Fischer CH, Afonso TR, Daminello E, et al. Early Changes in Myocardial Mechanics Detected by 3-Dimensional Speckle Tracking Echocardiography in Patients Treated with Low Doses of Anthracyclines. *JACC Cardiovasc Imaging*. 2018;11(11):1729-31. doi: 10.1016/j.jcmg.2018.04.014.
67. Nagueh SF, Smiseth OA, Appleton CP, Byrd BF 3rd, Dokainish H, Edvardsen T, et al. Recommendations for the Evaluation of Left Ventricular Diastolic Function by Echocardiography: An Update from the American Society of Echocardiography and the European Association of Cardiovascular Imaging. *Eur Heart J Cardiovasc Imaging*. 2016;17(12):1321-60. doi: 10.1093/ehjci/jew082.
68. Redfield MM, Jacobsen SJ, Burnett JC Jr, Mahoney DW, Bailey KR, Rodeheffer RJ. Burden of Systolic and Diastolic Ventricular Dysfunction in the Community: Appreciating the Scope of the Heart Failure Epidemic. *JAMA*. 2003;289(2):194-202. doi: 10.1001/jama.289.2.194.
69. Senni M, Tribouilloy CM, Rodeheffer RJ, Jacobsen SJ, Evans JM, Bailey KR, et al. Congestive Heart Failure in the Community: A Study of All Incident Cases in Olmsted County, Minnesota, in 1991. *Circulation*. 1998;98(21):2282-9. doi: 10.1161/01.cir.98.21.2282.
70. Nagueh SF. Left Ventricular Diastolic Function: Understanding Pathophysiology, Diagnosis, and Prognosis with Echocardiography. *JACC Cardiovasc Imaging*. 2020;13(1 Pt 2):228-44. doi: 10.1016/j.jcmg.2018.10.038.
71. Almeida JG, Fontes-Carvalho R, Sampaio F, Ribeiro J, Bettencourt P, Flachskampf FA, et al. Impact of the 2016 ASE/EACVI Recommendations on the Prevalence of Diastolic Dysfunction in the General Population. *Eur Heart J Cardiovasc Imaging*. 2018;19(4):380-6. doi: 10.1093/ehjci/jex252.
72. Kosmala W, Rojek A, Przewlocka-Kosmala M, Mysiak A, Karolko B, Marwick TH. Contributions of Nondiastolic Factors to Exercise Intolerance in Heart Failure with Preserved Ejection Fraction. *J Am Coll Cardiol*. 2016;67(6):659-70. doi: 10.1016/j.jacc.2015.10.096.
73. Freed BH, Daruwalla V, Cheng JY, Aguilar FG, Beussink L, Choi A, et al. Prognostic Utility and Clinical Significance of Cardiac Mechanics in Heart Failure with Preserved Ejection Fraction: Importance of Left Atrial Strain. *Circ Cardiovasc Imaging*. 2016;9(3):10.1161/CIRCIMAGING.115.003754. doi: 10.1161/CIRCIMAGING.115.003754.
74. Oh JK, Miranda WR, Bird JG, Kane GC, Nagueh SF. The 2016 Diastolic Function Guideline: Is it Already Time to Revisit or Revise Them? *JACC Cardiovasc Imaging*. 2020;13(1 Pt 2):327-35. doi: 10.1016/j.jcmg.2019.12.004.
75. Lejeune S, Roy C, Ciocea V, Slimani A, Meester C, Amzulescu M, et al. Right Ventricular Global Longitudinal Strain and Outcomes in Heart Failure with Preserved Ejection Fraction. *J Am Soc Echocardiogr*. 2020;33(8):973-984. e2. doi: 10.1016/j.echo.2020.02.016.
76. Wang J, Khoury DS, Thohan V, Torre-Amione G, Nagueh SF. Global Diastolic Strain Rate for the Assessment of Left Ventricular Relaxation and Filling Pressures. *Circulation*. 2007;115(11):1376-83. doi: 10.1161/CIRCULATIONAHA.106.662882.
77. Dokainish H, Sengupta R, Pillai M, Bobek J, Lakkis N. Usefulness of New Diastolic Strain and Strain Rate Indexes for the Estimation of Left Ventricular Filling Pressure. *Am J Cardiol*. 2008;101(10):1504-9. doi: 10.1016/j.amjcard.2008.01.037.
78. Hayashi T, Yamada S, Iwano H, Nakabachi M, Sakakibara M, Okada K, et al. Left Ventricular Global Strain for Estimating Relaxation and Filling Pressure—A Multicenter Study. *Circ J*. 2016;80(5):1163-70. doi: 10.1253/circj.CJ-16-0106.
79. Stokke TM, Hasselberg NE, Smedsrud MK, Sarvari SI, Haugaa KH, Smiseth OA, et al. Geometry as a Confounder when Assessing Ventricular Systolic Function: Comparison between Ejection Fraction and Strain. *J Am Coll Cardiol*. 2017;70(8):942-54. doi: 10.1016/j.jacc.2017.06.046.
80. Shah AM, Claggett B, Sweitzer NK, Shah SJ, Anand IS, Liu L, et al. Prognostic Importance of Impaired Systolic Function in Heart Failure with Preserved Ejection Fraction and the Impact of Spironolactone. *Circulation*. 2015;132(5):402-14. doi: 10.1161/CIRCULATIONAHA.115.015884.
81. Bianco CM, Farjo PD, Ghaffar YA, Sengupta PP. Myocardial Mechanics in Patients with Normal LVEF and Diastolic Dysfunction. *JACC Cardiovasc Imaging*. 2020;13(1 Pt 2):258-71. doi: 10.1016/j.jcmg.2018.12.035.
82. Morris DA, Ma XX, Belyavskiy E, Kumar RA, Kropf M, Kraft R, et al. Left Ventricular Longitudinal Systolic Function Analysed by 2D Speckle-Tracking Echocardiography in Heart Failure with Preserved Ejection Fraction: A Meta-Analysis. *Open Heart*. 2017;4(2):e000630. doi: 10.1136/openhrt-2017-000630.
83. Pieske B, Tschöpe C, Boer RA, Fraser AG, Anker SD, Donal E, et al. How to Diagnose Heart Failure with Preserved Ejection Fraction: The HFA-PEFF Diagnostic Algorithm: A Consensus Recommendation from the Heart Failure Association (HFA) of the European Society of Cardiology (ESC). *Eur Heart J*. 2019;40(40):3297-317. doi: 10.1093/eurheartj/ehz641.
84. Genovese D, Singh A, Volpato V, Kruse E, Weinert L, Yamat M, et al. Load Dependency of Left Atrial Strain in Normal Subjects. *J Am Soc Echocardiogr*. 2018;31(11):1221-8. doi: 10.1016/j.echo.2018.07.016.
85. Mandoli GE, Sisti N, Mondillo S, Cameli M. Left Atrial Strain in Left Ventricular Diastolic Dysfunction: Have we Finally Found the Missing Piece of the Puzzle? *Heart Fail Rev*. 2020;25(3):409-17. doi: 10.1007/s10741-019-09889-9.
86. Brecht A, Oertelt-Prigione S, Seeland U, Rütke M, Hättasch R, Wägelöhner T, et al. Left Atrial Function in Preclinical Diastolic Dysfunction: Two-Dimensional Speckle-Tracking Echocardiography-Derived Results from the BEFRI Trial. *J Am Soc Echocardiogr*. 2016;29(8):750-8. doi: 10.1016/j.echo.2016.03.013.
87. Thomas L, Abhayaratna WP. Left Atrial Reverse Remodeling: Mechanisms, Evaluation, and Clinical Significance. *JACC Cardiovasc Imaging*. 2017;10(1):65-77. doi: 10.1016/j.jcmg.2016.11.003.
88. Santos AB, Roca GQ, Claggett B, Sweitzer NK, Shah SJ, Anand IS, et al. Prognostic Relevance of Left Atrial Dysfunction in Heart Failure with Preserved Ejection Fraction. *Circ Heart Fail*. 2016;9(4):e002763. doi: 10.1161/CIRCHEARTFAILURE.115.002763.
89. Fernandes RM, Le Bihan D, Vilela AA, Barretto RBM, Santos ES, Asses JE, et al. Association between Left Atrial Strain and Left Ventricular Diastolic Function in Patients with Acute Coronary Syndrome. *J Echocardiogr*. 2019;17(3):138-46. doi: 10.1007/s12574-018-0403-7.
90. Singh A, Addetia K, Maffessanti F, Mor-Avi V, Lang RM. LA Strain for Categorization of LV Diastolic Dysfunction. *JACC Cardiovasc Imaging*. 2017;10(7):735-43. doi: 10.1016/j.jcmg.2016.08.014.
91. Thomas L, Muraru D, Popescu BA, Sitges M, Rosca M, Pedrizzetti G, et al. Evaluation of Left Atrial Size and Function: Relevance for Clinical Practice. *J Am Soc Echocardiogr*. 2020;33(8):934-52. doi: 10.1016/j.echo.2020.03.021.

Statement

92. Badano LP, Kolias TJ, Muraru D, Abraham TP, Aurigemma G, Edvardsen T, et al. Standardization of Left Atrial, Right Ventricular, and Right Atrial Deformation Imaging Using Two-Dimensional Speckle Tracking Echocardiography: A Consensus Document of the EACVI/ASE/Industry Task Force to Standardize Deformation Imaging. *Eur Heart J Cardiovasc Imaging*. 2018;19(6):591-600. doi: 10.1093/ehjci/ey042.
93. Morris DA, Belyavskiy E, Aravind-Kumar R, Kropf M, Frydas A, Braunaer K, et al. Potential Usefulness and Clinical Relevance of Adding Left Atrial Strain to Left Atrial Volume Index in the Detection of Left Ventricular Diastolic Dysfunction. *JACC Cardiovasc Imaging*. 2018;11(10):1405-15. doi: 10.1016/j.jcmg.2017.07.029.
94. Tossavainen E, Henein MY, Grönlund C, Lindqvist P. Left Atrial Intrinsic Strain Rate Correcting for Pulmonary Wedge Pressure Is Accurate in Estimating Pulmonary Vascular Resistance in Breathless Patients. *Echocardiography*. 2016;33(8):1156-65. doi: 10.1111/echo.13226.
95. Singh A, Medvedofsky D, Mediratta A, Balaney B, Kruse E, Cizek B, et al. Peak Left Atrial Strain as a Single Measure for the Non-Invasive Assessment of Left Ventricular Filling Pressures. *Int J Cardiovasc Imaging*. 2019;35(1):23-32. doi: 10.1007/s10554-018-1425-y.
96. Cameli M, Mandoli GE, Loiacono F, Dini FL, Henein M, Mondillo S. Left Atrial Strain: A New Parameter for Assessment of Left Ventricular Filling Pressure. *Heart Fail Rev*. 2016;21(1):65-76. doi: 10.1007/s10741-015-9520-9.
97. Potter EL, Ramkumar S, Kawakami H, Yang H, Wright L, Negishi T, et al. Association of Asymptomatic Diastolic Dysfunction Assessed by Left Atrial Strain with Incident Heart Failure. *JACC Cardiovasc Imaging*. 2020;13(11):2316-26. doi: 10.1016/j.jcmg.2020.04.028.
98. Park JJ, Park JH, Hwang IC, Park JB, Cho GY, Marwick TH. Left Atrial Strain as a Predictor of New-Onset Atrial Fibrillation in Patients with Heart Failure. *JACC Cardiovasc Imaging*. 2020;13(10):2071-81. doi: 10.1016/j.jcmg.2020.04.031.
99. Marwick TH, Chandrashekar Y. Left Atrial Strain: Part of the Solution to Taming the Vicious Twins. *JACC Cardiovasc Imaging*. 2020;13(10):2278-79. doi: 10.1016/j.jcmg.2020.09.001.
100. Negishi K, Negishi T, Kurosawa K, Hristova K, Popescu BA, Vinereanu D, et al. Practical Guidance in Echocardiographic Assessment of Global Longitudinal Strain. *JACC Cardiovasc Imaging*. 2015;8(4):489-92. doi: 10.1016/j.jcmg.2014.06.013.
101. Haji K, Wong C, Wright L, Ramkumar S, Marwick TH. Left Atrial Strain Performance and its Application in Clinical Practice. *JACC Cardiovasc Imaging*. 2019;12(6):1093-101. doi: 10.1016/j.jcmg.2018.11.009.
102. Report of the WHO/ISFC Task Force on The Definition and Classification of Cardiomyopathies. *Br Heart J*. 1980;44(6):672-3. doi: 10.1136/hrt.44.6.672.
103. Richardson P, McKenna W, Bristow M, Maisch B, Mautner B, O'Connell J, et al. Report of the 1995 World Health Organization/International Society and Federation of Cardiology Task Force on the Definition and Classification of Cardiomyopathies. *Circulation*. 1996;93(5):841-2. doi: 10.1161/01.cir.93.5.841.
104. Dec GW, Fuster V. Idiopathic Dilated Cardiomyopathy. *N Engl J Med*. 1994;331(23):1564-75. doi: 10.1056/NEJM199412083312307.
105. Luk A, Ahn E, Soor GS, Butany J. Dilated Cardiomyopathy: A Review. *J Clin Pathol*. 2009;62(3):219-25. doi: 10.1136/jcp.2008.060731.
106. Elliott P. Cardiomyopathy. Diagnosis and Management of Dilated Cardiomyopathy. *Heart*. 2000;84(1):106-12. doi: 10.1136/heart.84.1.106.
107. Manolio TA, Baughman KL, Rodeheffer R, Pearson TA, Bristow JD, Michels VV, et al. Prevalence and Etiology of Idiopathic Dilated Cardiomyopathy (Summary of a National Heart, Lung, and Blood Institute Workshop). *Am J Cardiol*. 1992;69(17):1458-66. doi: 10.1016/0002-9149(92)90901-a.
108. Abduch MC, Salgo I, Tsang W, Vieira ML, Cruz V, Lima M, et al. Myocardial Deformation by Speckle Tracking in Severe Dilated Cardiomyopathy. *Arq Bras Cardiol*. 2012;99(3):834-43. doi: 10.1590/s0066-782x2012005000086.
109. Lima MS, Villarraga HR, Abduch MC, Lima MF, Cruz CB, Bittencourt MS, et al. Comprehensive Left Ventricular Mechanics Analysis by Speckle Tracking Echocardiography in Chagas disease. *Cardiovasc Ultrasound*. 2016;14(1):20. doi: 10.1186/s12947-016-0062-7.
110. Meluzin J, Spinarova L, Hude P, Krejci J, Poloczkova H, Podrouzkova H, et al. Left Ventricular Mechanics in Idiopathic Dilated Cardiomyopathy: Systolic-Diastolic Coupling and Torsion. *J Am Soc Echocardiogr*. 2009;22(5):486-93. doi: 10.1016/j.echo.2009.02.022.
111. Saito M, Okayama H, Nishimura K, Ogimoto A, Ohtsuka T, Inoue K, et al. Determinants of Left Ventricular Untwisting Behaviour in Patients with Dilated Cardiomyopathy: Analysis by Two-Dimensional Speckle Tracking. *Heart*. 2009;95(4):290-6. doi: 10.1136/hrt.2008.145979.
112. Abduch MC, Alencar AM, Mathias W Jr, Vieira ML. Cardiac Mechanics Evaluated by Speckle Tracking Echocardiography. *Arq Bras Cardiol*. 2014;102(4):403-12. doi: 10.5935/abc.20140041.
113. Sengeløv M, Jørgensen PG, Jensen JS, Bruun NE, Olsen FJ, Fritz-Hansen T, et al. Global Longitudinal Strain Is a Superior Predictor of All-Cause Mortality in Heart Failure with Reduced Ejection Fraction. *JACC Cardiovasc Imaging*. 2015;8(12):1351-9. doi: 10.1016/j.jcmg.2015.07.013.
114. Adamo L, Perry A, Novak E, Makan M, Lindman BR, Mann DL. Abnormal Global Longitudinal Strain Predicts Future Deterioration of Left Ventricular Function in Heart Failure Patients with a Recovered Left Ventricular Ejection Fraction. *Circ Heart Fail*. 2017;10(6):e003788. doi: 10.1161/CIRCHEARTFAILURE.116.003788.
115. Sen-Chowdhry S, Lowe MD, Sporton SC, McKenna WJ. Arrhythmogenic Right Ventricular Cardiomyopathy: Clinical Presentation, Diagnosis, and Management. *Am J Med*. 2004;117(9):685-95. doi: 10.1016/j.amjmed.2004.04.028.
116. Gemayel C, Pelliccia A, Thompson PD. Arrhythmogenic Right Ventricular Cardiomyopathy. *J Am Coll Cardiol*. 2001;38(7):1773-81. doi: 10.1016/s0735-1097(01)01654-0.
117. Al-Khatib SM, Stevenson WG, Ackerman MJ, Bryant WJ, Callans DJ, Curtis AB, et al. 2017 AHA/ACC/HRS Guideline for Management of Patients with Ventricular Arrhythmias and the Prevention of Sudden Cardiac Death: Executive Summary: A Report of the American College of Cardiology/American Heart Association Task Force on Clinical Practice Guidelines and the Heart Rhythm Society. *Heart Rhythm*. 2018;15(10):e190-e252. doi: 10.1016/j.hrthm.2017.10.035.
118. Prakasa KR, Wang J, Tandri H, Dalal D, Bomma C, Chojnowski R, et al. Utility of Tissue Doppler and Strain Echocardiography in Arrhythmogenic Right Ventricular Dysplasia/Cardiomyopathy. *Am J Cardiol*. 2007;100(3):507-12. doi: 10.1016/j.amjcard.2007.03.053.
119. Malik N, Win S, James CA, Kutty S, Mukherjee M, Gilotra NA, et al. Right Ventricular Strain Predicts Structural Disease Progression in Patients with Arrhythmogenic Right Ventricular Cardiomyopathy. *J Am Heart Assoc*. 2020;9(7):e015016. doi: 10.1161/JAHA.119.015016.
120. Anwer S, Guastafierro F, Erhart L, Costa S, Akdis D, Schuermann M, et al. Right Atrial Strain and Cardiovascular Outcome in Arrhythmogenic Right Ventricular Cardiomyopathy. *Eur Heart J Cardiovasc Imaging*. 2022;23(7):970-8. doi: 10.1093/ehjci/jeac070.
121. Klues HG, Schiffrers A, Maron BJ. Phenotypic Spectrum and Patterns of Left Ventricular Hypertrophy in Hypertrophic Cardiomyopathy: Morphologic Observations and Significance as Assessed by Two-Dimensional Echocardiography in 600 Patients. *J Am Coll Cardiol*. 1995;26(7):1699-708. doi: 10.1016/0735-1097(95)00390-8.
122. Olivetto I, Cecchi F, Casey SA, Dolar A, Traverse JH, Maron BJ. Impact of Atrial Fibrillation on the Clinical Course of Hypertrophic Cardiomyopathy. *Circulation*. 2001;104(21):2517-24. doi: 10.1161/hc4601.097997.
123. Elliott PM, Anastakis A, Borger MA, Borggrefe M, Cecchi F, Charron P, et al. 2014 ESC Guidelines on Diagnosis and Management of Hypertrophic Cardiomyopathy: The Task Force for the Diagnosis and Management of Hypertrophic Cardiomyopathy of the European Society of Cardiology (ESC). *Eur Heart J*. 2014;35(39):2733-79. doi: 10.1093/eurheartj/ehu284.

124. Maron MS, Olivetto I, Betocchi S, Casey SA, Lesser JR, Losi MA, et al. Effect of Left Ventricular Outflow Tract Obstruction on Clinical Outcome in Hypertrophic Cardiomyopathy. *N Engl J Med.* 2003;348(4):295-303. doi: 10.1056/NEJMoa021332.
125. Panza JA, Petrone RK, Fananapazir L, Maron BJ. Utility of Continuous Wave Doppler Echocardiography in the Noninvasive Assessment of Left Ventricular Outflow Tract Pressure Gradient in Patients with Hypertrophic Cardiomyopathy. *J Am Coll Cardiol.* 1992;19(1):91-9. doi: 10.1016/0735-1097(92)90057-t.
126. Tigen K, Sunbul M, Karaahmet T, Dundar C, Ozben B, Guler A, et al. Left Ventricular and Atrial Functions in Hypertrophic Cardiomyopathy Patients with Very High LVOT Gradient: A Speckle Tracking Echocardiographic Study. *Echocardiography.* 2014;31(7):833-41. doi: 10.1111/echo.12482.
127. Serri K, Reant P, Lafitte M, Berhouet M, Le Bouffos V, Roudaut R, et al. Global and Regional Myocardial Function Quantification by Two-Dimensional Strain: Application in Hypertrophic Cardiomyopathy. *J Am Coll Cardiol.* 2006;47(6):1175-81. doi: 10.1016/j.jacc.2005.10.061.
128. Chen S, Yuan J, Qiao S, Duan F, Zhang J, Wang H. Evaluation of Left Ventricular Diastolic Function by Global Strain Rate Imaging in Patients with Obstructive Hypertrophic Cardiomyopathy: A Simultaneous Speckle Tracking Echocardiography and Cardiac Catheterization Study. *Echocardiography.* 2014;31(5):615-22. doi: 10.1111/echo.12424.
129. Almaas VM, Haugaa KH, Strøm EH, Scott H, Smith HJ, Dahl CP, et al. Noninvasive Assessment of Myocardial Fibrosis in Patients with Obstructive Hypertrophic Cardiomyopathy. *Heart.* 2014;100(8):631-8. doi: 10.1136/heartjnl-2013-304923.
130. Haland TF, Almaas VM, Hasselberg NE, Saberniak J, Leren IS, Hopp E, et al. Strain Echocardiography is Related to Fibrosis and Ventricular Arrhythmias in Hypertrophic Cardiomyopathy. *Eur Heart J Cardiovasc Imaging.* 2016;17(6):613-21. doi: 10.1093/ehjci/jew005.
131. Liu H, Pozios I, Haileselassie B, Nowbar A, Sorensen LL, Phillip S, et al. Role of Global Longitudinal Strain in Predicting Outcomes in Hypertrophic Cardiomyopathy. *Am J Cardiol.* 2017;120(4):670-5. doi: 10.1016/j.amjcard.2017.05.039.
132. Badran HM, Faheem N, Ibrahim WA, Elnomany MF, Elseddi M, Yacoub M. Systolic Function Reserve Using Two-Dimensional Strain Imaging in Hypertrophic Cardiomyopathy: Comparison with Essential Hypertension. *J Am Soc Echocardiogr.* 2013;26(12):1397-406. doi: 10.1016/j.echo.2013.08.026.
133. Hiemstra YL, Debonnaire P, Bootsma M, van Zwet EW, Delgado V, Schalij MJ, et al. Global Longitudinal Strain and Left Atrial Volume Index Provide Incremental Prognostic Value in Patients with Hypertrophic Cardiomyopathy. *Circ Cardiovasc Imaging.* 2017;10(7):e005706. doi: 10.1161/CIRCIMAGING.116.005706.
134. Zegkos T, Parcharidou D, Ntelios D, Efthimiadis G, Karvounis H. The Prognostic Implications of Two-Dimensional Speckle Tracking Echocardiography in Hypertrophic Cardiomyopathy: Current and Future Perspectives. *Cardiol Rev.* 2018;26(3):130-6. doi: 10.1097/CRD.000000000000172.
135. Salemi VM, Leite JJ, Picard MH, Oliveira LM, Reis SF, Pena JL, et al. Echocardiographic Predictors of Functional Capacity in Endomyocardial Fibrosis Patients. *Eur J Echocardiogr.* 2009;10(3):400-5. doi: 10.1093/ejehocardi/jen297.
136. Scatularo CE, Martínez ELP, Saldarriaga C, Ballesteros OA, Baranchuk A, Liprandi AS, et al. Endomyocardial fibrosis: A Systematic Review. *Curr Probl Cardiol.* 2021;46(4):100784. doi: 10.1016/j.cpcardiol.2020.100784.
137. Valero AR, Orts FJC, Muci T, Blasco PM. Endomyocardial Fibrosis and Apical Thrombus in Patient with Hypereosinophilia. *Eur Heart J.* 2019;40(40):3364-5. doi: 10.1093/eurheartj/ehz529.
138. Badami VM, Reece J, Sengupta S. Biventricular Thrombosis in a Young Male. *Eur Heart J Cardiovasc Imaging.* 2019;20(10):1179. doi: 10.1093/ehjci/jez064.
139. Ashwal AJ, Mugula SR, Samanth J, Paramasivam G, Nayak K, Padmakumar R. Role of Deformation Imaging in Left Ventricular Non-Compaction and Hypertrophic Cardiomyopathy: An Indian Perspective. *Egypt Heart J.* 2020;72(1):6. doi: 10.1186/s43044-020-0041-z.
140. Tarando F, Coisne D, Galli E, Rousseau C, Viera F, Bosseau C, et al. Left Ventricular Non-Compaction and Idiopathic Dilated Cardiomyopathy: The Significant Diagnostic Value of Longitudinal Strain. *Int J Cardiovasc Imaging.* 2017;33(1):83-95. doi: 10.1007/s10554-016-0980-3.
141. van Dalen BM, Caliskan K, Soliman OI, Kauer F, van der Zwaan HB, Vletter WB, et al. Diagnostic Value of Rigid Body Rotation in Noncompaction Cardiomyopathy. *J Am Soc Echocardiogr.* 2011;24(5):548-55. doi: 10.1016/j.echo.2011.01.002.
142. Peters F, Khandheria BK, Libhaber E, Maharaj N, Santos C, Matioda H, et al. Left Ventricular Twist in Left Ventricular Noncompaction. *Eur Heart J Cardiovasc Imaging.* 2014;15(1):48-55. doi: 10.1093/ehjci/etj076.
143. Nawaytou HM, Montero AE, Yubbu P, Calderón-Anyosa RJC, Sato T, O'Connor MJ, et al. A Preliminary Study of Left Ventricular Rotational Mechanics in Children with Noncompaction Cardiomyopathy: Do They Influence Ventricular Function? *J Am Soc Echocardiogr.* 2018;31(8):951-61. doi: 10.1016/j.echo.2018.02.015.
144. Arunamata A, Stringer J, Balasubramanian S, Tacy TA, Silverman NH, Punn R. Cardiac Segmental Strain Analysis in Pediatric Left Ventricular Noncompaction Cardiomyopathy. *J Am Soc Echocardiogr.* 2019;32(6):763-773.e1. doi: 10.1016/j.echo.2019.01.014.
145. Tarasoutchi F, Montera MW, Ramos AIO, Sampaio RO, Rosa VEE, Accorsi TAD, et al. Update of the Brazilian Guidelines for Valvular Heart Disease - 2020. *Arq Bras Cardiol.* 2020;115(4):720-75. doi: 10.36660/abc.20201047.
146. Barberato SH, Romano MMD, Beck ALS, Rodrigues ACT, Almeida ALC, Assunção BMBL, et al. Position Statement on Indications of Echocardiography in Adults - 2019. *Arq Bras Cardiol.* 2019;113(1):135-81. doi: 10.5935/abc.20190129.
147. Baumgartner H, Falk V, Bax JJ, De Bonis M, Hamm C, Holm PJ, et al. 2017 ESC/EACTS Guidelines for the Management of Valvular Heart Disease. *Eur Heart J.* 2017;38(36):2739-91. doi: 10.1093/eurheartj/ehx391.
148. Nishimura RA, Otto CM, Bonow RO, Carabello BA, Erwin JP 3rd, Guyton RA, et al. 2014 AHA/ACC Guideline for the Management of Patients with Valvular Heart Disease: A Report of the American College of Cardiology/American Heart Association Task Force on Practice Guidelines. *J Am Coll Cardiol.* 2014;63(22):e57-185. doi: 10.1016/j.jacc.2014.02.536.
149. Vahanian A, Beyersdorf F, Praz F, Milojevic M, Baldus S, Bauersachs J, et al. 2021 ESC/EACTS Guidelines for the Management of Valvular Heart Disease. *Eur J Cardiothorac Surg.* 2021;60(4):727-800. doi: 10.1093/ejcts/ezab389.
150. Suri RM, Schaff HV, Dearani JA, Sundt TM, Daly RC, Mullany CJ, et al. Recovery of Left Ventricular Function after Surgical Correction of Mitral Regurgitation Caused by Leaflet Prolapse. *J Thorac Cardiovasc Surg.* 2009;137(5):1071-6. doi: 10.1016/j.jtcvs.2008.10.026.
151. Enriquez-Sarano M, Schaff HV, Orszulak TA, Bailey KR, Tajik AJ, Frye RL. Congestive Heart Failure after Surgical Correction of Mitral Regurgitation. A Long-Term Study. *Circulation.* 1995;92(9):2496-503. doi: 10.1161/01.cir.92.9.2496.
152. Pandis D, Sengupta PP, Castillo JG, Caracciolo G, Fischer GW, Narula J, et al. Assessment of Longitudinal Myocardial Mechanics in Patients with Degenerative Mitral Valve Regurgitation Predicts Postoperative Worsening of Left Ventricular Systolic Function. *J Am Soc Echocardiogr.* 2014;27(6):627-38. doi: 10.1016/j.echo.2014.02.008.
153. Mascle S, Schnell F, Thebault C, Corbiveau H, Laurent M, Hamonic S, et al. Predictive Value of Global Longitudinal Strain in a Surgical Population of Organic Mitral Regurgitation. *J Am Soc Echocardiogr.* 2012;25(7):766-72. doi: 10.1016/j.echo.2012.04.009.
154. Witkowski TG, Thomas JD, Debonnaire PJ, Delgado V, Hoke U, Ewe SH, et al. Global Longitudinal Strain Predicts Left Ventricular Dysfunction after

Statement

- Mitral Valve Repair. *Eur Heart J Cardiovasc Imaging*. 2013;14(1):69-76. doi: 10.1093/ehjci/ies155.
155. Kim HM, Cho GY, Hwang IC, Choi HM, Park JB, Yoon YE, et al. Myocardial Strain in Prediction of Outcomes after Surgery for Severe Mitral Regurgitation. *JACC Cardiovasc Imaging*. 2018;11(9):1235-44. doi: 10.1016/j.jcmg.2018.03.016.
156. Marciniak A, Sutherland GR, Marciniak M, Claus P, Bijmens B, Jahangiri M. Myocardial Deformation Abnormalities in Patients with Aortic Regurgitation: A Strain Rate Imaging Study. *Eur J Echocardiogr*. 2009;10(1):112-9. doi: 10.1093/ejehocardi/jen185.
157. Alashi A, Mentias A, Abdallah A, Feng K, Gillinov AM, Rodriguez LL, et al. Incremental Prognostic Utility of Left Ventricular Global Longitudinal Strain in Asymptomatic Patients with Significant Chronic Aortic Regurgitation and Preserved Left Ventricular Ejection Fraction. *JACC Cardiovasc Imaging*. 2018;11(5):673-82. doi: 10.1016/j.jcmg.2017.02.016.
158. Alashi A, Khullar T, Mentias A, Gillinov AM, Roselli EE, Svensson LG, et al. Long-Term Outcomes After Aortic Valve Surgery in Patients with Asymptomatic Chronic Aortic Regurgitation and Preserved LVEF: Impact of Baseline and Follow-Up Global Longitudinal Strain. *JACC Cardiovasc Imaging*. 2020;13(1 Pt 1):12-21. doi: 10.1016/j.jcmg.2018.12.021.
159. Dahl JS, Magne J, Pellikka PA, Donal E, Marwick TH. Assessment of Subclinical Left Ventricular Dysfunction in Aortic Stenosis. *JACC Cardiovasc Imaging*. 2019;12(1):163-71. doi: 10.1016/j.jcmg.2018.08.040.
160. Ng AC, Delgado V, Bertini M, Antoni ML, van Bommel RJ, van Rijnsoever EP, et al. Alterations in Multidirectional Myocardial Functions in Patients with Aortic Stenosis and preserved Ejection Fraction: A Two-Dimensional Speckle Tracking Analysis. *Eur Heart J*. 2011;32(12):1542-50. doi: 10.1093/eurheartj/ehr084.
161. Lafitte S, Perlant M, Reant P, Serri K, Douard H, DeMaria A, et al. Impact of Impaired Myocardial Deformations on Exercise Tolerance and Prognosis in Patients with Asymptomatic Aortic Stenosis. *Eur J Echocardiogr*. 2009;10(3):414-9. doi: 10.1093/ejehocardi/jen299.
162. Lancellotti P, Donal E, Magne J, Moonen M, O'Connor K, Daubert JC, et al. Risk Stratification in Asymptomatic Moderate to Severe Aortic Stenosis: The Importance of The Valvular, Arterial and Ventricular Interplay. *Heart*. 2010;96(17):1364-71. doi: 10.1136/hrt.2009.190942.
163. Yingchoncharoen T, Gibby C, Rodriguez LL, Grimm RA, Marwick TH. Association of Myocardial Deformation with Outcome in Asymptomatic Aortic Stenosis with Normal Ejection Fraction. *Circ Cardiovasc Imaging*. 2012;5(6):719-25. doi: 10.1161/CIRCIMAGING.112.977348.
164. Kearney LG, Lu K, Ord M, Patel SK, Profitis K, Matalanis G, et al. Global Longitudinal Strain is a Strong Independent Predictor of All-Cause Mortality in Patients with Aortic Stenosis. *Eur Heart J Cardiovasc Imaging*. 2012;13(10):827-33. doi: 10.1093/ehjci/ies115.
165. Magne J, Cosyns B, Popescu BA, Carstensen HG, Dahl J, Desai MY, et al. Distribution and Prognostic Significance of Left Ventricular Global Longitudinal Strain in Asymptomatic Significant Aortic Stenosis: An Individual Participant Data Meta-Analysis. *JACC Cardiovasc Imaging*. 2019;12(1):84-92. doi: 10.1016/j.jcmg.2018.11.005.
166. Liou K, Negishi K, Ho S, Russell EA, Cranney G, Ooi SY. Detection of Obstructive Coronary Artery Disease Using Peak Systolic Global Longitudinal Strain Derived by Two-Dimensional Speckle-Tracking: A Systematic Review and Meta-Analysis. *J Am Soc Echocardiogr*. 2016;29(8):724-735.e4. doi: 10.1016/j.echo.2016.03.002.
167. Hashimoto I, Li X, Bhat AH, Jones M, Zetts AD, Sahn DJ. Myocardial Strain Rate is a Superior Method for Evaluation of left Ventricular Subendocardial Function Compared with Tissue Doppler Imaging. *J Am Coll Cardiol*. 2003;42(9):1574-83. doi: 10.1016/j.jacc.2003.05.002.
168. Gjesdal O, Hopp E, Vardal T, Lunde K, Helle-Valle T, Aakhus S, et al. Global Longitudinal Strain Measured by Two-Dimensional Speckle Tracking Echocardiography is Closely Related to Myocardial Infarct Size in Chronic Ischaemic Heart Disease. *Clin Sci*. 2007;113(6):287-96. doi: 10.1042/CS20070066.
169. Delgado V, Mollema SA, Ypenburg C, Tops LF, van der Wall EE, Schalij MJ, et al. Relation between Global Left Ventricular Longitudinal Strain Assessed with Novel Automated Function Imaging and Biplane Left Ventricular Ejection Fraction in Patients with coronary artery disease. *J Am Soc Echocardiogr*. 2008;21(11):1244-50. doi: 10.1016/j.echo.2008.08.010.
170. Korosoglou G, Haars A, Humpert PM, Hardt S, Bekeredjian R, Giannitsis E, et al. Evaluation of Myocardial Perfusion and Deformation in Patients with Acute Myocardial Infarction Treated with Primary Angioplasty and Stent Placement. *Coron Artery Dis*. 2008;19(7):497-506. doi: 10.1097/MCA.0b013e328310904e.
171. Tanaka H, Kawai H, Tatsumi K, Kataoka T, Onishi T, Nose T, et al. Improved Regional Myocardial Diastolic Function Assessed by Strain Rate Imaging in Patients with coronary Artery Disease Undergoing Percutaneous Coronary Intervention. *J Am Soc Echocardiogr*. 2006;19(6):756-62. doi: 10.1016/j.echo.2006.01.008.
172. Esmaeilzadeh M, Khaledifar A, Maleki M, Sadeghpour A, Samiei N, Moladoust H, et al. Evaluation of Left Ventricular Systolic and Diastolic Regional Function after Enhanced External Counter Pulsation Therapy Using Strain Rate Imaging. *Eur J Echocardiogr*. 2009;10(1):120-6. doi: 10.1093/ejehocardi/jen183.
173. Takeuchi M, Nishikage T, Nakai H, Kokumai M, Otani S, Lang RM. The Assessment of Left Ventricular Twist in Anterior Wall Myocardial Infarction Using Two-Dimensional Speckle Tracking Imaging. *J Am Soc Echocardiogr*. 2007;20(1):36-44. doi: 10.1016/j.echo.2006.06.019.
174. Kim RJ, Wu E, Rafael A, Chen EL, Parker MA, Simonetti O, et al. The Use of Contrast-Enhanced Magnetic Resonance Imaging to Identify Reversible Myocardial Dysfunction. *N Engl J Med*. 2000;343(20):1445-53. doi: 10.1056/NEJM200011163432003.
175. Becker M, Hoffmann R, Kühl HP, Grawe H, Katoh M, Kramann R, et al. Analysis of Myocardial Deformation Based on Ultrasonic Pixel Tracking to Determine Transmurality in Chronic Myocardial Infarction. *Eur Heart J*. 2006;27(21):2560-6. doi: 10.1093/eurheartj/ehl288.
176. Roes SD, Mollema SA, Lamb HJ, van der Wall EE, Roos A, Bax JJ. Validation of Echocardiographic Two-Dimensional Speckle Tracking Longitudinal Strain Imaging for Viability Assessment in Patients with Chronic Ischemic Left Ventricular Dysfunction and Comparison with Contrast-Enhanced Magnetic Resonance Imaging. *Am J Cardiol*. 2009;104(3):312-7. doi: 10.1016/j.amjcard.2009.03.040.
177. Geyer H, Caracciolo G, Abe H, Wilansky S, Carerj S, Gentile F, et al. Assessment of Myocardial Mechanics Using Speckle Tracking Echocardiography: Fundamentals and Clinical Applications. *J Am Soc Echocardiogr*. 2010;23(4):351-69. doi: 10.1016/j.echo.2010.02.015.
178. Caspar T, Samet H, Ohana M, Germain P, El Ghannudi S, Talha S, et al. Longitudinal 2D Strain Can Help Diagnose Coronary Artery Disease in patients with Suspected Non-ST-Elevation Acute Coronary Syndrome but Apparent Normal Global and Segmental Systolic Function. *Int J Cardiol*. 2017;236:91-94. doi: 10.1016/j.ijcard.2017.02.068.
179. Prastaro M, Pirozzi E, Gaibazzi N, Paolillo S, Santoro C, Savarese G, et al. Expert Review on the Prognostic Role of Echocardiography after Acute Myocardial Infarction. *J Am Soc Echocardiogr*. 2017;30(5):431-443.e2. doi: 10.1016/j.echo.2017.01.020.
180. Eek C, Grenne B, Brunvand H, Aakhus S, Endresen K, Smiseth OA, et al. Strain Echocardiography Predicts Acute Coronary Occlusion in Patients with Non-ST-Segment Elevation Acute Coronary Syndrome. *Eur J Echocardiogr*. 2010;11(6):501-8. doi: 10.1093/ejehocardi/jeq008.
181. Mollema SA, Delgado V, Bertini M, Antoni ML, Boersma E, Holman ER, et al. Viability Assessment with Global Left Ventricular Longitudinal Strain Predicts Recovery of Left Ventricular Function after Acute Myocardial Infarction. *Circ Cardiovasc Imaging*. 2010;3(1):15-23. doi: 10.1161/CIRCIMAGING.108.802785.
182. Bhutani M, Vatsa D, Rahatekar P, Verma D, Nath RK, Pandit N. Role of Strain Imaging for Assessment of Myocardial Viability in Symptomatic Myocardial Infarction with Single Vessel Disease: An Observational Study. *Echocardiography*. 2020;37(1):55-61. doi: 10.1111/echo.14567.

183. Biering-Sørensen T, Hoffmann S, Mogelvang R, Iversen AZ, Galatius S, Fritz-Hansen T, et al. Myocardial Strain Analysis by 2-Dimensional Speckle Tracking Echocardiography Improves Diagnostics of Coronary Artery Stenosis in Stable Angina Pectoris. *Circ Cardiovasc Imaging*. 2014;7(1):58-65. doi: 10.1161/CIRCIMAGING.113.000989.
184. Skulstad H, Edvardsen T, Urheim S, Rabben SI, Stugaard M, Lyseggen E, et al. Postsystolic Shortening in Ischemic Myocardium: Active Contraction or Passive Recoil? *Circulation*. 2002;106(6):718-24. doi: 10.1161/01.cir.0000024102.55150.b6.
185. Dahlslett T, Karlsen S, Grenne B, Eek C, Sjøli B, Skulstad H, et al. Early Assessment of Strain Echocardiography Can Accurately Exclude Significant Coronary Artery Stenosis In Suspected Non-ST-Segment Elevation Acute Coronary Syndrome. *J Am Soc Echocardiogr*. 2014;27(5):512-9. doi: 10.1016/j.echo.2014.01.019.
186. Tsai WC, Liu YW, Huang YY, Lin CC, Lee CH, Tsai LM. Diagnostic Value of Segmental Longitudinal Strain by Automated Function Imaging in Coronary Artery Disease without Left Ventricular Dysfunction. *J Am Soc Echocardiogr*. 2010;23(11):1183-9. doi: 10.1016/j.echo.2010.08.011.
187. Mada RO, Duchenne J, Voigt JU. Tissue Doppler, Strain and Strain Rate in Ischemic Heart Disease "How I Do It". *Cardiovasc Ultrasound*. 2014;12:38. doi: 10.1186/1476-7120-12-38.
188. Voigt JU, Lindenmeier G, Exner B, Regenfus M, Werner D, Reulbach U, et al. Incidence and Characteristics of Segmental Postsystolic Longitudinal Shortening in Normal, Acutely Ischemic, and Scarred Myocardium. *J Am Soc Echocardiogr*. 2003;16(5):415-23. doi: 10.1016/s0894-7317(03)00111-1.
189. van Mourik MJW, Zaar DVJ, Smulders MW, Heijman J, Lumens J, Dokter JE, et al. Adding Speckle-Tracking Echocardiography to Visual Assessment of Systolic Wall Motion Abnormalities Improves the Detection of Myocardial Infarction. *J Am Soc Echocardiogr*. 2019;32(1):65-73. doi: 10.1016/j.echo.2018.09.007.
190. Joyce E, Hoogslag GE, Leong DP, Debonnaire P, Katsanos S, Boden H, et al. Association between Left Ventricular Global Longitudinal Strain and Adverse Left Ventricular Dilatation after ST-Segment-Elevation Myocardial Infarction. *Circ Cardiovasc Imaging*. 2014;7(1):74-81. doi: 10.1161/CIRCIMAGING.113.000982.
191. Ersbøll M, Valeur N, Mogensen UM, Andersen MJ, Møller JE, Velazquez EJ, et al. Prediction of All-Cause Mortality and Heart Failure Admissions from Global Left Ventricular Longitudinal Strain in Patients with Acute Myocardial Infarction and Preserved Left Ventricular Ejection Fraction. *J Am Coll Cardiol*. 2013;61(23):2365-73. doi: 10.1016/j.jacc.2013.02.061.
192. Bertini M, Ng AC, Antoni ML, Nucifora G, Ewe SH, Auger D, et al. Global Longitudinal Strain Predicts Long-Term Survival in Patients with Chronic Ischemic Cardiomyopathy. *Circ Cardiovasc Imaging*. 2012;5(3):383-91. doi: 10.1161/CIRCIMAGING.111.970434.
193. Haugaa KH, Smedsrud MK, Steen T, Kongsgaard E, Loennechen JP, Skjaerpe T, et al. Mechanical Dispersion Assessed by Myocardial Strain in Patients after Myocardial Infarction for Risk Prediction of Ventricular Arrhythmia. *JACC Cardiovasc Imaging*. 2010;3(3):247-56. doi: 10.1016/j.jcmg.2009.11.012.
194. Gecmen C, Candan O, Kahyaoglu M, Kalayci A, Cakmak EO, Karaduman A, et al. Echocardiographic Assessment of Right Ventricle Free Wall Strain for Prediction of Right Coronary Artery Proximal Lesion in Patients with Inferior Myocardial Infarction. *Int J Cardiovasc Imaging*. 2018;34(7):1109-16. doi: 10.1007/s10554-018-1325-1.
195. Chang WT, Tsai WC, Liu YW, Lee CH, Liu PY, Chen JY, et al. Changes in Right Ventricular Free Wall Strain in Patients with Coronary Artery Disease Involving the Right Coronary Artery. *J Am Soc Echocardiogr*. 2014;27(3):230-8. doi: 10.1016/j.echo.2013.11.010.
196. Wechalekar AD, Gillmore JD, Hawkins PN. Systemic Amyloidosis. *Lancet*. 2016;387(10038):2641-54. doi: 10.1016/S0140-6736(15)01274-X.
197. Vergaro G, Aimo A, Barison A, Genovesi D, Buda G, Passino C, et al. Keys to Early Diagnosis of Cardiac Amyloidosis: Red Flags from Clinical, Laboratory and Imaging Findings. *Eur J Prev Cardiol*. 2020;27(17):1806-15. doi: 10.1177/2047487319877708.
198. Ternacle J, Bodez D, Guellich A, Audureau E, Rappeneau S, Lim P, et al. Causes and Consequences of Longitudinal LV Dysfunction Assessed by 2D Strain Echocardiography in Cardiac Amyloidosis. *JACC Cardiovasc Imaging*. 2016;9(2):126-38. doi: 10.1016/j.jcmg.2015.05.014.
199. Liu D, Hu K, Niemann M, Herrmann S, Cikes M, Störk S, et al. Effect of Combined Systolic and Diastolic Functional Parameter Assessment for Differentiation of Cardiac Amyloidosis from Other Causes of Concentric Left Ventricular Hypertrophy. *Circ Cardiovasc Imaging*. 2013;6(6):1066-72. doi: 10.1161/CIRCIMAGING.113.000683.
200. Pagourelis ED, Mirea O, Duchenne J, van Cleemput J, Delforge M, Bogaert J, et al. Echo Parameters for Differential Diagnosis in Cardiac Amyloidosis: A Head-to-Head Comparison of Deformation and Nondeformation Parameters. *Circ Cardiovasc Imaging*. 2017;10(3):e005588. doi: 10.1161/CIRCIMAGING.116.005588.
201. Arvidsson S, Henein MY, Wikström G, Suhr OB, Lindqvist P. Right Ventricular Involvement in Transthyretin Amyloidosis. *Amyloid*. 2018;25(3):160-6. doi: 10.1080/13506129.2018.1493989.
202. Bellavia D, Pellikka PA, Dispenzieri A, Scott CG, Al-Zahrani GB, Grogan M, et al. Comparison of Right Ventricular Longitudinal Strain Imaging, Tricuspid Annular Plane Systolic Excursion, and Cardiac Biomarkers for Early Diagnosis of Cardiac Involvement and Risk Stratification in Primary Systemic (AL) Amyloidosis: A 5-Year Cohort Study. *Eur Heart J Cardiovasc Imaging*. 2012;13(8):680-9. doi: 10.1093/ehjci/ies009.
203. Di Bella G, Minutoli F, Pingitore A, Zito C, Mazzeo A, Aquaro GD, et al. Endocardial and Epicardial Deformations in Cardiac Amyloidosis and Hypertrophic Cardiomyopathy. *Circ J*. 2011;75(5):1200-8. doi: 10.1253/circj.cj-10-0844.
204. Sun JP, Stewart WJ, Yang XS, Donnell RO, Leon AR, Felner JM, et al. Differentiation of Hypertrophic Cardiomyopathy and Cardiac Amyloidosis from Other Causes of Ventricular Wall Thickening by two-Dimensional Strain Imaging Echocardiography. *Am J Cardiol*. 2009;103(3):411-5. doi: 10.1016/j.amjcard.2008.09.102.
205. Cappelli F, Porciani MC, Bergesio F, Perfetto F, De Antoniis F, Cania A, et al. Characteristics of Left Ventricular Rotational Mechanics in Patients with Systemic Amyloidosis, Systemic Hypertension and Normal Left Ventricular Mass. *Clin Physiol Funct Imaging*. 2011;31(2):159-65. doi: 10.1111/j.1475-097X.2010.00987.x.
206. Porciani MC, Cappelli F, Perfetto F, Giaccheri M, Castelli G, Ricceri I, et al. Rotational Mechanics of the Left Ventricle in AL Amyloidosis. *Echocardiography*. 2010;27(9):1061-8. doi: 10.1111/j.1540-8175.2010.01199.x.
207. Aimo A, Fabiani I, Giannoni A, Mandoli GE, Pastore MC, Vergaro G, et al. Multi-Chamber Speckle Tracking Imaging and Diagnostic Value of Left Atrial Strain in Cardiac Amyloidosis. *Eur Heart J Cardiovasc Imaging*. 2022;24(1):130-41. doi: 10.1093/ehjci/jeac057.
208. Santarone M, Corrado G, Tagliagambe LM, Manzillo GF, Tadeo G, Spata M, et al. Atrial Thrombosis in Cardiac Amyloidosis: Diagnostic Contribution of Transesophageal Echocardiography. *J Am Soc Echocardiogr*. 1999;12(6):533-6. doi: 10.1016/s0894-7317(99)70091-x.
209. Bandera F, Martone R, Chacko L, Ganesanathan S, Gilbertson JA, Ponticos M, et al. Clinical Importance of Left Atrial Infiltration in Cardiac Transthyretin Amyloidosis. *JACC Cardiovasc Imaging*. 2022;15(1):17-29. doi: 10.1016/j.jcmg.2021.06.022.
210. Feng D, Syed IS, Martinez M, Oh JK, Jaffe AS, Grogan M, et al. Intracardiac Thrombosis and Anticoagulation Therapy in Cardiac Amyloidosis. *Circulation*. 2009;119(18):2490-7. doi: 10.1161/CIRCULATIONAHA.108.785014.
211. D'Aloia A, Vizzardi E, Chiari E, Faggiano P, Squeri A, Ugo F, et al. Cardiac Arrest in a Patient with a Mobile Right Atrial Thrombus in Transit and Amyloidosis. *Eur J Echocardiogr*. 2008;9(1):141-2. doi: 10.1016/j.euje.2007.04.010.
212. Falk RH, Alexander KM, Liao R, Dorbala S. AL (Light-Chain) Cardiac Amyloidosis: A Review of Diagnosis and Therapy. *J Am Coll Cardiol*. 2016;68(12):1323-41. doi: 10.1016/j.jacc.2016.06.053.

Statement

213. Vitarelli A, Lai S, Petrucci MT, Gaudio C, Capotosto L, Mangieri E, et al. Biventricular Assessment of Light-Chain Amyloidosis Using 3D Speckle Tracking Echocardiography: Differentiation from Other Forms of Myocardial Hypertrophy. *Int J Cardiol.* 2018;271:371-7. doi: 10.1016/j.ijcard.2018.03.088.
214. Baccouche H, Maunz M, Beck T, Gaa E, Banzhaf M, Knayer U, et al. Differentiating Cardiac Amyloidosis and Hypertrophic Cardiomyopathy by Use of Three-Dimensional Speckle Tracking Echocardiography. *Echocardiography.* 2012;29(6):668-77. doi: 10.1111/j.1540-8175.2012.01680.x.
215. Clemmensen TS, Eiskjær H, Mikkelsen F, Granstam SO, Flachskampf FA, Sørensen J, et al. Left Ventricular Pressure-Strain-Derived Myocardial Work at Rest and during Exercise in Patients with Cardiac Amyloidosis. *J Am Soc Echocardiogr.* 2020;33(5):573-82. doi: 10.1016/j.echo.2019.11.018.
216. Giblin GT, Cuddy SAM, González-López E, Sewell A, Murphy A, Dorbala S, et al. Effect of Tafamidis on Global Longitudinal Strain and Myocardial Work in Transthyretin Cardiac Amyloidosis. *Eur Heart J Cardiovasc Imaging.* 2022;23(8):1029-39. doi: 10.1093/ehjci/jeac049.
217. Senapati A, Sperry BW, Grodin JL, Kusnuse K, Thavendiranathan P, Jaber W, et al. Prognostic Implication of Relative Regional Strain Ratio in Cardiac Amyloidosis. *Heart.* 2016;102(10):748-54. doi: 10.1136/heartjnl-2015-308657.
218. Buss SJ, Emami M, Mereles D, Korosoglou G, Kristen AV, Voss A, et al. Longitudinal Left Ventricular Function for Prediction of Survival in Systemic Light-Chain Amyloidosis: Incremental Value Compared with Clinical and Biochemical Markers. *J Am Coll Cardiol.* 2012;60(12):1067-76. doi: 10.1016/j.jacc.2012.04.043.
219. Liu Z, Zhang L, Liu M, Wang F, Xiong Y, Tang Z, et al. Myocardial Injury in Multiple Myeloma Patients with Preserved Left Ventricular Ejection Fraction: Noninvasive Left Ventricular Pressure-Strain Myocardial Work. *Front Cardiovasc Med.* 2022;8:782580. doi: 10.3389/fcvm.2021.782580.
220. Huntjens PR, Zhang KW, Soyama Y, Karpalioti M, Lenihan DJ, Gorscan J 3rd. Prognostic Utility of Echocardiographic Atrial and Ventricular Strain Imaging in Patients With Cardiac Amyloidosis. *JACC Cardiovasc Imaging.* 2021;14(8):1508-19. doi: 10.1016/j.jcmg.2021.01.016.
221. Nagueh SF. Anderson-Fabry Disease and Other Lysosomal Storage Disorders. *Circulation.* 2014;130(13):1081-90. doi: 10.1161/CIRCULATIONAHA.114.009789.
222. Wu JC, Ho CY, Skali H, Abichandani R, Wilcox WR, Banikazemi M, et al. Cardiovascular Manifestations of Fabry Disease: Relationships between Left Ventricular Hypertrophy, Disease Severity, and Alpha-Galactosidase: A activity. *Eur Heart J.* 2010;31(9):1088-97. doi: 10.1093/eurheartj/ehp588.
223. Pieroni M, Chimenti C, De Cobelli F, Morgante E, Del Maschio A, Gaudio C, et al. Fabry's Disease Cardiomyopathy: Echocardiographic Detection of Endomyocardial Glycosphingolipid Compartmentalization. *J Am Coll Cardiol.* 2006;47(8):1663-71. doi: 10.1016/j.jacc.2005.11.070.
224. Sachdev B, Takenaka T, Teraguchi H, Tei C, Lee P, McKenna WJ, et al. Prevalence of Anderson-Fabry Disease in Male Patients with Late Onset Hypertrophic Cardiomyopathy. *Circulation.* 2002;105(12):1407-11. doi: 10.1161/01.cir.0000012626.81324.38.
225. Chimenti C, Pieroni M, Morgante E, Antuzzi D, Russo A, Russo MA, et al. Prevalence of Fabry Disease in Female Patients with Late-Onset Hypertrophic Cardiomyopathy. *Circulation.* 2004;110(9):1047-53. doi: 10.1161/01.CIR.0000139847.74101.03.
226. Morris DA, Blaschke D, Canaan-Kühl S, Krebs A, Knobloch G, Walter TC, et al. Global Cardiac Alterations Detected by Speckle-Tracking Echocardiography in Fabry Disease: Left Ventricular, Right Ventricular, and Left Atrial Dysfunction are Common and Linked to Worse Symptomatic Status. *Int J Cardiovasc Imaging.* 2015;31(2):301-13. doi: 10.1007/s10554-014-0551-4.
227. Nordin S, Kozor R, Vijapurapu R, Augusto JB, Knott KD, Captur G, et al. Myocardial Storage, Inflammation, and Cardiac Phenotype in Fabry Disease After One Year of Enzyme Replacement Therapy. *Circ Cardiovasc Imaging.* 2019;12(12):e009430. doi: 10.1161/CIRCIMAGING.119.009430.
228. Germain DP, Hughes DA, Nicholls K, Bichet DG, Giugliani R, Wilcox WR, et al. Treatment of Fabry's Disease with the Pharmacologic Chaperone Migalastat. *N Engl J Med.* 2016;375(6):545-55. doi: 10.1056/NEJMoa1510198.
229. Kraigher-Krainer E, Shah AM, Gupta DK, Santos A, Claggett B, Pieske B, et al. Impaired Systolic Function by Strain Imaging in Heart Failure with Preserved Ejection Fraction. *J Am Coll Cardiol.* 2014;63(5):447-56. doi: 10.1016/j.jacc.2013.09.052.
230. Hunt SA, Abraham WT, Chin MH, Feldman AM, Francis GS, Ganiats TC, et al. ACC/AHA 2005 Guideline Update for the Diagnosis and Management of Chronic Heart Failure in the Adult: A Report of the American College of Cardiology/American Heart Association Task Force on Practice Guidelines (Writing Committee to Update the 2001 Guidelines for the Evaluation and Management of Heart Failure): Developed in Collaboration with the American College of Chest Physicians and the International Society for Heart and Lung Transplantation: Endorsed by the Heart Rhythm Society. *Circulation.* 2005;112(12):e154-235. doi: 10.1161/CIRCULATIONAHA.105.167586.
231. Contaldi C, Imbriaco M, Alcidi G, Ponsiglione A, Santoro C, Puglia M, et al. Assessment of the Relationships between Left Ventricular Filling Pressures and Longitudinal Dysfunction with Myocardial Fibrosis in Uncomplicated Hypertensive Patients. *Int J Cardiol.* 2016;202:84-6. doi: 10.1016/j.ijcard.2015.08.153.
232. Kishi S, Teixeira-Tura G, Ning H, Venkatesh BA, Wu C, Almeida A, et al. Cumulative Blood Pressure in Early Adulthood and Cardiac Dysfunction in Middle Age: The CARDIA Study. *J Am Coll Cardiol.* 2015;65(25):2679-87. doi: 10.1016/j.jacc.2015.04.042.
233. Lembo M, Esposito R, Lo Iudice F, Santoro C, Izzo R, De Luca N, et al. Impact of Pulse Pressure on Left Ventricular Global Longitudinal Strain in Normotensive and Newly Diagnosed, Untreated Hypertensive Patients. *J Hypertens.* 2016;34(6):1201-7. doi: 10.1097/HJH.0000000000000906.
234. Imbalzano E, Zito C, Carerj S, Oretto G, Mandraffino G, Cusmà-Piccione M, et al. Left Ventricular Function in Hypertension: New Insight by Speckle Tracking Echocardiography. *Echocardiography.* 2011;28(6):649-57. doi: 10.1111/j.1540-8175.2011.01410.x.
235. Cameli M, Mandoli GE, Lisi E, Ibrahim A, Incampo E, Buccoliero G, et al. Left Atrial, Ventricular and Atrio-Ventricular Strain in Patients with Subclinical Heart Dysfunction. *Int J Cardiovasc Imaging.* 2019;35(2):249-58. doi: 10.1007/s10554-018-1461-7.
236. Biering-Sørensen T, Biering-Sørensen SR, Olsen FJ, Sengeløv M, Jørgensen PG, Mogelvang R, et al. Global Longitudinal Strain by Echocardiography Predicts Long-Term Risk of Cardiovascular Morbidity and Mortality in a Low-Risk General Population: The Copenhagen City Heart Study. *Circ Cardiovasc Imaging.* 2017;10(3):e005521. doi: 10.1161/CIRCIMAGING.116.005521.
237. Xu L, Wang N, Chen X, Liang Y, Zhou H, Yan J. Quantitative Evaluation of Myocardial Layer-Specific Strain Using Two-Dimensional Speckle Tracking Echocardiography among Young Adults with Essential Hypertension in China. *Medicine.* 2018;97(39):e12448. doi: 10.1097/MD.00000000000012448.
238. Di Bello V, Talini E, Dell'omo G, Giannini C, Delle Donne MG, Canale ML, et al. Early Left Ventricular Mechanics Abnormalities in Prehypertension: A Two-Dimensional Strain Echocardiography Study. *Am J Hypertens.* 2010;23(4):405-12. doi: 10.1038/ajh.2009.258.
239. Kang SJ, Lim HS, Choi BJ, Choi SY, Hwang GS, Yoon MH, et al. Longitudinal Strain and Torsion Assessed by Two-Dimensional Speckle Tracking Correlate with the Serum Level of Tissue Inhibitor of Matrix Metalloproteinase-1, a Marker of Myocardial Fibrosis, in Patients with Hypertension. *J Am Soc Echocardiogr.* 2008;21(8):907-11. doi: 10.1016/j.echo.2008.01.015.
240. Galderisi M, Lomoriello VS, Santoro A, Esposito R, Olibet M, Raia R, et al. Differences of Myocardial Systolic Deformation and Correlates of Diastolic Function in Competitive Rowers and Young Hypertensives: A Speckle-Tracking Echocardiography Study. *J Am Soc Echocardiogr.* 2010;23(11):1190-8. doi: 10.1016/j.echo.2010.07.010.

241. Kosmala W, Plaksej R, Strotmann JM, Weigel C, Herrmann S, Niemann M, et al. Progression of Left Ventricular Functional Abnormalities in Hypertensive Patients with Heart Failure: An Ultrasonic Two-Dimensional Speckle Tracking Study. *J Am Soc Echocardiogr.* 2008;21(12):1309-17. doi: 10.1016/j.echo.2008.10.006.
242. Kim SA, Park SM, Kim MN, Shim WJ. Assessment of Left Ventricular Function by Layer-Specific Strain and Its Relationship to Structural Remodelling in Patients with Hypertension. *Can J Cardiol.* 2016;32(2):211-6. doi: 10.1016/j.cjca.2015.04.025.
243. Lee WH, Liu YW, Yang LT, Tsai WC. Prognostic Value of Longitudinal Strain of Subepicardial Myocardium in Patients with Hypertension. *J Hypertens.* 2016;34(6):1195-200. doi: 10.1097/HJH.0000000000000903.
244. Cheng S, McCabe EL, Larson MG, Merz AA, Osypiuk E, Lehman BT, et al. Distinct Aspects of Left Ventricular Mechanical Function are Differentially Associated with Cardiovascular Outcomes and All-Cause Mortality in the Community. *J Am Heart Assoc.* 2015;4(10):e002071. doi: 10.1161/JAHA.115.002071.
245. Tadic M, Cuspidi C, Vukomanovic V, Celic V, Tasic I, Stevanovic A, et al. Does Masked Hypertension Impact Left Ventricular Deformation? *J Am Soc Hypertens.* 2016;10(9):694-701. doi: 10.1016/j.jash.2016.06.032.
246. Tadic M, Cuspidi C, Ivanovic B, Ilic I, Celic V, Kocijancic V. Influence of White-Coat Hypertension on Left Ventricular Deformation 2- and 3-Dimensional Speckle Tracking Study. *Hypertension.* 2016;67(3):592-6. doi: 10.1161/HYPERTENSIONAHA.115.06822.
247. Kuznetsova T, Nijs E, Cauwenberghs N, Knez J, Thijs L, Haddad F, et al. Temporal Changes in Left Ventricular Longitudinal Strain in General Population: Clinical Correlates and Impact on Cardiac Remodeling. *Echocardiography.* 2019;36(3):458-68. doi: 10.1111/echo.14246.
248. Drazner MH. The Progression of Hypertensive Heart Disease. *Circulation.* 2011;123(3):327-34. doi: 10.1161/CIRCULATIONAHA.108.845792.
249. Mizuguchi Y, Oishi Y, Miyoshi H, Iuchi A, Nagase N, Oki T. Concentric Left Ventricular Hypertrophy Brings Deterioration of Systolic Longitudinal, Circumferential, and Radial Myocardial Deformation in Hypertensive Patients with Preserved Left Ventricular Pump Function. *J Cardiol.* 2010;55(1):23-33. doi: 10.1016/j.jjcc.2009.07.006.
250. Tadic M, Cuspidi C, Majstorovic A, Kocijancic V, Celic V. The Relationship between Left Ventricular Deformation and Different Geometric Patterns According to the Updated Classification: Findings from the Hypertensive Population. *J Hypertens.* 2015;33(9):1954-61. doi: 10.1097/HJH.0000000000000618.
251. Bendiab NST, Meziane-Tani A, Ouabdesselam S, Methia N, Latreche S, Henaoui L, et al. Factors Associated with Global Longitudinal Strain Decline in Hypertensive Patients with Normal Left Ventricular Ejection Fraction. *Eur J Prev Cardiol.* 2017;24(14):1463-72. doi: 10.1177/2047487317721644.
252. Kouzu H, Yuda S, Muranaka A, Doi T, Yamamoto H, Shimoshige S, et al. Left Ventricular Hypertrophy Causes Different Changes in Longitudinal, Radial, and Circumferential Mechanics in Patients with Hypertension: A Two-Dimensional Speckle Tracking Study. *J Am Soc Echocardiogr.* 2011;24(2):192-9. doi: 10.1016/j.echo.2010.10.020.
253. Cameli M, Lisi M, Righini FM, Massoni A, Mondillo S. Left Ventricular Remodeling and Torsion Dynamics in Hypertensive Patients. *Int J Cardiovasc Imaging.* 2013;29(1):79-86. doi: 10.1007/s10554-012-0054-0.
254. Sun JP, Xu TY, Ni XD, Yang XS, Hu JL, Wang SC, et al. Echocardiographic Strain in Hypertrophic Cardiomyopathy and Hypertensive Left Ventricular Hypertrophy. *Echocardiography.* 2019;36(2):257-65. doi: 10.1111/echo.14222.
255. Tzortzis S, Ikonomidis I, Triantafyllidi H, Trivilou P, Pavlidis G, Katsanos S, et al. Optimal Blood Pressure Control Improves Left Ventricular Torsional Deformation and Vascular Function in Newly Diagnosed Hypertensives: A 3-Year Follow-up Study. *J Cardiovasc Transl Res.* 2020;13(5):814-25. doi: 10.1007/s12265-019-09951-9.
256. Kotini-Shah P, Cuadros S, Huang F, Colla JS. Strain Analysis for the Identification of Hypertensive Cardiac End-Organ Damage in the Emergency Department. *Crit Ultrasound J.* 2018;10(1):29. doi: 10.1186/s13089-018-0110-7.
257. Sera F, Jin Z, Russo C, Lee ES, Schwartz JE, Rundek T, et al. Ambulatory Blood Pressure Control and Subclinical Left Ventricular Dysfunction in Treated Hypertensive Subjects. *J Am Coll Cardiol.* 2015;66(12):1408-9. doi: 10.1016/j.jacc.2015.05.083.
258. Ghorayeb N, Stein R, Daher DJ, Silveira AD, Ritt LEF, Santos DFP, et al. Atualização da Diretriz em Cardiologia do Esporte e do Exercício da Sociedade Brasileira de Cardiologia e da Sociedade Brasileira de Medicina do Esporte - 2019. *Arq Bras Cardiol.* 2019; 112(3):326-68. doi: 10.5935/abc.20190048.
259. Richand V, Lafitte S, Reant P, Serri K, Lafitte M, Brette S, et al. An Ultrasound Speckle Tracking (Two-Dimensional Strain) Analysis of Myocardial Deformation in Professional Soccer Players Compared with Healthy Subjects and Hypertrophic Cardiomyopathy. *Am J Cardiol.* 2007;100(1):128-32. doi: 10.1016/j.amjcard.2007.02.063.
260. D'Andrea A, Limongelli G, Caso P, Sarubbi B, Della Pietra A, Brancaccio P, et al. Association between Left Ventricular Structure and Cardiac Performance During Effort in Two Morphological Forms of Athlete's Heart. *Int J Cardiol.* 2002;86(2-3):177-84. doi: 10.1016/s0167-5273(02)00194-8.
261. Beaumont A, Grace F, Richards J, Hough J, Oxborough D, Sculthorpe N. Left Ventricular Speckle Tracking-Derived Cardiac Strain and Cardiac Twist Mechanics in Athletes: A Systematic Review and Meta-Analysis of Controlled Studies. *Sports Med.* 2017;47(6):1145-70. doi: 10.1007/s40279-016-0644-4.
262. Saghir M, Areces M, Makan M. Strain Rate Imaging Differentiates Hypertensive Cardiac Hypertrophy from Physiologic Cardiac Hypertrophy (Athlete's Heart). *J Am Soc Echocardiogr.* 2007;20(2):151-7. doi: 10.1016/j.echo.2006.08.006.
263. Pena JLB, Santos WC, Araújo SA, Dias GM, Sternick EB. How Echocardiographic Deformation Indices Can Distinguish Different Types of Left Ventricular Hypertrophy. *Arq Bras Cardiol.* 2018;111(5):758-9. doi: 10.5935/abc.20180223.
264. Fudge J, Harmon KG, Owens DS, Prutkin JM, Salerno JC, Asif IM, et al. Cardiovascular Screening in Adolescents and Young Adults: A Prospective Study Comparing the Pre-Participation Physical Evaluation Monograph 4th Edition and ECG. *Br J Sports Med.* 2014;48(15):1172-8. doi: 10.1136/bjsports-2014-093840.
265. Zeltser I, Cannon B, Silvana L, Fenrich A, George J, Schleifer J, et al. Lessons Learned from Preparticipation Cardiovascular Screening in a State Funded Program. *Am J Cardiol.* 2012;110(6):902-8. doi: 10.1016/j.amjcard.2012.05.018.
266. Gianrossi R, Detrano R, Mulvihill D, Lehmann K, Dubach P, Colombo A, et al. Exercise-Induced ST Depression in the Diagnosis of Coronary Artery Disease. A Meta-Analysis. *Circulation.* 1989;80(1):87-98. doi: 10.1161/01.cir.80.1.87.
267. Corrado D, Schimied C, Basso C, Borjesson M, Schiavon M, Pelliccia A, et al. Risk of Sports: Do we Need a Pre-Participation Screening for Competitive and Leisure Athletes? *Eur Heart J.* 2011;32(8):934-44. doi: 10.1093/eurheartj/ehq482.
268. Mont L, Pelliccia A, Sharma S, Biffi A, Borjesson M, Terradellas JB, et al. Pre-Participation Cardiovascular Evaluation for Athletic Participants to Prevent Sudden Death: Position Paper from the EHRA and the EACPR, Branches of the ESC. Endorsed by APHRS, HRS, and SOLAECE. *Eur J Prev Cardiol.* 2017;24(1):41-69. doi: 10.1177/2047487316676042.
269. King C, Almutaser I, Murphy RT, La Gerche A, Mahoney N, Bennet K, et al. Reduced Right Ventricular Myocardial Strain in the Elite Athlete May Not Be a Consequence of Myocardial Damage. "Cream Masquerades as Skimmed Milk". *Echocardiography.* 2013;30(8):929-35. doi: 10.1111/echo.12153.
270. La Gerche A, Burns AT, D'Hooge J, Macisaac AI, Heidbüchel H, Prior DL. Exercise Strain Rate Imaging Demonstrates Normal Right Ventricular Contractile Reserve and Clarifies Ambiguous Resting Measures in Endurance

Statement

- Athletes. *J Am Soc Echocardiogr.* 2012;25(3):253-262.e1. doi: 10.1016/j.echo.2011.11.023.
271. Franckowiak SC, Dobrosielski DA, Reilley SM, Walston JD, Andersen RE. Maximal Heart Rate Prediction in Adults that are Overweight or Obese. *J Strength Cond Res.* 2011;25(5):1407-12. doi: 10.1519/JSC.0b013e3181d682d2.
272. Vanhees L, Stevens A. Exercise Intensity: A Matter of Measuring or of Talking? *J Cardiopulm Rehabil.* 2006;26(2):78-9. doi: 10.1097/00008483-200603000-00004.
273. Baggish AL, Wang F, Weiner RB, Elinoff JM, Tournoux F, Boland A, et al. Training-Specific Changes in Cardiac Structure and Function: A Prospective and Longitudinal Assessment of Competitive Athletes. *J Appl Physiol.* 2008;104(4):1121-8. doi: 10.1152/japplphysiol.01170.2007.
274. Silva CES. Appropriate Use of Diastolic Function Guideline when Evaluating Athletes: It is not Always what it Seems to Be. *Arq Bras Cardiol.* 2020;115(1):134-38. doi: 10.36660/abc.20190689.
275. Pelliccia A, Sharma S, Gati S, Bäck M, Björjesson M, Caselli S, et al. 2020 ESC Guidelines on Sports Cardiology and Exercise in Patients with Cardiovascular Disease. *Eur Heart J.* 2021;42(1):17-96. doi: 10.1093/eurheartj/ehaa605.
276. Reant P, Labrousse L, Lafitte S, Bor P, Pillois X, Tariosse L, et al. Experimental Validation of Circumferential, Longitudinal, and Radial 2-Dimensional Strain During Dobutamine Stress Echocardiography in Ischemic Conditions. *J Am Coll Cardiol.* 2008;51(2):149-57. doi: 10.1016/j.jacc.2007.07.088.
277. Yu Y, Villarraga HR, Saleh HK, Cha SS, Pellikka PA. Can Ischemia and Dyssynchrony Be Detected During Early Stages of Dobutamine Stress Echocardiography By 2-Dimensional Speckle Tracking Echocardiography? *Int J Cardiovasc Imaging.* 2013;29(1):95-102. doi: 10.1007/s10554-012-0074-9.
278. Hanekom L, Cho GY, Leano R, Jeffriess L, Marwick TH. Comparison of Two-Dimensional Speckle and Tissue Doppler Strain Measurement During Dobutamine Stress Echocardiography: An Angiographic Correlation. *Eur Heart J.* 2007;28(14):1765-72. doi: 10.1093/eurheartj/ehm188.
279. Paraskevaidis IA, Tsougos E, Panou F, Dagnes N, Karatzas D, Boutati E, et al. Diastolic Stress Echocardiography Detects Coronary Artery Disease in Patients with Asymptomatic Type II Diabetes. *Coron Artery Dis.* 2010;21(2):104-12. doi: 10.1097/MCA.0b013e328335a05d.
280. Ishii K, Imai M, Suyama T, Maenaka M, Nagai T, Kawanami M, et al. Exercise-Induced Post-Ischemic Left Ventricular Delayed Relaxation or Diastolic Stunning: Is It a Reliable Marker in Detecting Coronary Artery Disease? *J Am Coll Cardiol.* 2009;53(8):698-705. doi: 10.1016/j.jacc.2008.09.057.
281. Rambaldi R, Poldermans D, Bax JJ, Boersma E, Elhendy A, Vletter W, et al. Doppler Tissue Velocity Sampling Improves Diagnostic Accuracy During Dobutamine Stress Echocardiography for the Assessment of Viable Myocardium in Patients with Severe Left Ventricular Dysfunction. *Eur Heart J.* 2000;21(13):1091-8. doi: 10.1053/eurh.1999.1857.
282. Gong L, Li D, Chen J, Wang X, Xu T, Li W, et al. Assessment of Myocardial Viability in Patients with Acute Myocardial Infarction by Two-Dimensional Speckle Tracking Echocardiography Combined with Low-Dose Dobutamine Stress Echocardiography. *Int J Cardiovasc Imaging.* 2013;29(5):1017-28. doi: 10.1007/s10554-013-0185-y.
283. Rösner A, How OJ, Aarsaether E, Stenberg TA, Andreassen T, Kondratiev TV, et al. High Resolution Speckle Tracking Dobutamine Stress Echocardiography Reveals Heterogeneous Responses in Different Myocardial Layers: Implication for Viability Assessments. *J Am Soc Echocardiogr.* 2010;23(4):439-47. doi: 10.1016/j.echo.2009.12.023.
284. Voigt JU, Exner B, Schmiedehausen K, Huchzermeyer C, Reulbach U, Nixdorff U, et al. Strain-Rate Imaging During Dobutamine Stress Echocardiography Provides Objective Evidence of Inducible Ischemia. *Circulation.* 2003;107(16):2120-6. doi: 10.1161/01.CIR.0000065249.69988.AA.
285. Bountiokos M, Schinkel AF, Bax JJ, Rizzello V, Valkema R, Krenning BJ, et al. Pulsed Wave Tissue Doppler Imaging for the Quantification of Contractile Reserve in Stunned, Hibernating, and Scarred Myocardium. *Heart.* 2004;90(5):506-10. doi: 10.1136/hrt.2003.018531.
286. Bartko PE, Heinze G, Graf S, Clavel MA, Khorsand A, Bergler-Klein J, et al. Two-Dimensional Strain for the Assessment of Left Ventricular Function in Low Flow-Low Gradient Aortic Stenosis, Relationship to Hemodynamics, and Outcome: A Substudy of the Multicenter TOPAS Study. *Circ Cardiovasc Imaging.* 2013;6(2):268-76. doi: 10.1161/CIRCIMAGING.112.980201.
287. Dahou A, Bartko PE, Capoulade R, Clavel MA, Mundigler G, Grondin SL, et al. Usefulness of Global Left Ventricular Longitudinal Strain for Risk Stratification in Low Ejection Fraction, Low-Gradient Aortic Stenosis: Results from the Multicenter True or Pseudo-Severe Aortic Stenosis Study. *Circ Cardiovasc Imaging.* 2015;8(3):e002117. doi: 10.1161/CIRCIMAGING.114.002117.
288. Hensel KO, Jenke A, Leischik R. Speckle-Tracking and Tissue-Doppler Stress Echocardiography in Arterial Hypertension: A Sensitive Tool for Detection of Subclinical LV Impairment. *Biomed Res Int.* 2014;2014:472562. doi: 10.1155/2014/472562.
289. Cadeddu C, Nocco S, Piano D, Deidda M, Cossu E, Baroni MG, et al. Early Impairment of Contractility Reserve in Patients with Insulin Resistance in Comparison with Healthy Subjects. *Cardiovasc Diabetol.* 2013;12:66. doi: 10.1186/1475-2840-12-66.
290. Jellis CL, Stanton T, Leano R, Martin J, Marwick TH. Usefulness of at Rest and Exercise Hemodynamics to Detect Subclinical Myocardial Disease in Type 2 Diabetes Mellitus. *Am J Cardiol.* 2011;107(4):615-21. doi: 10.1016/j.amjcard.2010.10.024.
291. Vitarelli A, Morichetti MC, Capotosto L, De Cicco V, Ricci S, Caranci F, et al. Utility of Strain Echocardiography at Rest and after Stress Testing in Arrhythmogenic Right Ventricular Dysplasia. *Am J Cardiol.* 2013;111(9):1344-50. doi: 10.1016/j.amjcard.2013.01.279.
292. Matsumoto K, Tanaka H, Imanishi J, Tatsumi K, Motoji Y, Miyoshi T, et al. Preliminary Observations of Prognostic Value of Left Atrial Functional Reserve During Dobutamine Infusion in Patients with Dilated Cardiomyopathy. *J Am Soc Echocardiogr.* 2014;27(4):430-9. doi: 10.1016/j.echo.2013.12.016.
293. Yang HS, Mookadam F, Warsame TA, Khandheria BK, Tajik JA, Chandrasekaran K. Evaluation of Right Ventricular Global and Regional Function During Stress Echocardiography Using Novel Velocity Vector Imaging. *Eur J Echocardiogr.* 2010;11(2):157-64. doi: 10.1093/ejchocard/jep190.
294. D'Ascenzi F, Caselli S, Solari M, Pelliccia A, Cameli M, Focardi M, et al. Novel Echocardiographic Techniques for the Evaluation of Athletes' Heart: A Focus on Speckle-Tracking Echocardiography. *Eur J Prev Cardiol.* 2016;23(4):437-46. doi: 10.1177/2047487315586095.
295. Simsek Z, Gundogdu F, Alpaydin S, Gerek Z, Ercis S, Sen I, et al. Analysis of Athletes' Heart by Tissue Doppler and Strain/Strain Rate Imaging. *Int J Cardiovasc Imaging.* 2011;27(1):105-11. doi: 10.1007/s10554-010-9669-1.
296. Forsey J, Friedberg MK, Mertens L. Speckle Tracking Echocardiography in Pediatric and Congenital Heart Disease. *Echocardiography.* 2013;30(4):447-59. doi: 10.1111/echo.12131.
297. Levy PT, Mejia AAS, Machefsky A, Fowler S, Holland MR, Singh GK. Normal Ranges of Right Ventricular Systolic and Diastolic Strain Measures in Children: A Systematic Review and Meta-Analysis. *J Am Soc Echocardiogr.* 2014;27(5):549-6. doi: 10.1016/j.echo.2014.01.015.
298. Levy PT, Machefsky A, Sanchez AA, Patel MD, Rogal S, Fowler S, et al. Reference Ranges of Left Ventricular Strain Measures by Two-Dimensional Speckle-Tracking Echocardiography in Children: A Systematic Review and Meta-Analysis. *J Am Soc Echocardiogr.* 2016;29(3):209-225.e6. doi: 10.1016/j.echo.2015.11.016.
299. Kutty S, Padiyath A, Li L, Peng Q, Rangamani S, Schuster A, et al. Functional Maturation of Left and Right Atrial Systolic and Diastolic Performance in Infants, Children, and Adolescents. *J Am Soc Echocardiogr.* 2013;26(4):398-409.e2. doi: 10.1016/j.echo.2012.12.016.

300. Cantinotti M, Scalese M, Giordano R, Franchi E, Assanta N, Marotta M, et al. Normative Data for Left and Right Ventricular Systolic Strain in Healthy Caucasian Italian Children by Two-Dimensional Speckle-Tracking Echocardiography. *J Am Soc Echocardiogr*. 2018;31(6):712-720.e6. doi: 10.1016/j.echo.2018.01.006.
301. Cantinotti M, Scalese M, Giordano R, Franchi E, Assanta N, Molinaro S, et al. Left and Right Atrial Strain in Healthy Caucasian Children by Two-Dimensional Speckle-Tracking Echocardiography. *J Am Soc Echocardiogr*. 2019;32(1):165-168.e3. doi: 10.1016/j.echo.2018.10.002.
302. Muntean I, Benedek T, Melinte M, Suteu C, Togănel R. Deformation Pattern and Predictive Value of Right Ventricular Longitudinal Strain in Children with Pulmonary Arterial Hypertension. *Cardiovasc Ultrasound*. 2016;14(1):27. doi: 10.1186/s12947-016-0074-3.
303. Kühn A, Meierhofer C, Rutz T, Rondak IC, Röhlig C, Schreiber C, et al. Non-Volumetric Echocardiographic Indices and Qualitative Assessment of Right Ventricular Systolic Function in Ebstein's Anomaly: Comparison with CMR-Derived Ejection Fraction in 49 Patients. *Eur Heart J Cardiovasc Imaging*. 2016;17(8):930-5. doi: 10.1093/ehjci/jev243.
304. Lipczyńska M, Szymański P, Kumor M, Klisiewicz A, Mazurkiewicz Ł, Hoffman P. Global Longitudinal Strain May Identify Preserved Systolic Function of the Systemic Right Ventricle. *Can J Cardiol*. 2015;31(6):760-6. doi: 10.1016/j.cjca.2015.02.028.
305. Kowalik E, Mazurkiewicz Ł, Kowalski M, Klisiewicz A, Marczak M, Hoffman P. Echocardiography vs Magnetic Resonance Imaging in Assessing Ventricular Function and Systemic Atrioventricular Valve Status in Adults with Congenitally Corrected Transposition of the Great Arteries. *Echocardiography*. 2016;33(11):1697-702. doi: 10.1111/echo.13339.
306. Castaldi B, Vida V, Reffo E, Padalino M, Daniels Q, Stellin G, Milanese O. Speckle Tracking in ALCAPA Patients after Surgical Repair as Predictor of Residual Coronary Disease. *Pediatr Cardiol*. 2017;38(4):794-800. doi: 10.1007/s00246-017-1583-z.
307. Park PW, Atz AM, Taylor CL, Chowdhury SM. Speckle-Tracking Echocardiography Improves Pre-operative Risk Stratification Before the Total Cavopulmonary Connection. *J Am Soc Echocardiogr*. 2017;30(5):478-84. doi: 10.1016/j.echo.2017.01.008.
308. Meyer P, Filippatos GS, Ahmed MI, Iskandrian AE, Bittner V, Perry GJ, et al. Effects of Right Ventricular Ejection Fraction on Outcomes in Chronic Systolic Heart Failure. *Circulation*. 2010;121(2):252-8. doi: 10.1161/CIRCULATIONAHA.109.887570.
309. Ghio S, Gavazzi A, Campana C, Inserra C, Klersy C, Sebastiani R, et al. Independent and Additive Prognostic Value of Right Ventricular Systolic Function and Pulmonary Artery Pressure in Patients with Chronic Heart Failure. *J Am Coll Cardiol*. 2001;37(1):183-8. doi: 10.1016/s0735-1097(00)01102-5.
310. Haddad F, Doyle R, Murphy DJ, Hunt SA. Right Ventricular Function in Cardiovascular Disease, Part II: Pathophysiology, Clinical Importance, and Management of Right Ventricular Failure. *Circulation*. 2008;117(13):1717-31. doi: 10.1161/CIRCULATIONAHA.107.653584.
311. D'Alonzo GE, Barst RJ, Ayres SM, Bergofsky EH, Brundage BH, Detre KM, et al. Survival in Patients with Primary Pulmonary Hypertension. Results from a National Prospective Registry. *Ann Intern Med*. 1991;115(5):343-9. doi: 10.7326/0003-4819-115-5-343.
312. Forfia PR, Fisher MR, Mathai SC, Houston-Harris T, Hemnes AR, Borlaug BA, et al. Tricuspid Annular Displacement Predicts Survival in Pulmonary Hypertension. *Am J Respir Crit Care Med*. 2006;174(9):1034-41. doi: 10.1164/rccm.200604-547OC.
313. Warnes CA. Adult Congenital Heart Disease Importance of the Right Ventricle. *J Am Coll Cardiol*. 2009;54(21):1903-10. doi: 10.1016/j.jacc.2009.06.048.
314. Tadic M. Multimodality Evaluation of the Right Ventricle: An Updated Review. *Clin Cardiol*. 2015;38(12):770-6. doi: 10.1002/clc.22443.
315. Haddad F, Hunt SA, Rosenthal DN, Murphy DJ. Right Ventricular Function in Cardiovascular Disease, Part I: Anatomy, Physiology, Aging, and Functional Assessment of the Right Ventricle. *Circulation*. 2008;117(11):1436-48. doi: 10.1161/CIRCULATIONAHA.107.653576.
316. Zito C, Longobardo L, Cadeddu C, Monte I, Novo G, Dell'Oglio S, et al. Cardiovascular Imaging in the Diagnosis and Monitoring of Cardiotoxicity: Role of Echocardiography. *J Cardiovasc Med*. 2016;17(Suppl 1):e35-e44. doi: 10.2459/JCM.0000000000000374.
317. Ho SY, Nihoyannopoulos P. Anatomy, Echocardiography, and Normal Right Ventricular Dimensions. *Heart*. 2006;92(Suppl 1):i2-13. doi: 10.1136/hrt.2005.077875.
318. Dell'Italia LJ. The Right Ventricle: Anatomy, Physiology, and Clinical Importance. *Curr Probl Cardiol*. 1991;16(10):653-720. doi: 10.1016/0146-2806(91)90009-y.
319. Santamore WP, Dell'Italia LJ. Ventricular Interdependence: Significant Left Ventricular Contributions to Right Ventricular Systolic Function. *Prog Cardiovasc Dis*. 1998;40(4):289-308. doi: 10.1016/s0033-0620(98)80049-2.
320. Lu KJ, Chen JX, Profitis K, Kearney LC, DeSilva D, Smith G, et al. Right Ventricular Global Longitudinal Strain is an Independent Predictor of Right Ventricular Function: A Multimodality Study of Cardiac Magnetic Resonance Imaging, Real Time Three-Dimensional Echocardiography and Speckle Tracking Echocardiography. *Echocardiography*. 2015;32(6):966-74. doi: 10.1111/echo.12783.
321. Wang J, Prakasa K, Bomma C, Tandri H, Dalal D, James C, et al. Comparison of Novel Echocardiographic Parameters of Right Ventricular Function with Ejection Fraction by Cardiac Magnetic Resonance. *J Am Soc Echocardiogr*. 2007;20(9):1058-64. doi: 10.1016/j.echo.2007.01.038.
322. Vizzardi E, Bonadei I, Sciatti E, Pezzali N, Farina D, D'Aloia A, et al. Quantitative Analysis of Right Ventricular (RV) Function with Echocardiography in Chronic Heart Failure with No or Mild RV Dysfunction: Comparison with Cardiac Magnetic Resonance Imaging. *J Ultrasound Med*. 2015;34(2):247-55. doi: 10.7863/ultra.34.2.247.
323. Freed BH, Tsang W, Bhave NM, Patel AR, Weinert L, Yamat M, et al. Right Ventricular Strain in Pulmonary Arterial Hypertension: A 2D Echocardiography and Cardiac Magnetic Resonance Study. *Echocardiography*. 2015;32(2):257-63. doi: 10.1111/echo.12662.
324. Hulshof HG, Eijsvogels TMH, Kleinnibbelink G, van Dijk AP, George KP, Oxborough DL, et al. Prognostic Value of Right Ventricular Longitudinal Strain in Patients with Pulmonary Hypertension: A Systematic Review and Meta-Analysis. *Eur Heart J Cardiovasc Imaging*. 2019;20(4):475-484. doi: 10.1093/ehjci/jej120.
325. Houard L, Benaets MB, Ravenstein CM, Rousseau MF, Ahn SA, Amzulescu MS, et al. Additional Prognostic Value of 2D Right Ventricular Speckle-Tracking Strain for Prediction of Survival in Heart Failure and Reduced Ejection Fraction: A Comparative Study With Cardiac Magnetic Resonance. *JACC Cardiovasc Imaging*. 2019;12(12):2373-85. doi: 10.1016/j.jcmg.2018.11.028.
326. Medvedofsky D, Koifman E, Jarrett H, Miyoshi T, Rogers T, Ben-Dor I, et al. Association of Right Ventricular Longitudinal Strain with Mortality in Patients Undergoing Transcatheter Aortic Valve Replacement. *J Am Soc Echocardiogr*. 2020;33(4):452-60. doi: 10.1016/j.echo.2019.11.014.
327. Gandjbakhch E, Redheuil A, Pousset F, Charron P, Frank R. Clinical Diagnosis, Imaging, and Genetics of Arrhythmogenic Right Ventricular Cardiomyopathy/Dysplasia: JACC State-of-the-Art Review. *J Am Coll Cardiol*. 2018;72(7):784-804. doi: 10.1016/j.jacc.2018.05.065.
328. Prihadi EA, van der Bijl P, Dietz M, Abou R, Vollema EM, Marsan NA, et al. Prognostic Implications of Right Ventricular Free Wall Longitudinal Strain in Patients with Significant Functional Tricuspid Regurgitation. *Circ Cardiovasc Imaging*. 2019;12(3):e008666. doi: 10.1161/CIRCIMAGING.118.008666.
329. Morris DA, Krisper M, Nakatani S, Köhncke C, Otsuji Y, Belyavskiy E, et al. Normal Range and Usefulness of Right Ventricular Systolic Strain to Detect Subtle Right Ventricular Systolic Abnormalities in Patients with Heart Failure: A Multicentre Study. *Eur Heart J Cardiovasc Imaging*. 2017;18(2):212-23. doi: 10.1093/ehjci/jew011.

Statement

330. Lee JH, Park JH, Park KI, Kim MJ, Kim JH, Ahn MS, et al. A Comparison of Different Techniques of Two-Dimensional Speckle-Tracking Strain Measurements of Right Ventricular Systolic Function in Patients with Acute Pulmonary Embolism. *J Cardiovasc Ultrasound*. 2014;22(2):65-71. doi: 10.4250/jcu.2014.22.2.65.
331. Genovese D, Mor-Avi V, Palermo C, Muraru D, Volpato V, Kruse E, et al. Comparison between Four-Chamber and Right Ventricular-Focused Views for the Quantitative Evaluation of Right Ventricular Size and Function. *J Am Soc Echocardiogr*. 2019;32(4):484-94. doi: 10.1016/j.echo.2018.11.014.
332. Badano LP, Muraru D, Parati G, Haugaa K, Voigt JU. How to do Right Ventricular Strain. *Eur Heart J Cardiovasc Imaging*. 2020;21(8):825-7. doi: 10.1093/ehjci/jeaa126.
333. Muraru D, Onciul S, Peluso D, Soriani N, Cucchini U, Aruta P, et al. Sex- and Method-Specific Reference Values for Right Ventricular Strain by 2-Dimensional Speckle-Tracking Echocardiography. *Circ Cardiovasc Imaging*. 2016;9(2):e003866. doi: 10.1161/CIRCIMAGING.115.003866.
334. Focardi M, Cameli M, Carbone SF, Massoni A, De Vito R, Lisi M, et al. Traditional and Innovative Echocardiographic Parameters for the Analysis of Right Ventricular Performance in Comparison with Cardiac Magnetic Resonance. *Eur Heart J Cardiovasc Imaging*. 2015;16(1):47-52. doi: 10.1093/ehjci/jeu156.
335. Li YD, Wang YD, Zhai ZG, Guo XJ, Wu YF, Yang YH, et al. Relationship between Echocardiographic and Cardiac Magnetic Resonance Imaging-Derived Measures of Right Ventricular Function in Patients with Chronic Thromboembolic Pulmonary Hypertension. *Thromb Res*. 2015;135(4):602-6. doi: 10.1016/j.thromres.2015.01.008.
336. Leong DP, Grover S, Molaee P, Chakrabarty A, Shirazi M, Cheng YH, et al. Nonvolumetric Echocardiographic Indices of Right Ventricular Systolic Function: Validation with Cardiovascular Magnetic Resonance and Relationship with Functional Capacity. *Echocardiography*. 2012;29(4):455-63. doi: 10.1111/j.1540-8175.2011.01594.x.
337. Fukuda Y, Tanaka H, Sugiyama D, Ryo K, Onishi T, Fukuya H, et al. Utility of Right Ventricular Free Wall Speckle-Tracking Strain for Evaluation of Right Ventricular Performance in Patients with Pulmonary Hypertension. *J Am Soc Echocardiogr*. 2011;24(10):1101-8. doi: 10.1016/j.echo.2011.06.005.
338. Cameli M, Lisi M, Righini FM, Tsioulpas C, Bernazzali S, Maccherini M, et al. Right Ventricular Longitudinal Strain Correlates Well With right Ventricular Stroke Work Index in Patients with Advanced Heart Failure Referred for Heart Transplantation. *J Card Fail*. 2012;18(3):208-15. doi: 10.1016/j.cardfail.2011.12.002.
339. Grant AD, Smedira NG, Starling RC, Marwick TH. Independent and Incremental Role of Quantitative Right Ventricular Evaluation for the Prediction of Right Ventricular Failure after Left Ventricular Assist Device Implantation. *J Am Coll Cardiol*. 2012;60(6):521-8. doi: 10.1016/j.jacc.2012.02.073.
340. Mingo-Santos S, Moñivas-Palmero V, Garcia-Lunar I, Mitroi CD, Goirgolzarri-Artaza J, Rivero B, et al. Usefulness of Two-Dimensional Strain Parameters to Diagnose Acute Rejection after Heart Transplantation. *J Am Soc Echocardiogr*. 2015;28(10):1149-56. doi: 10.1016/j.echo.2015.06.005.
341. Lemarié J, Huttin O, Girerd N, Mandry D, Juillière Y, Moulin F, et al. Usefulness of Speckle-Tracking Imaging for Right Ventricular Assessment after Acute Myocardial Infarction: A Magnetic Resonance Imaging/Echocardiographic Comparison within the Relation between Aldosterone and Cardiac Remodeling after Myocardial Infarction Study. *J Am Soc Echocardiogr*. 2015;28(7):818-27.e4. doi: 10.1016/j.echo.2015.02.019.
342. Park JH, Park MM, Farha S, Sharp J, Lundgrin E, Comhair S, et al. Impaired Global Right Ventricular Longitudinal Strain Predicts Long-Term Adverse Outcomes in Patients with Pulmonary Arterial Hypertension. *J Cardiovasc Ultrasound*. 2015;23(2):91-9. doi: 10.4250/jcu.2015.23.2.91.
343. Roşca M, Cîlin A, Beladan CC, Enache R, Mateescu AD, Gurzun MM, et al. Right Ventricular Remodeling, Its Correlates, and Its Clinical Impact in Hypertrophic Cardiomyopathy. *J Am Soc Echocardiogr*. 2015;28(11):1329-38. doi: 10.1016/j.echo.2015.07.015. Epub 2015 Aug 19.
344. Afonso L, Briasoulis A, Mahajan N, Kondur A, Siddiqui F, Siddiqui S, et al. Comparison of Right Ventricular Contractile Abnormalities in Hypertrophic Cardiomyopathy versus Hypertensive Heart Disease Using Two Dimensional Strain Imaging: A Cross-Sectional Study. *Int J Cardiovasc Imaging*. 2015;31(8):1503-9. doi: 10.1007/s10554-015-0722-y.
345. Ozdemir AO, Kaya CT, Ozdol C, Candemir B, Turhan S, Dincer I, et al. Two-Dimensional Longitudinal Strain and Strain Rate Imaging for Assessing the Right Ventricular Function in Patients with Mitral Stenosis. *Echocardiography*. 2010;27(5):525-33. doi: 10.1111/j.1540-8175.2009.01078.x.
346. Roushdy AM, Raafat SS, Shams KA, El-Sayed MH. Immediate and Short-Term Effect of Balloon Mitral Valvuloplasty on Global and Regional Biventricular Function: A Two-Dimensional Strain Echocardiographic Study. *Eur Heart J Cardiovasc Imaging*. 2016;17(3):316-25. doi: 10.1093/ehjci/jev157.
347. Saraiva RM, Demirkol S, Buakhamsri A, Greenberg N, Popović ZB, Thomas JD, et al. Left Atrial Strain Measured by Two-Dimensional Speckle Tracking Represents a New Tool to Evaluate Left Atrial Function. *J Am Soc Echocardiogr*. 2010;23(2):172-80. doi: 10.1016/j.echo.2009.11.003.
348. Cameli M, Caputo M, Mondillo S, Ballo P, Palmerini E, Lisi M, et al. Feasibility and Reference Values of Left Atrial Longitudinal Strain Imaging by Two-Dimensional Speckle Tracking. *Cardiovasc Ultrasound*. 2009;7:6. doi: 10.1186/1476-7120-7-6.
349. Hoit BD. Left Atrial Size and Function: Role in Prognosis. *J Am Coll Cardiol*. 2014;63(6):493-505. doi: 10.1016/j.jacc.2013.10.055.
350. Carluccio E, Biagioli P, Mengoni A, Cerasa MF, Lauciello R, Zuchi C, et al. Left Atrial Reservoir Function and Outcome in Heart Failure with Reduced Ejection Fraction. *Circ Cardiovasc Imaging*. 2018;11(11):e007696. doi: 10.1161/CIRCIMAGING.118.007696.
351. D'Andrea A, Caso P, Romano S, Scarafire R, Cuomo S, Salerno G, et al. Association between Left Atrial Myocardial Function and Exercise Capacity in Patients with Either Idiopathic or Ischemic Dilated Cardiomyopathy: A Two-Dimensional Speckle Strain Study. *Int J Cardiol*. 2009;132(3):354-63. doi: 10.1016/j.ijcard.2007.11.102.
352. Cameli M, Lisi M, Mondillo S, Padeletti M, Ballo P, Tsioulpas C, et al. Left Atrial Longitudinal Strain by Speckle Tracking Echocardiography Correlates Well with Left Ventricular Filling Pressures in Patients with Heart Failure. *Cardiovasc Ultrasound*. 2010;8:14. doi: 10.1186/1476-7120-8-14.
353. Valzania C, Gadler F, Boriani G, Rapezzi C, Eriksson MJ. Effect of Cardiac Resynchronization Therapy on Left Atrial Size and Function as Expressed by Speckle Tracking 2-Dimensional Strain. *Am J Cardiol*. 2016;118(2):237-43. doi: 10.1016/j.amjcard.2016.04.042.
354. Reddy YNV, Obokata M, Egbe A, Yang JH, Pislaru S, Lin G, et al. Left Atrial Strain and Compliance in the Diagnostic Evaluation of Heart Failure with Preserved Ejection Fraction. *Eur J Heart Fail*. 2019;21(7):891-900. doi: 10.1002/ehf.1464.
355. Sanchis L, Andrea R, Falces C, Lopez-Sobrinho T, Montserrat S, Perez-Villa F, et al. Prognostic Value of Left Atrial Strain in Outpatients with De Novo Heart Failure. *J Am Soc Echocardiogr*. 2016;29(11):1035-1042.e1. doi: 10.1016/j.echo.2016.07.012.
356. Malagoli A, Rossi L, Bursi F, Zanni A, Sticozzi C, Piepoli MF, et al. Left Atrial Function Predicts Cardiovascular Events in Patients with Chronic Heart Failure with Reduced Ejection Fraction. *J Am Soc Echocardiogr*. 2019;32(2):248-56. doi: 10.1016/j.echo.2018.08.012.
357. Ancona R, Pinto SC, Caso P, Di Salvo G, Severino S, D'Andrea A, et al. Two-Dimensional Atrial Systolic Strain Imaging Predicts Atrial Fibrillation at 4-Year Follow-up in Asymptomatic Rheumatic Mitral Stenosis. *J Am Soc Echocardiogr*. 2013;26(3):270-7. doi: 10.1016/j.echo.2012.11.016.
358. Saraiva RM, Pacheco NP, Pereira TOJS, Costa AR, Holanda MT, Sangenis LHC, et al. Left Atrial Structure and Function Predictors of New-Onset Atrial Fibrillation in Patients with Chagas Disease. *J Am Soc Echocardiogr*. 2020;33(11):1363-74.e1. doi: 10.1016/j.echo.2020.06.003.
359. Kosmala W, Saito M, Kaye G, Negishi K, Linker N, Gammage M, et al. Incremental Value of Left Atrial Structural and Functional Characteristics

- for Prediction of Atrial Fibrillation in Patients Receiving Cardiac Pacing. *Circ Cardiovasc Imaging*. 2015;8(4):e002942. doi: 10.1161/CIRCIMAGING.114.002942.
360. Moreno-Ruiz LA, Madrid-Miller A, Martínez-Flores JE, González-Hermosillo JA, Arenas-Fonseca J, Zamorano-Velázquez N, et al. Left Atrial Longitudinal Strain by Speckle Tracking as Independent Predictor of Recurrence after Electrical Cardioversion in Persistent and Long Standing Persistent Non-Valvular Atrial Fibrillation. *Int J Cardiovasc Imaging*. 2019;35(9):1587-96. doi: 10.1007/s10554-019-01597-7.
361. Mochizuki A, Yuda S, Fujito T, Kawamukai M, Muranaka A, Nagahara D, et al. Left Atrial Strain Assessed by Three-Dimensional Speckle Tracking Echocardiography Predicts Atrial Fibrillation Recurrence after Catheter Ablation in Patients with Paroxysmal Atrial Fibrillation. *J Echocardiogr*. 2017;15(2):79-87. doi: 10.1007/s12574-017-0329-5.
362. Parwani AS, Morris DA, Blaschke F, Huemer M, Pieske B, Haverkamp W, et al. Left Atrial Strain Predicts Recurrence of Atrial Arrhythmias after Catheter Ablation of Persistent Atrial Fibrillation. *Open Heart*. 2017;4(1):e000572. doi: 10.1136/openhrt-2016-000572.
363. Nielsen AB, Skaarup KG, Lassen MCH, Djernæs K, Hansen ML, Svendsen JH, et al. Usefulness of Left Atrial Speckle Tracking Echocardiography in Predicting Recurrence of Atrial Fibrillation after Radiofrequency Ablation: A Systematic Review and Meta-Analysis. *Int J Cardiovasc Imaging*. 2020;36(7):1293-309. doi: 10.1007/s10554-020-01828-2.
364. Leung M, van Rosendaal PJ, Abou R, Marsan NA, Leung DY, Delgado V, et al. Left Atrial Function to Identify Patients with Atrial Fibrillation at High Risk of Stroke: New Insights from a Large Registry. *Eur Heart J*. 2018;39(16):1416-25. doi: 10.1093/eurheartj/ehx736.
365. Marques-Alves P, Marinho AV, Domingues C, Baptista R, Castro G, Martins R, et al. Left Atrial Mechanics in Moderate Mitral Valve Disease: Earlier Markers of Damage. *Int J Cardiovasc Imaging*. 2020;36(1):23-31. doi: 10.1007/s10554-019-01683-w.
366. Cameli M, Sciacaluga C, Mandoli GE, D'Ascenzi F, Tsioulpas C, Mondillo S. The Role of the Left Atrial Function in the Surgical Management of Aortic and Mitral Valve Disease. *Echocardiography*. 2019;36(8):1559-65. doi: 10.1111/echo.14426.
367. Mandoli GE, Pastore MC, Benfari G, Bisleri G, Maccherini M, Lisi G, et al. Left Atrial Strain as a pre-Operative Prognostic Marker for Patients with Severe Mitral Regurgitation. *Int J Cardiol*. 2021;324:139-45. doi: 10.1016/j.ijcard.2020.09.009.
368. Debonnaire P, Leong DP, Witkowski TG, Al Amri I, Joyce E, Katsanos S, et al. Left Atrial Function by Two-Dimensional Speckle-Tracking Echocardiography in Patients with Severe Organic Mitral Regurgitation: Association with Guidelines-Based Surgical Indication and Postoperative (Long-Term) Survival. *J Am Soc Echocardiogr*. 2013;26(9):1053-62. doi: 10.1016/j.echo.2013.05.019.
369. Guichard JB, Nattel S. Atrial Cardiomyopathy: A Useful Notion in Cardiac Disease Management or a Passing Fad? *J Am Coll Cardiol*. 2017;70(6):756-65. doi: 10.1016/j.jacc.2017.06.033.
370. Antoni ML, Ten Brinke EA, Marsan NA, Atary JZ, Holman ER, van der Wall EE, et al. Comprehensive Assessment of Changes in Left Atrial Volumes and Function after ST-Segment Elevation Acute Myocardial Infarction: Role of Two-Dimensional Speckle-Tracking Strain Imaging. *J Am Soc Echocardiogr*. 2011;24(10):1126-33. doi: 10.1016/j.echo.2011.06.017.
371. Antoni ML, ten Brinke EA, Atary JZ, Marsan NA, Holman ER, Schlij MJ, et al. Left Atrial Strain is Related to Adverse Events in Patients after Acute Myocardial Infarction Treated with Primary Percutaneous Coronary Intervention. *Heart*. 2011;97(16):1332-7. doi: 10.1136/hrt.2011.227678.
372. Padeletti M, Cameli M, Lisi M, Malandrino A, Zacà V, Mondillo S. Reference Values of Right Atrial Longitudinal Strain Imaging by Two-Dimensional Speckle Tracking. *Echocardiography*. 2012;29(2):147-52. doi: 10.1111/j.1540-8175.2011.01564.x.
373. Vitarelli A, Mangieri E, Gaudio C, Tanzilli G, Miraldi F, Capotosto L. Right Atrial Function by Speckle Tracking Echocardiography in Atrial Septal Defect: Prediction of Atrial Fibrillation. *Clin Cardiol*. 2018;41(10):1341-47. doi: 10.1002/clc.23051.
374. Alenezi F, Mandawat A, Il'Giovine ZJ, Shaw LK, Siddiqui I, Tapson VF, et al. Clinical Utility and Prognostic Value of Right Atrial Function in Pulmonary Hypertension. *Circ Cardiovasc Imaging*. 2018;11(11):e006984. doi: 10.1161/CIRCIMAGING.117.006984.
375. Sengupta PP, Korinek J, Belohlavek M, Narula J, Vannan MA, Jahangir A, et al. Left Ventricular Structure and Function: Basic Science for Cardiac Imaging. *J Am Coll Cardiol*. 2006;48(10):1988-2001. doi: 10.1016/j.jacc.2006.08.030.
376. Torrent-Guasp F, Ballester M, Buckberg GD, Carreras F, Flotats A, et al. Spatial Orientation of the Ventricular Muscle Band: Physiologic Contribution and Surgical Implications. *J Thorac Cardiovasc Surg*. 2001;122(2):389-92. doi: 10.1067/mtc.2001.113745.
377. Taber LA, Yang M, Podszus WW. Mechanics of Ventricular Torsion. *J Biomech*. 1996;29(6):745-52. doi: 10.1016/0021-9290(95)00129-8.
378. Henson RE, Song SK, Pastorek JS, Ackerman JJ, Lorenz CH. Left Ventricular Torsion is Equal in Mice and Humans. *Am J Physiol Heart Circ Physiol*. 2000;278(4):H1117-23. doi: 10.1152/ajpheart.2000.278.4.H1117.
379. Granzier HL, Labeit S. The Giant Protein Titin: A Major Player in Myocardial Mechanics, Signaling, and Disease. *Circ Res*. 2004;94(3):284-95. doi: 10.1161/01.RES.0000117769.88862.F8.
380. Notomi Y, Martin-Miklovic MG, Oryszak SJ, Shiota T, Deserranno D, Popovic ZB, et al. Enhanced Ventricular Untwisting During Exercise: A Mechanistic Manifestation of Elastic Recoil Described by Doppler Tissue Imaging. *Circulation*. 2006;113(21):2524-33. doi: 10.1161/CIRCULATIONAHA.105.596502.
381. Dong SJ, Hees PS, Huang WM, Buffer SA Jr, Weiss JL, Shapiro EP. Independent Effects of Preload, Afterload, and Contractility on Left Ventricular Torsion. *Am J Physiol*. 1999;277(3):H1053-60. doi: 10.1152/ajpheart.1999.277.3.H1053.
382. Helle-Valle T, Crosby J, Edvardsen T, Lyseggen E, Amundsen BH, Smith HJ, et al. New Noninvasive Method for Assessment of Left Ventricular Rotation: Speckle Tracking Echocardiography. *Circulation*. 2005;112(20):3149-56. doi: 10.1161/CIRCULATIONAHA.104.531558.
383. Gayat E, Ahmad H, Weinert L, Lang RM, Mor-Avi V. Reproducibility and Inter-Vendor Variability of Left Ventricular Deformation Measurements by Three-Dimensional Speckle-Tracking Echocardiography. *J Am Soc Echocardiogr*. 2011;24(8):878-85. doi: 10.1016/j.echo.2011.04.016.
384. Stöhr EJ, Shave RE, Baggish AL, Weiner RB. Left Ventricular Twist Mechanics in the Context of Normal Physiology and Cardiovascular Disease: A Review of Studies Using Speckle Tracking Echocardiography. *Am J Physiol Heart Circ Physiol*. 2016;311(3):H633-44. doi: 10.1152/ajpheart.00104.2016.
385. Yancy CW, Jessup M, Bozkurt B, Butler J, Casey DE Jr, Colvin MM, et al. 2017 ACC/AHA/HFSA Focused Update of the 2013 ACCF/AHA Guideline for the Management of Heart Failure: A Report of the American College of Cardiology/American Heart Association Task Force on Clinical Practice Guidelines and the Heart Failure Society of America. *Circulation*. 2017;136(6):e137-e161. doi: 10.1161/CIR.0000000000000509.
386. Gorcsan J 3rd, Tanabe M, Bleeker GB, Suffoletto MS, Thomas NC, Saba S, et al. Combined Longitudinal and Radial Dyssynchrony Predicts Ventricular Response after Resynchronization Therapy. *J Am Coll Cardiol*. 2007;50(15):1476-83. doi: 10.1016/j.jacc.2007.06.043.
387. Leenders GE, De Boeck BW, Teske AJ, Meine M, Bogaard MD, Prinzen FW, et al. Septal Rebound Stretch is a Strong Predictor of Outcome after Cardiac Resynchronization Therapy. *J Card Fail*. 2012;18(5):404-12. doi: 10.1016/j.cardfail.2012.02.001.
388. Risum N, Strauss D, Sogaard P, Loring Z, Hansen TF, Bruun NE, et al. Left Bundle-Branch Block: The Relationship between Electrocardiogram Electrical Activation and Echocardiography Mechanical Contraction. *Am Heart J*. 2013;166(2):340-8. doi: 10.1016/j.ahj.2013.04.005.

Statement

389. van der Bijl P, Vo NM, Kostyukevich MV, Mertens B, Marsan NA, Delgado V, et al. Prognostic Implications of Global, Left Ventricular Myocardial Work Efficiency Before Cardiac Resynchronization Therapy. *Eur Heart J Cardiovasc Imaging*. 2019;20(12):1388-94. doi: 10.1093/ehjci/jez095.
390. Khan FZ, Virdee MS, Palmer CR, Pugh PJ, O'Halloran D, Elsik M, et al. Targeted Left Ventricular Lead Placement to Guide Cardiac Resynchronization Therapy: The TARGET Study: A Randomized, Controlled Trial. *J Am Coll Cardiol*. 2012;59(17):1509-18. doi: 10.1016/j.jacc.2011.12.030.
391. Marek JJ, Saba S, Onishi T, Ryo K, Schwartzman D, Adelstein EC, et al. Usefulness of Echocardiographically Guided Left Ventricular Lead Placement for Cardiac Resynchronization Therapy in Patients with Intermediate QRS width and Non-Left Bundle Branch Block Morphology. *Am J Cardiol*. 2014;113(1):107-16. doi: 10.1016/j.amjcard.2013.09.024.
392. Tayal B, Gorcsan J 3rd, Delgado-Montero A, Marek JJ, Haugaa KH, Ryo K, et al. Mechanical Dyssynchrony by Tissue Doppler Cross-Correlation is Associated with Risk for Complex Ventricular Arrhythmias after Cardiac Resynchronization Therapy. *J Am Soc Echocardiogr*. 2015;28(12):1474-81. doi: 10.1016/j.echo.2015.07.021.
393. Chung ES, Leon AR, Tavazzi L, Sun JP, Nihoyannopoulos P, Merlino J, et al. Results of the Predictors of Response to CRT (PROSPECT) trial. *Circulation*. 2008;117(20):2608-16. doi: 10.1161/CIRCULATIONAHA.107.743120.
394. Šipula D, Kozák M, Šipula J, Homza M, Plášek J. Cardiac Strains As a Tool for Optimization of Cardiac Resynchronization Therapy in Non-responders: a Pilot Study. *Open Med*. 2019;14:945-952. doi: 10.1515/med-2019-0111.
395. Suga H. Total Mechanical Energy of a Ventricle Model and Cardiac Oxygen Consumption. *Am J Physiol*. 1979;236(3):H498-505. doi: 10.1152/ajpheart.1979.236.3.H498.
396. Hisano R, Cooper G 4th. Correlation of Force-Length Area with Oxygen Consumption in Ferret Papillary Muscle. *Circ Res*. 1987;61(3):318-28. doi: 10.1161/01.res.61.3.318.
397. Takaoka H, Takeuchi M, Odake M, Yokoyama M. Assessment of Myocardial Oxygen Consumption (Vo₂) and Systolic Pressure-Volume Area (PVA) in Human Hearts. *Eur Heart J*. 1992;13(Suppl E):85-90. doi: 10.1093/eurheartj/13.suppl_e.85.
398. Russell K, Eriksen M, Aaberge L, Wilhelmssen N, Skulstad H, Remme EW, et al. A Novel Clinical Method for Quantification of Regional Left Ventricular Pressure-Strain Loop Area: A Non-Invasive Index of Myocardial Work. *Eur Heart J*. 2012;33(6):724-33. doi: 10.1093/eurheartj/ehs016.
399. Russell K, Opdahl A, Remme EW, Gjesdal O, Skulstad H, Kongsgaard E, et al. Evaluation of Left Ventricular Dyssynchrony by Onset of Active Myocardial Force Generation: A Novel Method that Differentiates between Electrical and Mechanical Etiologies. *Circ Cardiovasc Imaging*. 2010;3(4):405-14. doi: 10.1161/CIRCIMAGING.109.905539.
400. Gjesdal O, Remme EW, Opdahl A, Skulstad H, Russell K, Kongsgaard E, et al. Mechanisms of Abnormal Systolic Motion of the Interventricular Septum During Left Bundle-Branch Block. *Circ Cardiovasc Imaging*. 2011;4(3):264-73. doi: 10.1161/CIRCIMAGING.110.961417.
401. Russell K, Smiseth OA, Gjesdal O, Qvigstad E, Norseng PA, Sjaastad I, et al. Mechanism of Prolonged Electromechanical Delay in Late Activated Myocardium During Left Bundle Branch Block. *Am J Physiol Heart Circ Physiol*. 2011;301(6):H2334-43. doi: 10.1152/ajpheart.00644.2011.
402. Sletten OJ, Aalen J, Khan FH, Larsen CK, Inoue K, Remme EW, et al. Myocardial Work Exposes Afterload-Dependent Changes in Strain. *Eur Heart J Cardiovasc Imaging*. 2020;21(Suppl 1):i40. doi: 10.1093/ehjci/jez319.036.
403. Manganaro R, Marchetta S, Dulgheru R, Ilardi F, Sugimoto T, Robinet S, et al. Echocardiographic Reference Ranges for Normal Non-Invasive Myocardial Work Indices: Results from the EACVI NORRE Study. *Eur Heart J Cardiovasc Imaging*. 2019;20(5):582-90. doi: 10.1093/ehjci/jey188.
404. Galli E, John-Matthwes B, Rousseau C, Schnell F, Leclercq C, Donal E. Echocardiographic Reference Ranges for Myocardial Work in Healthy Subjects: A Preliminary Study. *Echocardiography*. 2019;36(10):1814-24. doi: 10.1111/echo.14494.
405. Galli E, Leclercq C, Hubert A, Bernard A, Smiseth OA, Mabo P, et al. Role of Myocardial Constructive Work in the Identification of Responders to CRT. *Eur Heart J Cardiovasc Imaging*. 2018;19(9):1010-8. doi: 10.1093/ehjci/jex191.
406. Vecera J, Penicka M, Eriksen M, Russell K, Bartunek J, Vanderheyden M, et al. Wasted Septal Work in Left Ventricular Dyssynchrony: A Novel Principle to Predict Response to Cardiac Resynchronization Therapy. *Eur Heart J Cardiovasc Imaging*. 2016;17(6):624-32. doi: 10.1093/ehjci/jew019.
407. Edwards NFA, Scalia GM, Shiino K, Sabapathy S, Anderson B, Chamberlain R, et al. Global Myocardial Work Is Superior to Global Longitudinal Strain to Predict Significant Coronary Artery Disease in Patients with Normal Left Ventricular Function and Wall Motion. *J Am Soc Echocardiogr*. 2019;32(8):947-57. doi: 10.1016/j.echo.2019.02.014.
408. Meimoun P, Abdani S, Stracchi V, Elmki F, Boulanger J, Botoro T, et al. Usefulness of Noninvasive Myocardial Work to Predict Left Ventricular Recovery and Acute Complications after Acute Anterior Myocardial Infarction Treated by Percutaneous Coronary Intervention. *J Am Soc Echocardiogr*. 2020;33(10):1180-90. doi: 10.1016/j.echo.2020.07.008.
409. Lustosa RP, Butcher SC, van der Bijl P, El Mahdi M, Montero-Cabezas JM, Kostyukevich MV, et al. Global Left Ventricular Myocardial Work Efficiency and Long-Term Prognosis in Patients after ST-Segment-Elevation Myocardial Infarction. *Circ Cardiovasc Imaging*. 2021;14(3):e012072. doi: 10.1161/CIRCIMAGING.120.012072.
410. Nabeshima Y, Seo Y, Takeuchi M. A Review of Current Trends in Three-Dimensional Analysis of Left Ventricular Myocardial Strain. *Cardiovasc Ultrasound*. 2020;18(1):23. doi: 10.1186/s12947-020-00204-3.
411. Muraru D, Cucchini U, Mihajilic S, Miglioranza MH, Aruta P, Cavalli G, et al. Left Ventricular Myocardial Strain by Three-Dimensional Speckle-Tracking Echocardiography in Healthy Subjects: Reference Values and Analysis of Their Physiologic and Technical Determinants. *J Am Soc Echocardiogr*. 2014;27(8):858-871.e1. doi: 10.1016/j.echo.2014.05.010.
412. Badano LP, Boccacini F, Muraru D, Bianco LD, Peluso D, Bellu R, et al. Current Clinical Applications of Transthoracic Three-Dimensional Echocardiography. *J Cardiovasc Ultrasound*. 2012;20(1):1-22. doi: 10.4250/jcu.2012.20.1.1.
413. Mor-Avi V, Lang RM, Badano LP, Belohlavek M, Cardim NM, Derumeaux G, et al. Current and Evolving Echocardiographic Techniques for the Quantitative Evaluation of Cardiac Mechanics: ASE/EAE Consensus Statement on Methodology and Indications Endorsed by the Japanese Society of Echocardiography. *J Am Soc Echocardiogr*. 2011;24(3):277-313. doi: 10.1016/j.echo.2011.01.015.
414. Teixeira R. Three-Dimensional Speckle Tracking Echocardiography: The Future Is Now. *Rev Port Cardiol*. 2018 Apr;37(4):339-40. doi: 10.1016/j.repc.2018.03.008.
415. Smith BC, Dobson G, Dawson D, Charalampopoulos A, Grapsa J, Nihoyannopoulos P. Three-Dimensional Speckle Tracking of the Right Ventricle: Toward Optimal Quantification of Right Ventricular Dysfunction in Pulmonary Hypertension. *J Am Coll Cardiol*. 2014;64(1):41-51. doi: 10.1016/j.jacc.2014.01.084.
416. Cuspidi C, Tadic M, Sala C, Gherbesi E, Grassi G, Mancia G. Left Atrial Function in Elite Athletes: A Meta-Analysis of Two-Dimensional Speckle Tracking Echocardiographic Studies. *Clin Cardiol*. 2019;42(5):579-87. doi: 10.1002/clc.23180.
417. Sabatino J, Di Salvo G, Prota C, Bucciarelli V, Josen M, Paredes J, et al. Left Atrial Strain to Identify Diastolic Dysfunction in Children with Cardiomyopathies. *J Clin Med*. 2019;8(8):1243. doi: 10.3390/jcm8081243.
418. Simpson RM, Keegan J, Firmin DN. MR Assessment of Regional Myocardial Mechanics. *J Magn Reson Imaging*. 2013;37(3):576-99. doi: 10.1002/jmri.23756.
419. Andre F, Steen H, Matheis P, Westkott M, Breuninger K, Sander Y, et al. Age- and Gender-Related Normal Left Ventricular Deformation Assessed by Cardiovascular Magnetic Resonance Feature Tracking. *J Cardiovasc Magn Reson*. 2015;17(1):25. doi: 10.1186/s12968-015-0123-3.

420. Schuster A, Stahnke VC, Unterberg-Buchwald C, Kowallick JT, Lamata P, Steinmetz M, et al. Cardiovascular Magnetic Resonance Feature-Tracking Assessment of Myocardial Mechanics: Intervendor Agreement and Considerations Regarding Reproducibility. *Clin Radiol*. 2015;70(9):989-98. doi: 10.1016/j.crad.2015.05.006.
421. Augustine D, Lewandowski AJ, Lazdam M, Rai A, Francis J, Myerson S, et al. Global and Regional Left Ventricular Myocardial Deformation Measures by Magnetic Resonance Feature Tracking in Healthy Volunteers: Comparison with Tagging and Relevance of Gender. *J Cardiovasc Magn Reson*. 2013;15(1):8. doi: 10.1186/1532-429X-15-8.
422. Taylor RJ, Moody WE, Umar F, Edwards NC, Taylor TJ, Stegemann B, et al. Myocardial Strain Measurement with Feature-Tracking Cardiovascular Magnetic Resonance: normal values. *Eur Heart J Cardiovasc Imaging*. 2015;16(8):871-81. doi: 10.1093/ehjci/jev006.
423. Heiberg J, Ringgaard S, Schmidt MR, Redington A, Hjortdal VE. Structural and Functional Alterations of the Right Ventricle are Common in Adults Operated for Ventricular Septal Defect as Toddlers. *Eur Heart J Cardiovasc Imaging*. 2015;16(5):483-9. doi: 10.1093/ehjci/jeu292.
424. Vo HQ, Marwick TH, Negishi K. MRI-Derived Myocardial Strain Measures in Normal Subjects. *JACC Cardiovasc Imaging*. 2018 Feb;11(2 Pt 1):196-205. doi: 10.1016/j.jcmg.2016.12.025.
425. Erley J, Genovese D, Tapaskar N, Alvi N, Rashedi N, Besser SA, et al. Echocardiography and Cardiovascular Magnetic Resonance Based Evaluation of Myocardial Strain and Relationship with Late Gadolinium Enhancement. *J Cardiovasc Magn Reson*. 2019;21(1):46. doi: 10.1186/s12968-019-0559-y.
426. Buss SJ, Breuninger K, Lehrke S, Voss A, Galuschky C, Lossnitzer D, et al. Assessment of Myocardial Deformation with Cardiac Magnetic Resonance Strain Imaging Improves Risk Stratification in Patients with Dilated Cardiomyopathy. *Eur Heart J Cardiovasc Imaging*. 2015;16(3):307-15. doi: 10.1093/ehjci/jeu181.
427. Ito H, Ishida M, Makino W, Goto Y, Ichikawa Y, Kitagawa K, et al. Cardiovascular Magnetic Resonance Feature Tracking for Characterization of Patients with Heart Failure with Preserved Ejection Fraction: Correlation of Global Longitudinal Strain with Invasive Diastolic Functional Indices. *J Cardiovasc Magn Reson*. 2020;22(1):42. doi: 10.1186/s12968-020-00636-w.
428. Amaki M, Savino J, Ain DL, Sanz J, Pedrizzetti G, Kulkarni H, et al. Diagnostic Concordance of Echocardiography and Cardiac Magnetic Resonance-Based Tissue Tracking for Differentiating Constrictive Pericarditis from Restrictive Cardiomyopathy. *Circ Cardiovasc Imaging*. 2014;7(5):819-27. doi: 10.1161/CIRCIMAGING.114.002103.
429. Weigand J, Nielsen JC, Sengupta PP, Sanz J, Srivastava S, Uppu S. Feature Tracking-Derived Peak Systolic Strain Compared to Late Gadolinium Enhancement in Troponin-Positive Myocarditis: A Case-Control Study. *Pediatr Cardiol*. 2016;37(4):696-703. doi: 10.1007/s00246-015-1333-z.
430. Oda S, Utsunomiya D, Nakaura T, Yuki H, Kidoh M, Morita K, et al. Identification and Assessment of Cardiac Amyloidosis by Myocardial Strain Analysis of Cardiac Magnetic Resonance Imaging. *Circ J*. 2017;81(7):1014-21. doi: 10.1253/circj.CJ-16-1259.
431. Mathur S, Dreisbach JG, Karur GR, Iwanochko RM, Morel CF, Wasim S, et al. Loss of Base-To-Apex Circumferential Strain Gradient Assessed by Cardiovascular Magnetic Resonance in Fabry Disease: Relationship to T1 Mapping, Late Gadolinium Enhancement and Hypertrophy. *J Cardiovasc Magn Reson*. 2019;21(1):45. doi: 10.1186/s12968-019-0557-0.
432. Smith BM, Dorfman AL, Yu S, Russell MW, Agarwal PP, Mahani MG, et al. Relation of Strain by Feature Tracking and Clinical Outcome in Children, Adolescents, and Young Adults with Hypertrophic Cardiomyopathy. *Am J Cardiol*. 2014;114(8):1275-80. doi: 10.1016/j.amjcard.2014.07.051.
433. Neisius U, Myerson L, Fahmy AS, Nakamori S, El-Rewaify H, Joshi G, et al. Cardiovascular Magnetic Resonance Feature Tracking Strain Analysis for Discrimination between Hypertensive Heart Disease and Hypertrophic Cardiomyopathy. *PLoS One*. 2019;14(8):e0221061. doi: 10.1371/journal.pone.0221061.
434. Schneeweis C, Qiu J, Schnackenburg B, Berger A, Kelle S, Fleck E, et al. Value of Additional Strain Analysis with Feature Tracking in Dobutamine Stress Cardiovascular Magnetic Resonance for Detecting Coronary Artery Disease. *J Cardiovasc Magn Reson*. 2014;16(1):72. doi: 10.1186/s12968-014-0072-2.
435. Reindl M, Tiller C, Holzknicht M, Lechner I, Beck A, Plappert D, et al. Prognostic Implications of Global Longitudinal Strain by Feature-Tracking Cardiac Magnetic Resonance in ST-Elevation Myocardial Infarction. *Circ Cardiovasc Imaging*. 2019;12(11):e009404. doi: 10.1161/CIRCIMAGING.119.009404.
436. Al Musa T, Uddin A, Swoboda PP, Garg P, Fairbairn TA, Dobson LE, et al. Myocardial Strain and Symptom Severity in Severe Aortic Stenosis: Insights from Cardiovascular Magnetic Resonance. *Quant Imaging Med Surg*. 2017;7(1):38-47. doi: 10.21037/qims.2017.02.05.
437. Burris NS, Lima APS, Hope MD, Ordovas KG. Feature Tracking Cardiac MRI Reveals Abnormalities in Ventricular Function in Patients with Bicuspid Aortic Valve and Preserved Ejection Fraction. *Tomography*. 2018;4(1):26-32. doi: 10.18383/j.tom.2018.00005.
438. Nakano S, Takahashi M, Kimura F, Senoo T, Saeki T, Ueda S, et al. Cardiac Magnetic Resonance Imaging-Based Myocardial Strain Study for Evaluation of Cardiotoxicity in Breast Cancer Patients Treated with Trastuzumab: A Pilot Study to Evaluate the Feasibility of the Method. *Cardiol J*. 2016;23(3):270-80. doi: 10.5603/CJ.a2016.0023.
439. Romano S, Judd RM, Kim RJ, Kim HW, Klem I, Heitner JF, et al. Feature-Tracking Global Longitudinal Strain Predicts Death in a Multicenter Population of Patients with Ischemic and Nonischemic Dilated Cardiomyopathy Incremental to Ejection Fraction and Late Gadolinium Enhancement. *JACC Cardiovasc Imaging*. 2018;11(10):1419-29. doi: 10.1016/j.jcmg.2017.10.024.
440. Scatteia A, Baritussio A, Bucciarelli-Ducci C. Strain Imaging Using Cardiac Magnetic Resonance. *Heart Fail Rev*. 2017;22(4):465-476. doi: 10.1007/s10741-017-9621-8.
441. Kowallick JT, Kutty S, Edelmann F, Chiribiri A, Villa A, Steinmetz M, et al. Quantification of Left Atrial Strain and Strain Rate Using Cardiovascular Magnetic Resonance Myocardial Feature Tracking: A Feasibility Study. *J Cardiovasc Magn Reson*. 2014;16(1):60. doi: 10.1186/s12968-014-0060-6.
442. Habibi M, Chahal H, Opdahl A, Gjesdal O, Helle-Valle TM, Heckbert SR, et al. Association of CMR-Measured LA Function with Heart Failure Development: Results from the MESA Study. *JACC Cardiovasc Imaging*. 2014;7(6):570-9. doi: 10.1016/j.jcmg.2014.01.016.
443. Chirinos JA, Sardana M, Ansari B, Sattija V, Kuriakose D, Edelstein I, et al. Left Atrial Phasic Function by Cardiac Magnetic Resonance Feature Tracking Is a Strong Predictor of Incident Cardiovascular Events. *Circ Cardiovasc Imaging*. 2018;11(12):e007512. doi: 10.1161/CIRCIMAGING.117.007512.
444. Fukui M, Xu J, Abdelkarim I, Sharbaugh MS, Thoma FW, Althouse AD, et al. Global Longitudinal Strain Assessment by Computed Tomography in Severe Aortic Stenosis Patients - Feasibility Using Feature Tracking Analysis. *J Cardiovasc Comput Tomogr*. 2019;13(2):157-62. doi: 10.1016/j.jcct.2018.10.020.
445. Szilveszter B, Nagy AI, Vattay B, Apor A, Kolosváry M, Bartykowszki A, et al. Left Ventricular and Atrial Strain Imaging with Cardiac Computed Tomography: Validation Against Echocardiography. *J Cardiovasc Comput Tomogr*. 2020;14(4):363-9. doi: 10.1016/j.jcct.2019.12.004.
446. Han X, Cao Y, Ju Z, Liu J, Li N, Li Y, et al. Assessment of Regional Left Ventricular Myocardial Strain in Patients with Left Anterior Descending Coronary Stenosis Using Computed Tomography Feature Tracking. *BMC Cardiovasc Disord*. 2020;20(1):362. doi: 10.1186/s12872-020-01644-5.

